TECHNISCHE UNIVERSITÄT WIEN
Vienna | Austria

Master Thesis

Beneficial traits of coronary sinus interventions with focus on pressure-controlled intermittent coronary sinus occlusion

carried out for the purpose of obtaining the degree of Master of Science (MSc),
submitting at TU Wien, Faculty of Analysis and Scientific Computing, by

Johannes GNONG
Mat.nr.: 1026063

under the supervision of
Ao.Univ.Prof. Dipl.-Ing. Dr.rer.nat. Dr.sc.med. Dr.techn. Frank Rattay
Institut of Analysis and Scientific Computing, E101

Vienna, 9th of February 2018

Abstract

According to World Health Organization (WHO) cardiovascular diseases are the number one cause of death globally, where most cardiovascular diseases can be prevented by addressing behavioral risk factors such as tobacco use, unhealthy diet and obesity, physical inactivity and harmful use of alcohol using population-wide strategies.

The high death rate leads to an increased demand of diagnosis and treatment of these diseases. One of many imaging methods is cardiac magnetic resonance imaging and coronary sinus interventions as a treatment are methods of temporary protection of ischemic myocardium via the coronary venous system. They include retroinfusion of cardioplegia during cardiac arrest in surgery, retroperfusion of arterial blood in settings of myocardial infarction (synchronized retroperfusion), retroperfusion of pharmaceutical agents, and manipulations of venous blood drainage by pressure-controlled intermittent coronary sinus occlusion.

The present thesis aims to emphasize the beneficial traits of these coronary sinus interventions with the focus on pressure-controlled intermittent coronary sinus occlusion. Mathematical modeling of pressure-controlled intermittent coronary sinus occlusion in a phenomenological and in a mechanistic way are described to give insights of the treatment, as well as the clinical application of this coronary sinus intervention.

In phenomenological modeling, parameterized mathematical functions are fitted to systolic and diastolic coronary sinus pressure envelopes in order to characterize numerically specific parameters of shape of coronary sinus pressure rise.
Mechanistic modeling is achieved by coupled differential equations which describes flows, pressures and volume changes in a mechanical model which was developed to resemble the key features of the coronary circulation in the presence of coronary sinus interventions.

Clinical studies investigated the long-term effects of intermittent coronary sinus occlusion as an adjunct to reperfusion in acute myocardial infarction; the intracoronary hemodynamics effects of pressure-controlled intermittent coronary sinus occlusion; pressure-controlled intermittent coronary sinus occlusion in acute ST-segment elevation myocardial infarction and the safety and feasibility; preservation of left ventricular ejection fraction of early pressure-controlled intermittent coronary sinus occlusion in porcine acute myocardial infarction; the reduction of infarct size and functional recovery after ST-segment elevation myocardial infarction and finally the reduction of infarct size after primary percutaneous coronary intervention.

Results of the mathematical model show the impact of squeezing on phasic flows; forward, retrograde and mean flows, and the impact of squeezing on plateau and rise time of venous pressure. The left ascending coronary artery and left circumflex coronary artery asymmetry and the addition of collaterals were also taken into account, which influenced the arterial flow, capillary volume and the venous volume and pressure.

Clinical studies have shown that long term data showed significant differences in re-infarction, as well as in major adverse cardiovascular events; the successful catheter delivery and that coronary sinus occlusion lead to an increase in mean coronary sinus pressure and coronary sinus pulse pressure. Furthermore, results have shown that pressure-controlled intermittent coronary sinus occlusion is safe, although feasibilty was limited and that the

treatment could be maintained for about 90 minutes. Greater left ventricular ejection fraction, better wall thickening and trends towards smaller infarct size could be shown as well. Finally, results have shown that initiation of pressure-controlled intermittent coronary sinus occlusion in patients with acute myocardial infarction immediatley after flow restoration but before stenting was associated with evidence of reduced microvascular obstruction and infarct size, with improved left ventricular function, and that initation of pressure-controlled intermittent coronary sinus occlusion in patients with acute anterior myocardial infarction immediately after flow restoration but before stenting was associated with a 47% relative reduction in infarct size.

Kurzfassung

Laut der Weltgesundheitsorganisation (WHO) sind Herz-Kreislauf-Erkrankungen, global gesehen, die häufigste Todesursache, wobei die meisten Herz-Kreislauf-Erkrankungen vorgebeugt werden können, bei adressieren der Risikofaktoren wie Tabakkonsum, ungesunde Ernährung und Übergewicht, körperliche Inaktivität und gesundheitsschädlichem Alkoholkonsum.

Diese hohe Sterberate führt zu einem erhöhten Anspruch auf Diagnose und Therapie dieser Krankheiten. Eine von vielen bildgebenden Methoden ist die kardiale Magnetresonanztomographie und Koronarsinusinterventionen als Behandlung sind Methoden die temporär das ischemische Myokard über das koronare Venensystem schützen. Sie beinhalten die Retroinfusion bei Herzstillstand während eines Kreislaufstillstandes, die Retroperfusion des arteriellen Blutes bei einem Myokardinfarkt (synchronisierte Retroperfusion) und das Manipulieren des Abflusses des venösen Blutes mit dem druck-kontrollierten intermittierenden Koronarsinusverschluss.

Ziel dieser Arbeit ist es die vorteilhaften Merkmale dieser Koronarsinusinterventionen zu unterstreichen, mit dem Fokus auf den druck-kontrollierten intermittierenden Koronarsinusverschluss. Mathematische Modelle vom druck-kontrollierten intermittierenden Koronarsinusverschluss, phänomenologisch und mechanistisch betrachtet, geben Einsicht in diese Therapie, sowie die klinische Anwendungen werden hier beschrieben.

Im phänomenologischen Modell werden die parametrisierten mathematischen Funktionen, den Einhüllenden des systolischen und diastolischen Koronarsinusdruckes angepasst, um die numerisch spezifischen Parametern der Gestalt des Koronarsinus-Druckanstiegs zu charakterisieren.
Mechanistisches Modell wird erreicht durch gekoppelte Differentialgleichungen, welche die Flüsse, Drücke und Volumsänderungen in einem mechanischen Modell, welches entwickelt wurde um die Hauptmerkmale des Herz-Kreislaufes in Anwesenheit von Koronarsinusinterventionen zu ähneln.

Klinische Studien untersuchten die Langzeiteffekte des intermittierenden Koronarsinusverschlusses als Zusatz zur Reperfusion im akuten Myokardinfarkt; intrakoronare hämodynamische Effekte vom druck-kontrollierten intermittierenden Koronarsinusverschluss; druck-kontrollierten intermittierenden Koronarsinusverschluss im akuten ST-Hebungs-Myokardinfarkt und die Sicherheit und Durchführbarkeit; Aufrechterhaltung der linksventrikulären Ejektionsfraktion vom vorzeitigen druck-kontrollierten intermittierenden Koronarsinusverschluss im akuten Myokardinfarkt in Schweinen; die Reduzierung der Infarktgröße und der funktionalen Erholung nach einem ST-Hebungs-Myokardinfarkt und schlussendlich die Reduzierung der Infarktgröße nach primärer perkutaner koronaren Intervention.

Ergebnisse des mathematischen Modells zeigt den Einfluss des Druckes auf die phasischen Flüsse; vorwärts, retrograder und Durchschnittsflüsse und den Einfluss des Druckes auf das Plateau und die Anstiegszeit des venösen Druckes. Ebenfalls wurde die Asymmetry des Ramus interventricularis anterior und Ramus circumflexus, sowie das Hinzufügen weiterer Herzbegleitungen einkalkuliert, welche den arteriellen Fluss, kapillare Volumen und venöse Volumen und Druck beeinflussen.

Klinische Studien zeigten, dass die Langzeitdaten sowohl einen signifikanten Unterschied für Reinfarktion aufwiesen,

als auch für schwere kardiale Komplikationen; die erfolgreiche Katheterplatzierung und dass Koronarsinusverschluss zu einem steigenden Durchschnitt des Koronarsinusdruckes und Koronarsinuspulsdruckes führt. Des Weiteren zeigten die Resultate, dass druck-kontrollierten intermittierenden Koronarsinusverschluss sicher ist, obwohl die Durchführbarkeit limitiert war und dass die Behandlung für rund 90 Minuten aufrechterhalten werden konnte. Größere linksventrikuläre Ejektionsfraktion, bessere Wandverdickung und eine Tendenz in Richtung kleinere Infarktgröße konnten gezeigt werden. Abschließend zeigten die Resultate, dass die Initiierung vom druck-kontrollierten intermittierenden Koronarsinusverschluss in Patienten mit akuten Myokardinfarkt, sofort nach der Wiederherstellung des Flusses, aber vor Stentimplantation, mit einer reduzierten mikrovaskulären Obstruktion und Infarktgröße in Verbindung gebracht werden konnte und dass die Initiierung vom druck-kontrollierten intermittierenden Koronarsinusverschluss in Patienten mit akuten vorderen Myokardinfarkt, sofort nach der Wiederherstellung des Flusses, aber vor Stentimplantation, mit einer 47% relativen Reduzierung der Infarktgröße in Verbindung gebracht werden konnte.

Abbreviations

ACS	acute coronary syndromes
AMI	acute myocardial infarction
CABG	coronary artery bypass grafting
CK	creatine kinase
cMRI	cardiac magnetic resonance imaging
CS	coronary sinus
CSI	coronary sinus intervention
CSO	coronary sinus occlusion
CSP	coronary sinus pressure
CSR	coronary sinus release
ECG	Electrocardiogram
GCV	great cardiac vein
IS	infarct size
LAD	left anterior descending artery
LCA	left coronary artery
LCX	left circumflex artery
LMV	left marginal vein
LV	left ventricle
LVEF	left ventricular ejection fraction
LVP	left ventricular pressure
MACE	major adverse cardiovascular events
MI	myocardial infarction
MSI	myocardial salvage index
MVO	microvascular obstruction
NSTEMI	non-ST-elevation myocardial infarction
PICSO	pressure-controlled intermittent coronary sinus occlusion
pPCI	primary percutaneous coronary interventions
RA	right atrium
SRP	synchronized retroperfusion
STEMI	ST-elevation myocardial infarction
TIMI	thrombolysis in,myocardial infarction

Contents

1 Introduction **1**

2 Medical Background **3**

2.1 Anatomy and physiology . . . 3
2.2 Coronary arteries . . . 5
2.3 Microcirculation . . . 6
2.4 Hemodynamics . . . 6

3 Diagnosis **8**

3.1 Imaging techniques . . . 8
3.1.1 Echocardiography . . . 8
3.1.2 Computed Tomography . . . 8
3.1.3 Magnetic Resonance Imaging . . . 8
3.2 Electrocardiogram . . . 11
3.2.1 Electrocardiographic leads . . . 12
3.2.2 Electrocardiographic detection of myocardial infarction . . . 16

4 Pathologies **17**

4.1 Acute coronary syndromes . . . 18
4.1.1 Myocardial infarction . . . 18
4.1.2 ST-elevated Myocardial Infarction . . . 20

5 Therapy **21**

5.1 Reperfusion therapy . . . 21
5.1.1 Coronary sinus intervention . . . 22
5.1.2 Advantages and disadvantages . . . 30
5.2 Pros and cons of CSIs vs. conventional therapy . . . 32

6 Mathematical Modelling Of Coronary Sinus Interventions **33**

6.1 Introduction . . . 33
6.2 Phenomenological modeling . . . 34
6.2.1 Model applications . . . 34
6.2.2 Derived quantities for model 1 . . . 36
6.2.3 Derived quantities for model 2 . . . 36

6.3 Mechanistic modeling . . . 37
6.3.1 Coronary circulation during coronary sinus interventions . . . 38
6.3.2 Description of compartments . . . 38
6.3.3 Model equations . . . 40

7 PICSO in Myocardial Infarction 46

8 Material and Methods 49
8.1 Phenomenological modeling . . . 49
8.1.1 Testing the models with experimental and clinical data . . . 49
8.1.2 Interpretation of quantities derived from phenomenological modeling . . . 50
8.1.3 Modes of adaption . . . 50
8.1.4 Relationship between coronary sinus pressure and coronary artery flow . . . 51
8.1.5 Methods . . . 51
8.2 Mechanistic modeling . . . 53
8.2.1 Simulation of PICSO under normal conditions, global loss of contractility and reduced perfusion pressure . . . 53
8.2.2 Simulation of PICSO during LAD stenosis and infarction . . . 54
8.2.3 Assessment of model parameters . . . 55
8.2.4 Modifications of Schreiner model for model Oswald . . . 57
8.3 Study oversight . . . 58
8.4 Patient population . . . 58
8.5 Study procedures . . . 60
8.6 Data analysis . . . 61
8.7 Endpoints and definitions . . . 62
8.8 Statistical methods . . . 62
8.9 Optimization of PICSO therapy . . . 63

9 Results 65
9.1 Phenomenological modeling . . . 65
9.2 Mechanistic modeling . . . 66
9.2.1 Overview of the model parameters . . . 66
9.2.2 Schreiner Model . . . 66
9.2.3 Comparison of experiment-model Oswald . . . 71
9.2.4 Model Kajgana . . . 72
9.3 Effects of PICSO in myocardial infarction . . . 75
9.3.1 Myocardial protection via the coronary sinus . . . 75
9.3.2 Intracoronary hemodynamic effects of PICSO . . . 77
9.3.3 Safety and feasibility . . . 80
9.3.4 From myocardial salvage to tissue regeneration . . . 82
9.3.5 Early PICSO preserves LVEF in porcine acute myocardial infarction . . . 84
9.3.6 Infarct size reduction and results in functional recovery . . . 84
9.3.7 Infarct size reduction after pPCI . . . 84

10 Discussion/Conclusion **85**
10.1 Phenomenological modeling 85
10.2 Mechanistic modeling 86
10.2.1 Further concepts 86
10.2.2 Discussion 86
10.2.3 Conclusion 90
10.3 PICSO in myocardial infarction 91
10.3.1 Myocardial protection via the coronary sinus 91
10.3.2 Intracoronary hemodynamic effects 94
10.3.3 Safety and feasibility study 95
10.3.4 Future developments 97
10.3.5 Conclusion 97
10.4 Coronary Sinus Intervention 98

Bibliography **99**

Chapter 1

Introduction

The World Health Organization, WHO (2017) stated that cardiovascular diseases (CVDs) are the number 1 cause of death globally: more people die annually from CVDs than from any other cause. An estimated 17.7 million people died from CVDs in 2015, representing 31% of all global deaths. Of these deaths, an estimated 7.4 million were due to coronary heart disease and 6.7 million were due to stroke. Most cardiovascular diseases can be prevented by addressing behavioral risk factors such as tobacco use, unhealthy diet and obesity, physical inactivity and harmful use of alcohol using population-wide strategies. People with cardiovascular disease or who are at high cardiovascular risk (due to the presence of one or more risk factors such as hypertension, diabetes, hyperlipidaemia or already established disease) need early detection and management using counselling and medicines, as appropriate.

The high death rate leads to an increased demand of diagnosis and treatment of these diseases. Myocardial perfusion diagnosis has turned out as a promising tool. This method of diagnosis allows to identify ischemic areas of the myocardium. Several imaging methods will be introduced, with the main focus on magnetic resonance imaging (MRI).

Mohl *et al.* (2015) found that in recent years, the demographics of patients admitted for coronary interventions and revascularization procedures have changed, and there is an increasing need for complex high-risk interventional procedures (CHIP). Despite the development of sophisticated reperfusion strategies and the availability of logistic treatment networks for acute coronary syndromes (ACS), the management of obstructed myocardial microcirculation and subsequent myocardial deterioration remains challenging. Furthermore, there are large variations in reperfusion treatment across Europe; a substantial number of ST-elevation myocardial infarction (STEMI) patients in Eastern and Southern Europe are not receiving any reperfusion therapy. Although mortality from acute events has decreased, therapies to prevent or attenuate post-infarction left ventricular remodeling have changed little, leaving an increasing cohort of patients at risk of severe heart failure. Current routine therapies in ACS focus on the ischemic/reperfused microcirculation and on structural regeneration.
Despite timely reperfusion, molecular, biochemical and immunological changes of the former deprived microcirculation persist, as well as areas of structural obstruction, particularly in the post capillary venules. Therefore there is a need for methods to further reduce microcirculatory obstruction, an important prognostic factor for morbidity, mortality and quality of life. In addition to restoring the microcirculation, cardioprotection and structural regenera-

tion remain important in the treatment of ACS.

Faxon (2015) reported that coronary revascularization can salvage ischemic myocardium, relieve symptoms, and prolong life in patients with high-risk acute coronary syndrome and in patients with severe coronary artery disease. It is no wonder that coronary artery bypass surgery and percutaneous coronary interventions (PCI) were performed on nearly 900 000 patients in the United States in 2010. Despite the advances with both revascularization techniques, there are many situations where improvement is still needed. For instance, myocardial salvage in ST-segment-elevation myocardial infarction with primary PCI averages only 40% to 50% of the area at risk despite timely reperfusion and many patients with multivessel disease continue to have severe angina and ischemia because of anatomy that is not amenable to revascularization. As many as 7% or 1.8 million individuals are estimated to be unrevascularizable and the treatment options for these patients are limited and often unsuccessful. Several articles have been published suggesting that retrograde perfusion via the coronary sinus may have promise as a treatment option for these patients.

In the following chapters, the general principle of coronary sinus interventions will be introduced with the main focus on the reperfusion technique pressure-controlled intermittent coronary sinus occlusion (PICSO) as a mathematical and a clinical approach with their corresponding results.

Chapter 2

Medical Background

2.1 Anatomy and physiology

The heart has two valved muscular pumps which are combined in a single organ. Each pump, the right and the left heart, is physiologically separated. There are four cardiac chambers, where the two atria receive venous blood as weakly contractile reservoirs for final filling of the two ventricles, which then provide the contraction that forces blood into the main arterial trunks. The right heart starts at the right atrium and receives venous blood from the superior and inferior vena cava and from the main venous inflow from the heart itself via the coronary sinus. The left heart starts at the left atrium and receives oxygenated blood from all the pulmonary inflow and some of the coronary venous inflow [Standring (2008)].

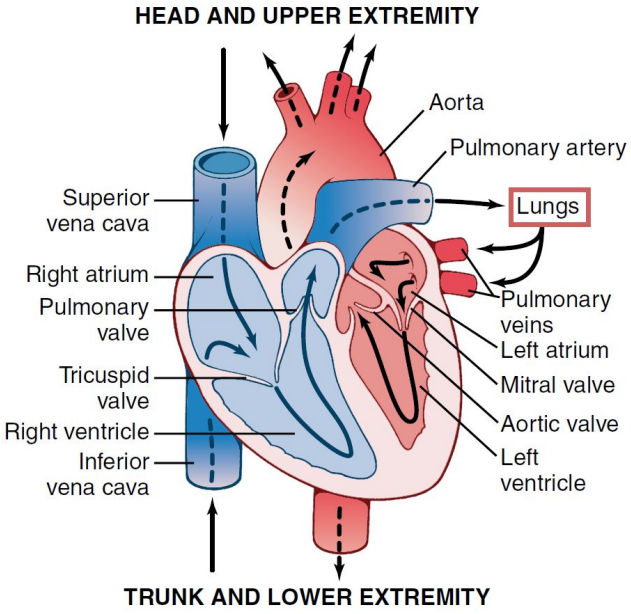

Figure 2.1: Illustration of the structure of the heart and the course of the blood flow through the heart chambers and heart valves [Hall *et al.* (2011)].

The cardiac cycle is a cardiac event that occurs from the beginning of one heartbeat to the beginning of the next

one. Each cycle is initiated by spontaneous generations of an action potential in the sinus node. This node is located in the superior lateral wall of the right atrium near the opening of the superior vena cava and the action potential travels from here rapidly through both atria and then through the atrio-ventricular (A-V) bundle into the ventricles [Hall *et al.* (2011)]. The nodes and networks constitute the cardiac conductions system. Its components are the sinus-atrial and the A-V nodes, the A-V bundle and the Purkinje fibres. Within this conductions system, the main pacemaker rhythm of the heart is generated and is influenced by nerves and is transmitted form atria to ventricles and then within the ventricles to all their musculature. Different parts of the ventricles are excited at slightly different time as illustrated in Figure 2.2 [Standring (2008)].

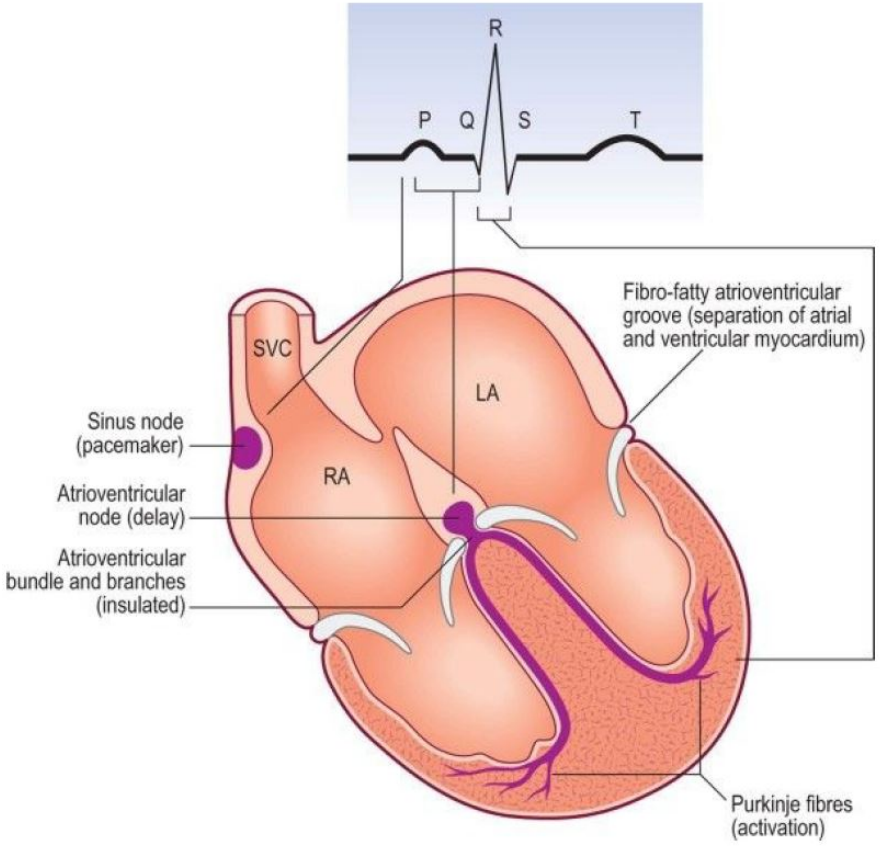

Figure 2.2: Illustration of the basic structure of the conduction system and its relationship with the electrocardiogram ECG. Note: right atrium (RA), left atrium (LA), superior vena cava (SCV) [Standring (2008)].

The cardiac cycle consists of two periods, namely the diastole and the systole. Diastole is the period of relaxation where the heart is filled with blood and systole is the period of contraction. The Figure 2.3 shows the different events that occur during a cardiac cycle for the left side of the heart. Pressure changes in the aorta, left ventricle and left atrium are shown at the top. Below are the changes in left ventricular volume, the electrocardiogram and the phonocardiogram, where the latter is recording the sounds produced by the heart [Hall *et al.* (2011)].
The ECG from the Figure 2.3 shows the P, Q, R, S and T waves which are electrical voltages that are generated by the heart and recorded by the electrocardiograph. The spread of depolarization through the atria causes the P wave, which is followed by atrial contraction. Shortly after, the QRS waves appear as a result of electrical depolarization of the ventricles, which causes its contraction and the rising of the ventricular pressure. The QRS

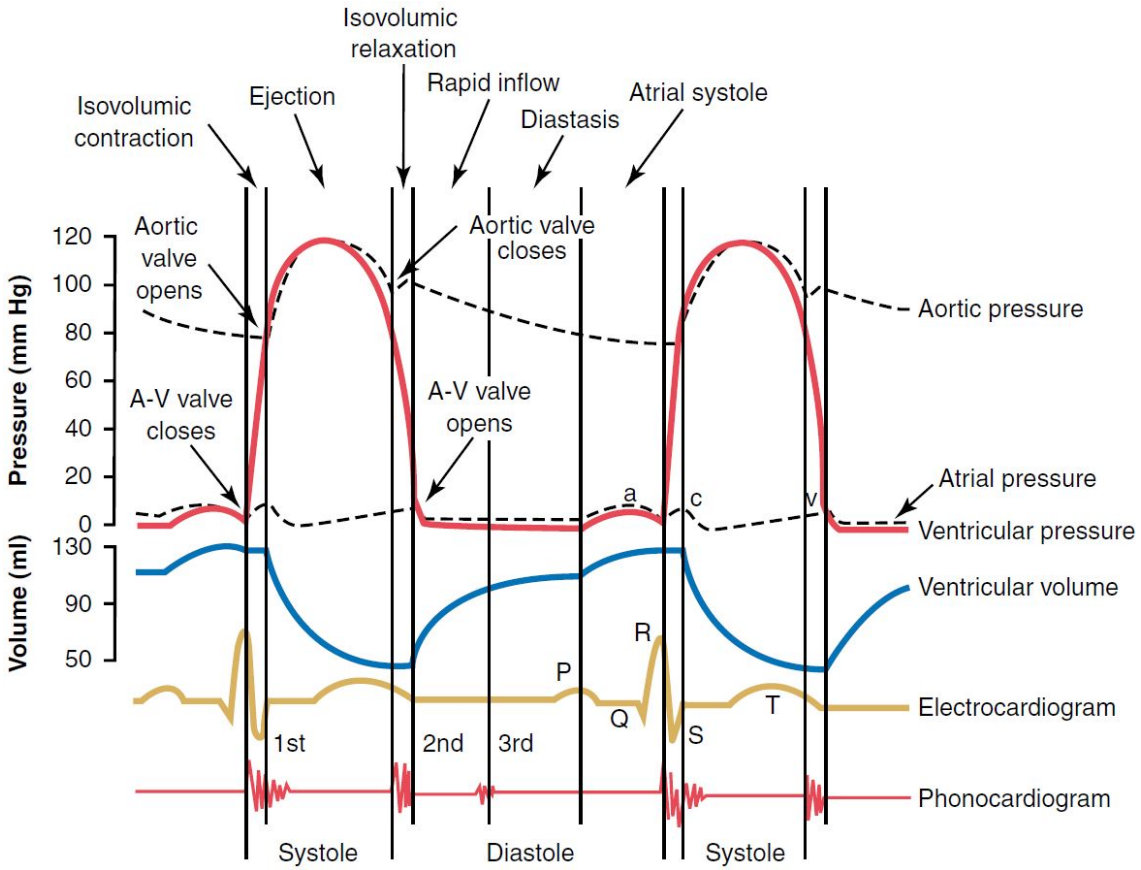

Figure 2.3: Illustration of the structure of the heart and the course of the blood flow through the heart chambers and heart valves [Hall *et al.* (2011)].

complex begins slightly before the systole. The T wave represents the stage of repolarization of the ventricles, i.e. the relaxation period and begins slightly before the end of contraction.
Normal filling of the ventricles that increases the volume of each ventricle to about 110 to 120 ml during diastole is called end-diastolic volume. The volume decreases then to about 70 ml during the systole, which is called the stroke volume output and the remaining volume in each ventricles of about 40 to 50 ml is called end-systolic volume. Ejection fraction is the fraction of the end-diastolic volume that is ejected [Hall *et al.* (2011)].

2.2 Coronary arteries

The main coronary arteries lie on the surface of the heart and smaller arteries penetrate the surface into the cardiac muscle mass. The heart receives its nutritive blood supply almost entirely through this arteries. The left coronary artery supplies mainly the anterior and left lateral portions of the left ventricle, whereas the right coronary artery supplies most of the right ventricle, as well as the posterior part of the left ventricle in 80 to 90 percent of people [Hall *et al.* (2011)].
Most of the coronary venous blood flow from the left ventricular muscle returns to the right atrium of the heart via the coronary sinus, which is about 75 percent of the total coronary blood flow [Hall *et al.* (2011)].

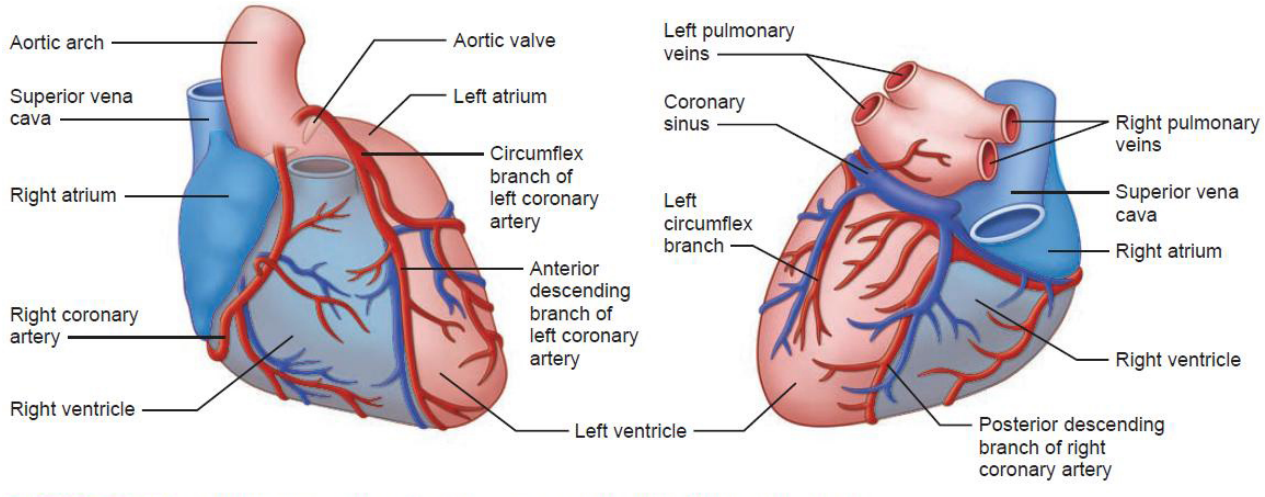

Figure 2.4: Anterior and posterior view of the coronary arteries and veins [Porth *et al.* (2009)].

Habib *et al.* (2009) stated that in providing access for different cardiac procedures, the coronary sinus has become important. The coronary venous systems is important in many electrophysiological procedures, including arrhythmia ablation, biventricular pacing, and for deployment of an array of cardiac devices.

2.3 Microcirculation

Pries *et al.* (2008) found that the need for adequate exchange of materials between blood and tissue, and particularly for oxygen delivery, is met by large numbers of closely spaced microvessels with small diameters and large cumulative surface area, interconnected in intricate network structures. Microvascular network is a system of conduits that distributes blood throughout tissues as needed. The distribution of flow and pressure can be analyzed by analogy to the distribution of current and voltage in a network of electrical resistances. The flow resistance of each segment depends on the segment geometry according to the Poiseuille relationship. The topological structure of microvascular networks is heterogeneous. The biophysical processes that govern distribution of blood flow within a microvascular network of given geometry have been studied for decades and, while areas of uncertainty remain, it may be claimed that a good overall level of understanding has been achieved. Much remains to be learned, however, about the active biological processes that control network geometry, including angiogenesis, structural adaptation, and control of vascular tone. The study of blood flow in microvascular networks thus represents a key step in the process of translating advances in molecular and cellular biology into improved understanding of cardiovascular function in health and disease. Also discussion of the relationship of network structure and flow to physiological aspects of the microvasculature including transport functions, inflammatory and immune functions, regulation of blood flow, and structural adaptation were presented.

2.4 Hemodynamics

Faber *et al.* (2017) stated that hemodynamics is concerned with the mechanical and physiologic properties controlling blood pressure and flow through the body. Kinetic energy is negligible compared to blood pressure at normal

cardiac output (CO) and thus blood flow is estimated using the pressure gradient and resistance. The primary parameter used in clinical medicine to describe blood flow through the systemic circulation is CO, which is the total volume of blood pumped by the ventricle per minute. To compare CO among individuals of different sizes, the cardiac index (CI) is used. The Frank-Starling law helps the heart match CO to venous return. While changes in venous return cause a ventricle to move along a single Frank-Starling curve, changes in contractility and afterload cause the heart to shift to a different Frank-Starling curve.

And McLaughin *et al.* (2017) stated that for the purpose of understanding clinical applications of physiologic testing of coronary blood flow, the intermediate and distal compartments can be lumped together, creating a two-component model. Coronary blood flow can increase two- to fivefold in the normal heart. In one study of adult patients with angiographically normal vessels and coronary artery disease risk factors, coronary blood flow increased by 2.7 $\pm$ 0.6 times with maximal coronary vasodilation. The ratio of maximal coronary flow to resting coronary blood flow is labeled coronary flow reserve (CFR). Coronary blood flow is primarily controlled by release of local metabolites such as adenosine or nitric oxide. There are several ways to measure coronary blood flow directly, but these are generally difficult, time consuming, and unable to measure rapid changes in coronary flow. More commonly, angioplasty wires with Doppler probes or pressure transducers are used to make clinical decisions and to study coronary physiology.

Chapter 3

Diagnosis

3.1 Imaging techniques

Thygesen *et al.* (2012) stated that non-invasive imaging plays many roles in patients with known or suspected myocardial infarction (MI) and therefore is important in the diagnosis and characterization of MI. The regional myocardial hypoperfusion and ischemia lead to several of events, including myocardial dysfunction, cell death and healing by fibrosis. Important imaging parameters are therefore perfusion, myocyte viability, myocardial thickness, thickening and motion and the effects of fibrosis on the kinetics of paramagnetic or radioopaque contrast agents. Commonly used imaging techniques in acute and chronic infarction are echocardiography, radionuclide ventriculography, myocardial perfusion scintigraphy (MPS) using single photon emission computed tomography (SPECT), and magnetic resonance imaging (MRI). Positron emission tomography (PET) and X-ray computed tomography (CT) are less common.

3.1.1 Echocardiography

The strength of echocardiography is the assessment of cardiac structure and function, in particular myocardial thickness, thickening and motion. Echocardiographic contrast agents can improve visualization of the endocardial border and can be used to assess myocardial perfusion and microvascular obstruction [Thygesen *et al.* (2012)].

3.1.2 Computed Tomography

Infarcted myocardium is initially visible as a focal area of decreased left ventricle (LV) enhancement, but later imaging shows hyper-enhancement, as with late gadolinium imaging by MRI. This finding is clinically relevant because contrast-enhanced CT may be performed for suspected pulmonary embolism and aortic dissection- conditions with clinical features that overlap with those of acute MI -but the technique is not used routinely. Similarly, CT assessment of myocardial perfusion is technically feasible but not yet fully validated [Thygesen *et al.* (2012)].

3.1.3 Magnetic Resonance Imaging

Grover *et al.* (2015) stated that the development of magnetic resonance imaging (MRI) for use in medical investigation has provided a huge forward leap in the field of diagnosis, particularly with avoidance of exposure to

potentially dangerous ionizing radiation.

The high tissue contrast of cardiovascular MRI provides an accurate assessment of myocardial function and it has similar capability to echocardiography in suspected acute MI. Paramagnetic contrast agents can be used to assess myocardial perfusion and the increase in extracellular space that is associated with the fibrosis of prior MI. These techniques have been used in the setting of acute MI and imaging of myocardial fibrosis by delayed contrast enhancement is able to detect even small areas of subendocardial MI. It is also of value in detecting myocardial disease states that can mimic MI, such as myocarditis [Thygesen *et al.* (2012)].

Moser *et al.* (2009) defined the MRI system as followed: The useable field-of-view (FOV) of an MRI system, in general, is defined by three hardware groups and their related parameters:

- the main magnet with its homogeneity over the imaging volume;
- the gradient system with its linearity over the imaging volume; and
- the radiofrequency (RF) system with its signal homogeneity and signal sensitivity over the active imaging volume.

Typically, a superconducting magnet provides the high magnetic field strength for producing a strong tissue magnetization and, thus, a basis for high signal-to-noise ratios (SNR). The gradient system plays an important role in signal localization: it must be strong enough to switch the highest possible gradient amplitudes in the shortest possible time to enable rapid data acquisition. The RF system is charged with receiving the weak MR signal with the very minimum of loss.

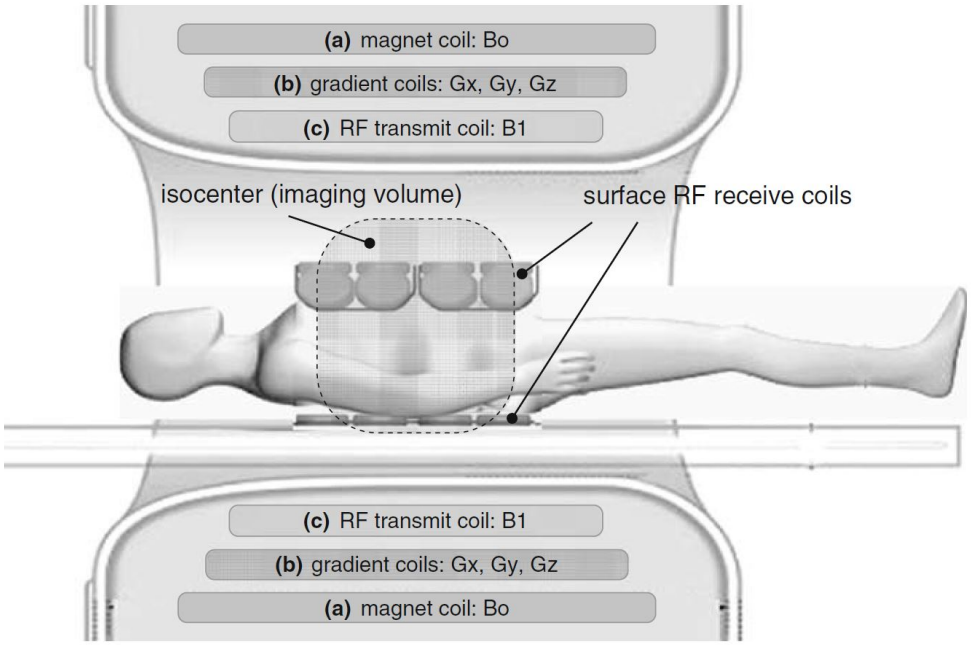

Figure 3.1: Scheme of a MRI system. (a) magnet coil to produce the homogeneous static magnetic field (B0) for spin alignment; (b) gradient coils to produce the time-varying gradient fields (Gx, Gy and Gz) for spatial encoding of the MR signals, and (c) transmitter radiofrequency (RF) coil to generate an RF field (B1) for spin excitation. The MR signal response from the excited spins within the subject is detected by a set of receive-only surface RF coils placed above and below the image volume [Moser *et al.* (2009)].

Furthermore, Ginat *et al.* (2011) stated that cardiac MRI is indicated for evaluating a wide variety of congenital and acquired heart diseases, including cardiac masses, myocardial ischemia or infarction, cardiomyopathies, valvular disease, coronary artery disease, pericardial disease, and complex congenital anomalies. However, the main limitation of cardiac MRI compared with CT is the evaluation of coronary calcifications.
There are certain technical challenges unique to cardiac MRI. Most notably is the rapid and complex motion of the heart and pulsatility of the great vessels due to normal contractility. Nevertheless, these issues are generally mitigated by implementation of ECG (cardiac) gating; navigator echo respiratory gating; breath-hold techniques; rapid, high-performance gradients; improved field homogeneity; and advanced pulse sequences.

3.1.3.1 Imaging planes

The body (scanner) planes and the cardiac planes are the two main coordinate systems that are used for cardiac MRI [Ginat *et al.* (2011)].

3.1.3.2 Body planes

Body planes are oriented orthogonal to the long axis of the body and consist of axial, sagittal and coronal planes, which are used to provide a qualitative overview of cardiac morphology. The axial plane can show the four chambers of the heart and the pericardium simultaneously, the sagittal plane the great vessels arising in continuity from the ventricles and the coronal plane can be used to assess the left ventricular outflow tract, the left atrium, and the pulmonary veins [Ginat *et al.* (2011)].

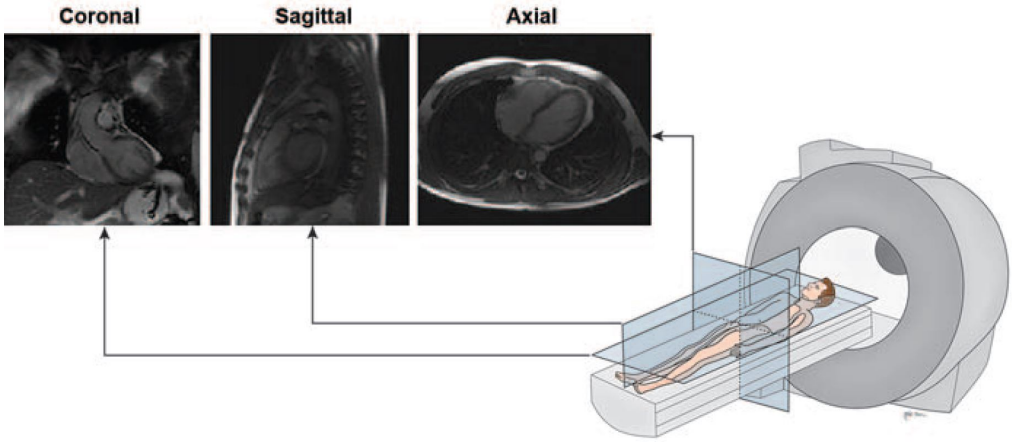

Figure 3.2: Illustration of major body planes with respect to patient and their corresponding appearance on bright blood imaging sequences, where latter describes the high signal intensity of fast-flowing blood and is typically used to evaluate cardiac function [Ginat *et al.* (2011)].

3.1.3.3 Cardiac planes

Accurate anatomic and functional characterization of the walls of the heart can be obtained from the specialized cardiac planes. The standard cardiac planes include short axis, horizontal long axis (four-chamber view), and vertical long axis (two-chamber view) [Ginat *et al.* (2011)].

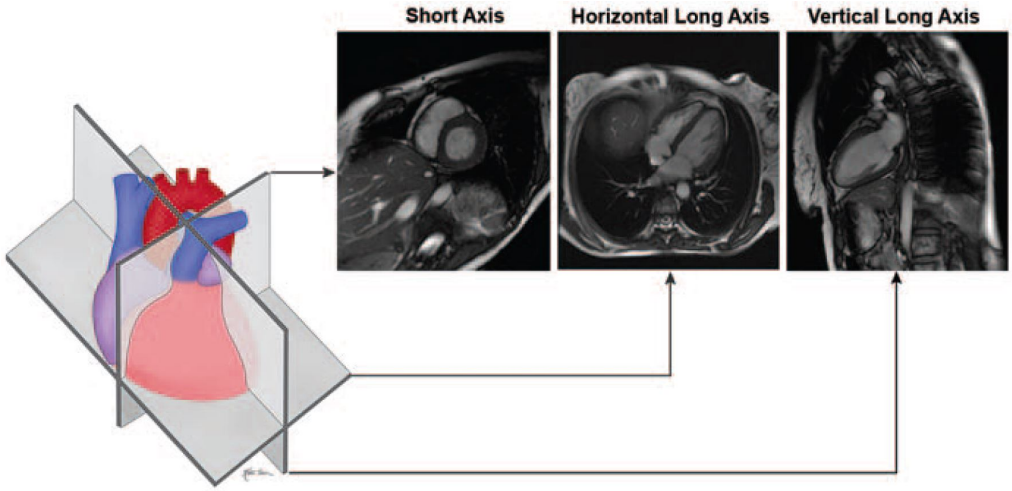

Figure 3.3: Illustration of major cardiac planes with respect to heart and their corresponding appearance on bright blood sequences [Ginat *et al.* (2011)].

3.2 Electrocardiogram

Electrical current spreads from the heart into the adjacent tissues that are surrounding the heart when the cardiac impulse passes through the heart. A small part of the electrical current spreads to the surface of the body. Therefore, the electrical current can be recorded by placing electrodes on the skin on opposite sides of the heart, which is then known as electrocardiogram. A normal one for two beats of the heart is shown in Figure 3.4 [Hall *et al.* (2011)].

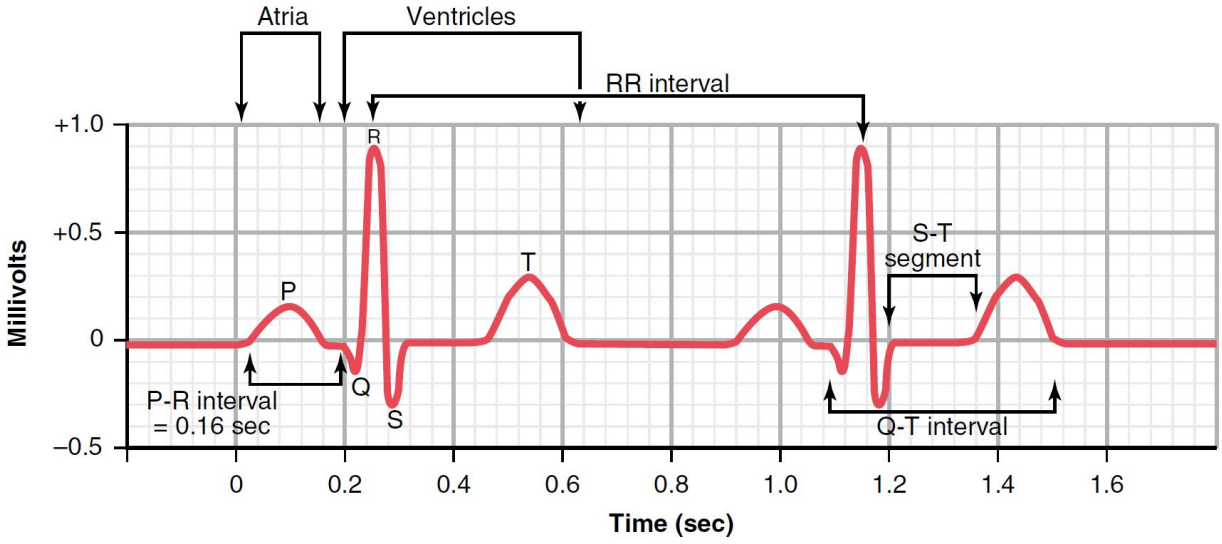

Figure 3.4: Normal electrocardiogram [Hall *et al.* (2011)].

3.2.1 Electrocardiographic leads

In the following sections, several electrode placements are introduced, whereas the 12-lead ECG is referred as standard ECG.

3.2.1.1 12-Lead ECG

Burghart (2011) described the standard ECG as followed. The 12-lead ECG records the heart's electrical activity using a series of electrodes placed on the patient's extremities and chest wall. The 12 leads include three bipolar limb leads (I, II, and III), three unipolar augmented limb leads (a_{VR}, a_{VL}, and a_{VF}), and six unipolar precordial, or chest, leads (V1, V2, V3, V4, V5, and V6). These leads provide 12 different views of the heart's electrical activity. A 12-lead ECG is usually performed on patients having a myocardial infarction. It may also be ordered for patients with other conditions that affect the heart, including:

- angina
- arrhythmias
- heart chamber enlargement
- digoxin or other drug toxicity
- electrolyte imbalances
- pulmonary embolism
- pericarditis
- hypothermia.

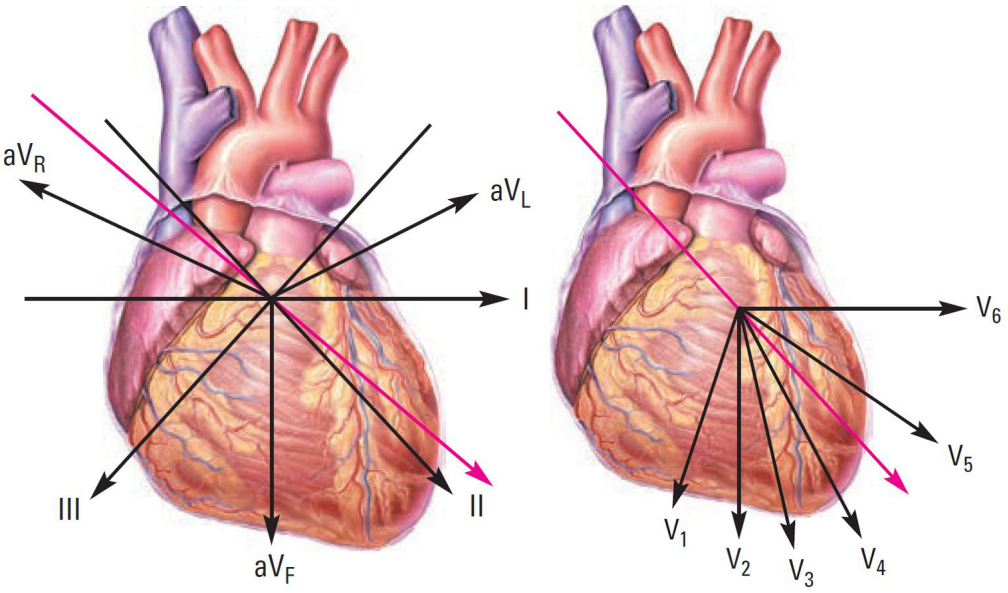

Figure 3.5: These illustrations show the direction of each lead relative to the wave of depolarization (shown in color) [Burghart (2011)].

Each of the 12 leads views the heart from a different angle.

Standard limb leads (bipolar)		**Augmented limb leads (unipolar)**	
Leads	View of the heart	Leads	View of the heart
I	Lateral wall	aVR	No specific view
II	Inferior wall	aVL	Lateral wall
III	Inferior wall	aVF	Inferior wall
Precordial, or chest, leads (unipolar)			
Leads	View of the heart	Leads	View of the heart
V1	Septal wall	V4	Anterior wall
V2	Septal wall	V5	Lateral wall
V3	Anterior wall	V6	Lateral wall

Table 3.1: List of the 12 views of the heart [Burghart (2011)].

The following illustrations (Fig.3.7 - Fig.3.8) show the electrode placements for recording the electrocardiogram for the six limb leads and the precordial leads to provide a complete view of the heart. Placing the bipolar and unipolar limb leads: electrodes on both arms and the left leg, ground on right leg.

- V1: Over fourth intercostal space at the right sternal border.
- V2: Over fourth intercostal space at the left sternal border.
- V3: Midway between leads V2 and V4.
- V4: Over fifth intercostal space at left midclavicular line.
- V5: Over fifth intercostal space at left anterior axillary line.
- V6: Over fifth intercostal space at left midaxillary line.

Note: right arm (RA), left arm (LA), right leg (RL) and left leg (LL). The plus sign (+) indicates the positive pole, the minus sign (-) indicates the negative pole, and G indicates the ground.

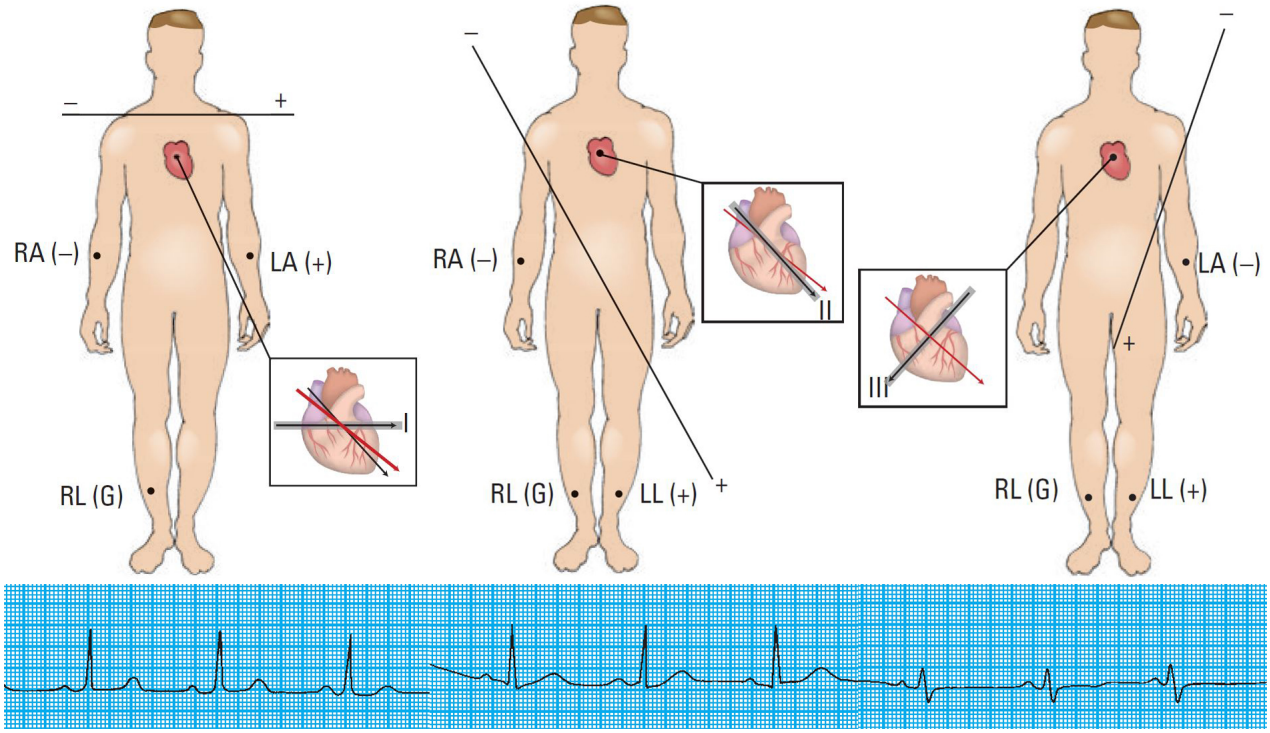

Figure 3.6: Lead I: This lead connects the right arm (negative pole) with the left arm (positive pole). Lead II:. This lead connects the right arm (negative pole) with the left leg (positive pole). Lead III: This lead connects the left arm (negative pole) with the left leg (positive pole) [Burghart (2011)].

Next to 12 Leads, there are also Three Bipolar Limb Leads, Chest Leads (Precordial Leads) and Augmented Unipolar Limb Leads.

3.2.1.2 Three bipolar limb leads

The term "bipolar" means that the electrocardiogram is recorded from two electrodes located on different sides of the heart, e.g. on the limbs. Thus, a "lead" is not a single wire connecting from the body but a combination of two wires and their electrodes to make a complete circuit between the body and the electrocardiograph [Hall *et al.* (2011)].

3.2.1.3 Chest leads (precordial leads)

Often electrocardiograms are recorded with one electrode placed on the anterior surface of the chest directly over the heart. This electrode is connected to the positive terminal of the electrocardiograph, and the negative electrode, called the indifferent electrode, is connected through equal electrical resistances to the right arm, left arm, and left leg all at the same time. Usually six standard chest leads are recorded, one at a time, from the anterior chest wall, the chest electrode being placed sequentially at the six points [Hall *et al.* (2011)].

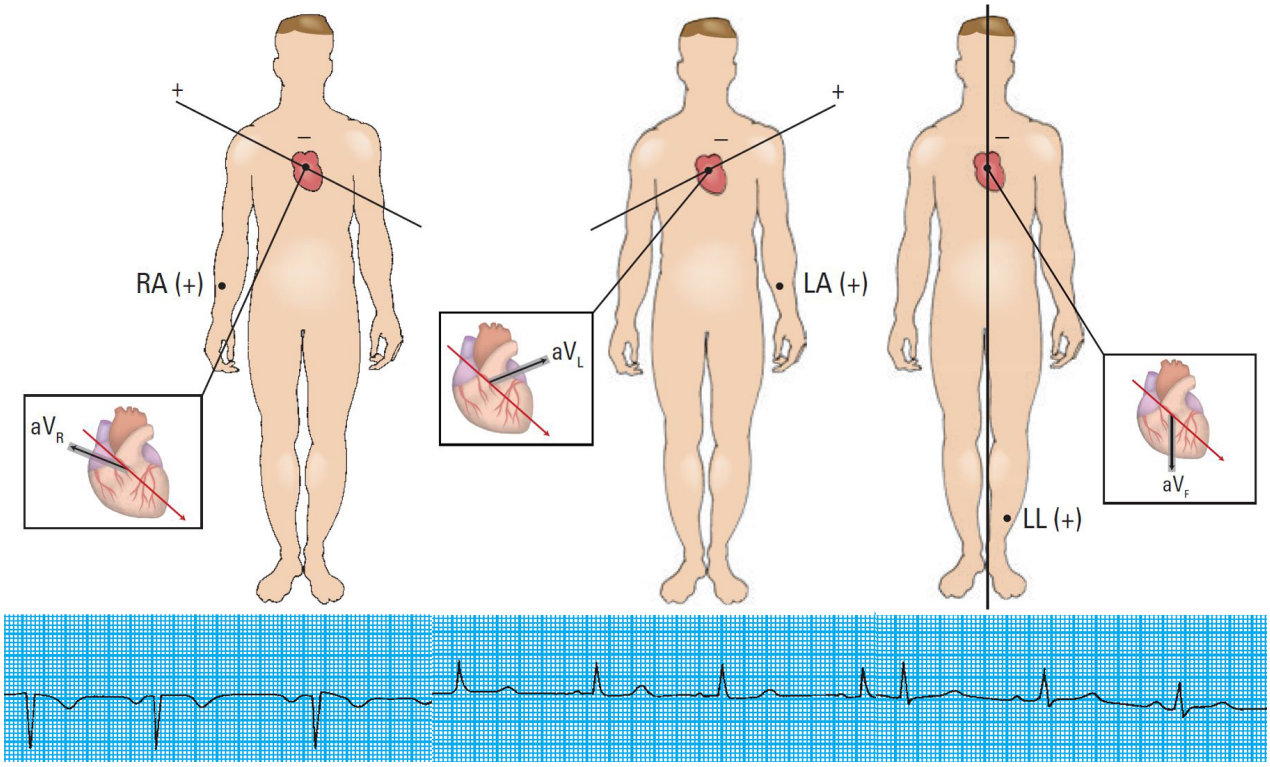

Figure 3.7: Lead a_{VR}: This lead connects the right arm (positive pole) with the heart (negative pole). Lead a_{VL}: This lead connects the left arm (positive pole) with the heart (negative pole). Lead a_{VF}: This lead connects the left leg (positive pole) with the heart (negative pole) [Burghart (2011)].

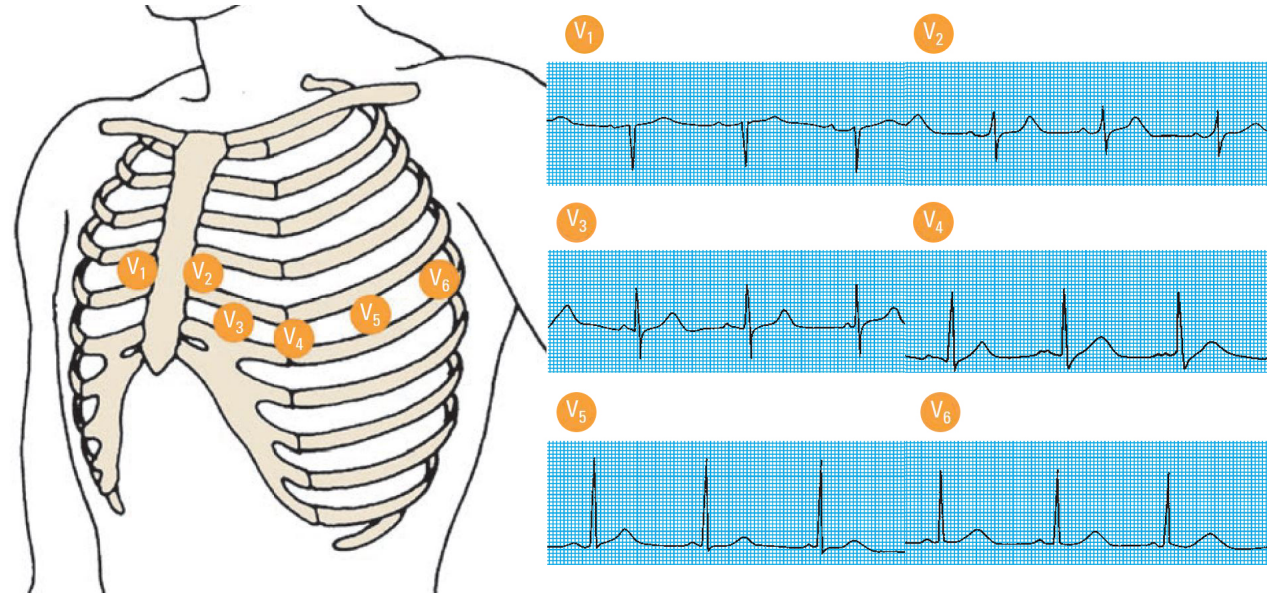

Figure 3.8: Placement of the precordial electrodes [Burghart (2011)].

3.2.1.4 Augmented unipolar limb leads

Another system of leads in wide use is the augmented unipolar limb lead. In this type of recording, two of the limbs are connected through electrical resistances to the negative terminal of the electrocardiograph, and the third limb

is connected to the positive terminal [Hall *et al.* (2011)].

3.2.2 Electrocardiographic detection of myocardial infarction

Trägårdh *et al.* (2007) found that one study of the Lund University Hospital suggests that electrocardiographic diagnosis of acute myocardial infarction should be improved. This might be done either by regarding all 24 aspects (both positive and negative leads), or a subset hereof (for example 19-lead ECG), of the conventional 12-lead ECG or by using additional electrodes. The purpose of the study was to investigate the accuracy of the different ECG methods in diagnosing acute ST-elevation MI.

Therefore 479 patients were admitted with acute chest pain. One conventional ECG plus leads V4R, V5R, V8, and V9 were recorded for each patient within 24 hours of admittance. The gold standard, namely biochemical markers were used for diagnosis of MI. ST-segment elevations in the 12-lead, 16-lead, and 24-lead postadmission ECGs as well as in the 12-lead, 19-lead and 24-lead admission ECGs were measured.

The result of this study was that the sensitivity for detecting acute MI was 28% for the postadmission 12-lead ECG, 33% for the 16-lead ECG, and 37% for the 24-lead ECG. The specificities were 97%, 93%, and 95%, respectively. For admission ECGs, the sensitivity was 33% for the 12-lead ECG, 45% for the 19-lead ECG and 49% for the 24-lead ECG, with specificities of 97%, 96%, and 94%, respectively.

The authors concluded that sensitivity for detecting acute MI was higher for the 16-, 19- and 24-lead ECGs than for the conventional 12-lead ECGs. However, their specifity was slightly slower. The 24-lead or 19-lead should be used if an increased sensitivity for detecting MI is desired, since no additional electrodes are required.

Chapter 4

Pathologies

Xu *et al.* (2016) described that large vessel arterial disease may be regarded as atherosclerotic or nonatherosclerotic. Nonatherosclerotic includes less common diseases related to known genetic abnormalities, degenerative conditions, and specific immune and infectious processes. Atherosclerosis is a chronic vascular disease initially involving the intima of elastic and larger muscular arteries, which is characterized by the presence of fibroinflammatory lipid plaques (atheromas). A function of the interplay between an individual's genetic disposition, environmental exposure, and living habits adopted by the individual is termed atherogenesis. The pathogenesis is complex, multifactorial and the relative importance of specific genetic and external factors vary among individuals. Growth of a plaque is a chronic dynamic inflammatory process, where the most serious acute events are plaque rupture and atherosclerotic aneurysm rupture. Thrombosis is associated with plaque growth, lumen occlusion, and plaque rupture. Complicated plaques may become destabilized and lead to plaque rupture and occlusive thrombosis. Organs with atherosclerosis in the supply arteries develop clinical disease, including ischemic heart disease, stroke, and peripheral vascular disease.
Risk factors are

- Hypertension
- Blood cholesterol level
- Diabetes mellitus
- Cigarette smoking
- Physical inactivity
- Obesity
- Alcohol consumption
- Stressful life pattern
- Increasing age
- Gender
- Family history

The number one killer of both men and women in industrialized countries is atherosclerotic cardiovascular disease. Occlusion of the arteries of the heart, in particular the coronary arteries, leads to myocardial ischemia, which

consequently leads to an imbalance between oxygen supply and demand in the heart muscle. If the ischemia is of sufficient severity and duration, death of myocardium, myocardial infarction (MI), occurs. This can lead to failure of the heart as a pump, or to electrical system failure leading to arrhythmias and sudden death. Other complications in individuals who survive, include aneurysms, ruptures, and/or valvular dysfunction of the heart. Reperfusion of the ischemic muscle is the only effective early treatment to date.
Fishbein *et al.* (2016) showed that impaired interaction between the coronary circulation and the myocardium can result in a spectrum of clinical disease, including typical angina pectoris, unstable angina pectoris, AMI, sudden cardiac death, and chronic ischemic heart disease (see table 4.1).

4.1 Acute coronary syndromes

Acute coronary syndromes is a term that Amsterdam *et al.* (2014) refers to a spectrum of conditions similar with acute myocardial ischemia and/or infarction that are due to an abrupt reduction in coronary blood flow. Kumar *et al.* (2009) also refers to unstable angina (UA), non-ST-segment elevation myocardial infection (NSTEMI) and ST-segment elevation myocardial infection (STEMI). And Thygesen *et al.* (2012) that many patients with MI develop Q waves (Q wave MI), but others do not (non-Q MI).

4.1.1 Myocardial infarction

Fishbein *et al.* (2016) defined ischemic myocardial injury by the changes that occur in the heart muscle as a result of an imbalance in oxygen and substrate supply and demand. Dependent on the severity and duration of the ischemic insult are the degree, time course, and type of injury. When ischemia is of sufficient duration and magnitude, such that compensation of flow does not prevent irreversible ischemic injury, myocardial necrosis, i.e., infarction occurs. The clinical disease that results from the imbalance in myocardial perfusion is often defined as coronary artery disease (CAD) or coronary heart disease because coronary artery lesions typically are implicated in the clinical manifestations. However, from a pathophysiological viewpoint, the condition is best designated as ischemic heart disease.
Acute MI (AMI) is classified based on the presence or absence of ST-segment elevation on the electrocardiogram (ECG): unstable angina/non-ST-elevation myocardial infarction (NSTEMI) and evolving ST-elevation myocardial infarction (STEMI). Rupture or erosion of an atherosclerotic plaque with superimposed thrombosis is the most common cause of AMI. The less common causes include vasospasm, vasculitis, myocardial bridging and thromboembolism associated with a variety of disorders.
Hall *et al.* (2011) stated: Blood flow stops in the coronary vessels beyond the occlusion after an acute coronary occlusion. The area of muscle that has either zero flow or so little flow that it cannot be supplied with nutritive blood is then called infarcted. The overall process is call myocardial infarction. Within a few hours of almost no blood supply, the cardiac muscle cells die.

Coronary arteries	Myocardium
Moderate coronary atherosclerosis	Adequate perfusion and function
Focal severe coronary atherosclerosis with >75% narrowing (cross sectional area) of one or more coronary arteries	Intermittent regional ischemia and contractile dysfunction
Coronary plaque(s) with acute alterations	Sustained regional ischemia and contractile dysfunction
Severe coronary atherosclerosis, often with coronary plaque(s) with acute alterations	Ischemic myocardium with ectopic electrical activity
Coronary plaque(s) with variable acute alterations	Irreversible injury and necrosis of ischemic myocardium limited to inner $\frac{1}{2}$ of LV wall
Coronary plaque(s) with acute alterations	Irreversible injury and necrosis of ischemic myocardial extending from subendocardium into subepicardium of LV
Severe coronary atherosclerosis	Variable myocardial functional impairment

Mechanisms	Clinical manifestations
Outward coronary remodeling; coronary flow reserve	No symptoms
Stress or exertion-induced increase in myocardial oxygen demand	Typical angina pectoris; stable angina pectoris
Coronary plaque erosion, rupture, platelet aggregation, vasospasm, mural thrombus, thromboemboli	Unstable angina pectoris
Marked coronary luminal narrowing; coronary plaque with acute alterations as above; ventricular fibrillation	Sudden cardiac death
Coronary plaque erosion or rupture with mural thrombus or stable coronary plaque with markedly decreased coronary perfusion	Acute subendocardial myocardial infarct
Coronary plaque erosion or rupture with occlusive thrombosis	Acute transmural myocardial infarction

Table 4.1: The Spectrum of Ischemic Heart Disease [Fishbein *et al.* (2016)].

Thygesen *et al.* (2012) classified MI in various types, based on pathological, clinical and prognostic differences:

- MI Type 1: Spontaneous Myocardial Infarction
- MI Type 2: Myocardial Infarction Secondary to an Ischemic Imbalance
- MI Type 3: Cardia Death due to Myocardial Infarction
- MI Type 4 and 5: Myocardial Infarction associated with Revascularization Procedures

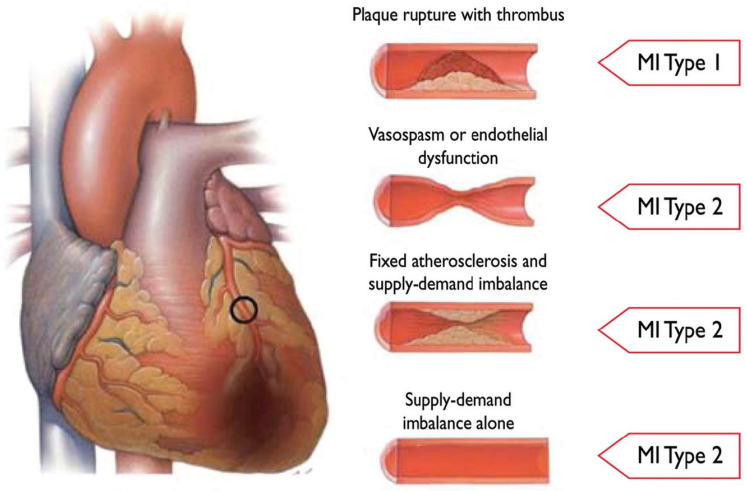

Figure 4.1: Illustration of the differences between type 1 and type 2 myocardial infarction according to the condition of the coronary arteries [Thygesen *et al.* (2012)].

4.1.2 ST-elevated Myocardial Infarction

Ibanez *et al.* (2017) stated that although the rate of mortality associated with ischemic heart disease have reduced in Europe over the last few decades, this is still the single most common cause of death worldwide. The relative incidences of STEMI and NSTEMI are decreasing and increasing, respectively.
The majority of STEMI patients are classified as a type 1 MI (with evidence of a coronary thrombus) and some STEMIs fall into other MI types. A diagnosis of STEMI is usually based on symptoms consistent with myocardial ischemia (i.e. persistent chest pain) and signs [i.e. 12-lead electrocardiogram (ECG)].

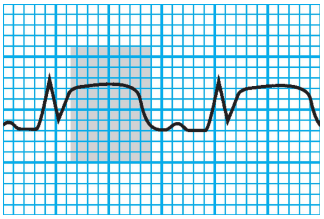

Figure 4.2: Illustration of ST-segment elevation, which is considered when it is 1 mm or more above the baseline [Burghart (2011)].

Chapter 5

Therapy

5.1 Reperfusion therapy

Bassand *et al.* (2005) stated that reperfusion therapy in the acute phase of STEMI has been shown to be the most important component of the treatment. When reperfusion therapy is applied in a timely manner, it can favorably influence short- and long-term patient outcome. Various strategies of reperfusion were developed and are available to the clinician, namely thrombolytic treatment, percutaneous coronary intervention (PCI), or a combination of both. Both thrombolytic therapy and PCI have been shown to improve outcome. But the efficacy and safety of their combination is still a matter of considerable debate.
Data have shown that reperfusion therapy is insufficiently implemented in many countries. A large proportion of patients with STEMI do not receive any reperfusion therapy, for a wide variety of reasons, despite its availability and the absence of any contraindication.

Ibanez *et al.* (2017) found that primary PCI is the preferred reperfusion strategy in patients with STEMI within 12 hours of symptom onset. It can be performed expeditiously if it is well provided i.e. 120min from STEMI diagnosis, by an experienced team, which includes not only interventional cardiologists but also skilled support staff.
In centres with a high volume of PCI procedures lower mortality rates among patients undergoing primary PCI can be observed. Real-life data confirm that primary PCI is performed faster and results in lower mortality if performed in high-volume centres. Randomized clinical trials in high-volume, experienced centres have repeatedly shown that, if delay to treatment is similar, primary PCI is superior to fibrinolysis in reducing mortality, reinfarction, or stroke. However, in some circumstances, primary PCI is not an immediate option and fibrinolysis could be initiated expeditiously. Patients should undergo a primary PCI strategy when a clinical compatible with AMI and a non-interpretable ST-segment on the ECG is present, such as those with bundle branch block or ventricular pacing.
There is general agreement that a primary PCI strategy should also be followed for patients with symptoms lasting > 12 h in the presence of:

- ECG evidence of ongoing ischemia;
- ongoing or recurrent pain and dynamic ECG changes; and
- ongoing or recurrent pain, symptoms, and signs of heart failure, shock, or malignant arrhythmias.

Reperfusion therapy is recommended when in all patients with symptoms of ischemia of $\leq$ 12 h duration and persistent ST-segment elevation is indicated.
A primary PCI strategy is recommended in the absence of ST-segment elevation, and in patients with suspected ongoing ischemic symptoms suggestive of MI and at least one of the following criteria:

- hemodynamic instability or cardiogenic shock
- recurrent or ongoing chest pain refractory to medical treatment
- life-threatening arrhythmias or cardiac arrest
- mechanical complications of MI
- acute heart failure
- recurrent dynamic ST-segment or T-wave changes, particularly with intermittent ST-segment elevation.

5.1.1 Coronary sinus intervention

Faxon (2015) found that coronary veins provide direct retrograde access to ischemic myocardium, which why coronary venous interventions are considered. Most of the left ventricular venous drainage occurs via the coronary sinus. The other major source of drainage is through the Thebesian veins that provide venous drainage directly into the left ventricle, where in some patients, this is the dominant venous outflow. In distinction to the left ventricle, the right ventricle drains primarily through the Thebesian veins. Past studies showed that occlusion of the coronary sinus increases venous pressure to 50% to 70% of left ventricular systolic pressure. But the diastolic pressure is identical to left ventricular diastolic pressure, presumably transmitted through Thebesian veins or from the myocardium or both.

Mohl (1988a) stated that coronary sinus interventions generally are understood to be methods of temporary protection of ischemic myocardium via the coronary venous system. They include retroinfusion of cardioplegia during cardiac arrest in surgery, retroperfusion of arterial blood in settings of myocardial infarction (synchronized retroperfusion or SRP), retroperfusion of pharmaceutical agents, and manipulations of venous blood drainage by pressure-controlled intermittent coronary sinus occlusion (PICSO).
There are two reasons why it makes sense to access ischemic myocardium via the coronary sinus in the presence of diseased coronary arteries that are jeopardizing the myocardium through deprivation:

- The coronary venous vasculature remains unaffected by the atherosclerotic disease process, which often causes severe coronary artery obstruction and may jeopardize regional myocardium deprived of essential perfusion and substrates. All of the several categories of CSIs have been extensively studied in the laboratory. Surgical retroinfusion of cardioplegia is applied in substantial, patient subsets. SRP and PICSO were tried in clinical treatment and aimed at extending myocardial viability during severe but reversible ischemic injury.
- The coronary venous vasculature is a dense meshwork with numerous interconnections, offering an approach for retrograde delivery that can be accomplished by increasing coronary vein outflow impedance (PICSO) and/or provision of supplemental reverse flow (SRP).

Furthermore Mohl *et al.* (2015) stated that the coronary venous route to access deprived myocardium and thus the obstructed microcirculation has a long history, beginning with retroperfusion of arterial blood in the late 19th

century and progressing to the development of pressure-controlled intermittent coronary sinus occlusion (PICSO) in the 1980s (Fig.5.1). Although there is little doubt that cardiac veins are useful access routes to jeopardized myocardium, few concepts have progressed to clinical development. The concept of PICSO, which uses the coronary

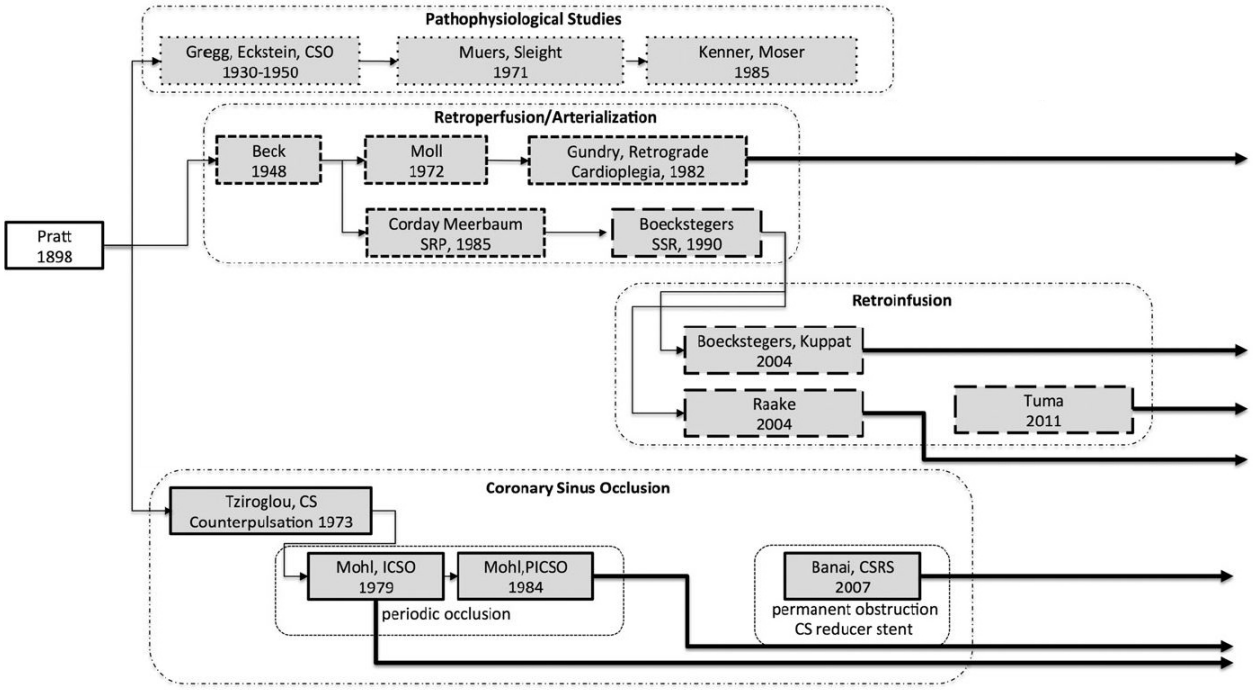

Figure 5.1: Historical overview of coronary sinus interventions [Mohl *et al.* (2015)]. Literature: Pratt (1898). Pathophysiological Studies: Gregg *et al.* (1938a), (1938b), (1940), (1947), and (1950); Eckstein *et al.* (1941a), (1941b), (1949), (1950), (1952) and (1953); Muers and Sleight (1972a) and (1972b) and Kenner *et al.* (1985). Retroperfusion/Arterialization: Beck *et al.* (1948); Moll *et al.* (1975); Gundry *et al.* (1984); Meerbaum *et al.* (1982) and Boekstegers *et al.* (1998). Retroinfusion: Boekstegers *et al.* (2004), Raake *et al.* (2004) and Tuma *et al.* (2011). Coronary Sinus Occlusion: Tziroglou *et al.* (1979), Mohl *et al.* (1982) and (1984) and Banai *et al.* (2007).

sinus pressure for termination of obstructing venous flow in contrast to fixed timed ICSO, has been further developed using new technology. There are abundant data on myocardial salvage in experimental ischemia as well as in patients with lysis therapy during or following ischemia as well as reperfusion. Clinical data also support the use of PICSO in patients after global ischemia and in heart failure patients. Presented data detail the application of PICSO during primary PCI in the early reperfusion period.

The primary aim of coronary sinus interventions was retroperfusion of arterial blood to the myocardium, but preclinical and clinical data have suggested other beneficial effects, primarily redistribution of flow towards underperfused zones and subsequent washout as well as offering the potential to revive regenerative pathways, ultimately restoring structural integrity. The first clinical application of the concept of using the coronary sinus to access ischemic myocardium was in the 1940s. A series of pathophysiologic studies enhanced understanding of the reaction to elevated pressure in cardiac veins as well as reflexes originating from the endocardium close to the orifice of the coronary sinus. Further studies showed the effects of coronary sinus occlusion techniques on the behavior of the coronary microcirculation. Meerbaum *et al.* (1982) and (1976) developed interventional retroperfusion methods such as synchronized retroperfusion (SRP) and applied them clinically. They forced arterial blood retrograde via

a catheter system during diastole into the ischemic microcirculation. Furthermore Boekstegers *et al.* (1998) and (2004) refined the retroperfusion technology using a selective perfusion technique with subsequent suction that showed positive results in the clinical setting. Meerbaum *et al.* (1983) achieved retrograde lysis of coronary artery thrombus by coronary venous streptokinase administration. In early clinical studies by Komamura *et al.* (1989), pICSO (pressure observed intermittent coronary sinus occlusion without automatic closed loop, but observer control of pressure increase) was also able to enhance clot lysis significantly, even when given intravenously as compared to controls.

Jacobs (2003a) also stated that numerous studies from multiple investigators support the fact that the coronary sinus interventions will play a role in the treatment of several ischemic syndromes. Furthermore techniques like synchronized retroperfusion (SRP) and pressure-controlled intermittent coronary sinus occlusion (PICSO) will be effective in salvaging myocardium during myocardial infarction as well as during reperfusion. The coronary sinus techniques offer a method of myocardial protection which provides access to an ischemic microvasculature. Coronary sinus catheterization is safe and also relative simple to accomplish. Major disadvantage is the potential to damage the venous system.

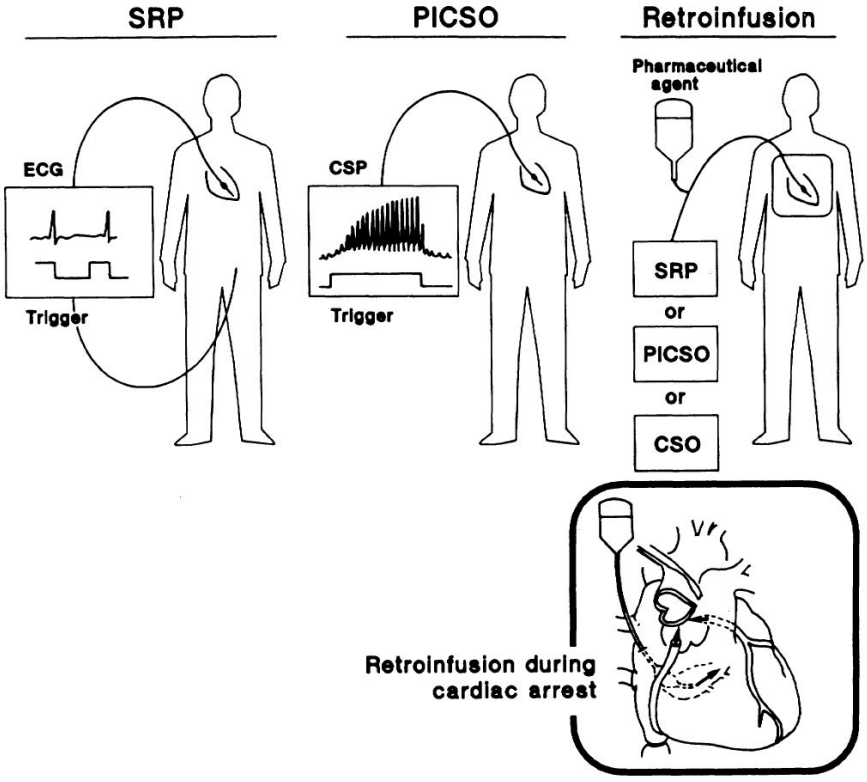

Figure 5.2: Schematic comparison between the three CSIs: SRP, PICSO, and retroinfusion in the normal working and arrested heart. During SRP arterial blood is shunted from the femoral artery into a pump console and pumped during diastole into the coronary sinus. Pump action is triggered by the electrocardiogram. During PICSO the coronary sinus pressure triggers the balloon occlusions (closed-loop control). Retroinfusion of pharmaceutical agents in the working heart can be performed by use of timed coronary sinus occlusion, PICSO, or SRP. In the arrested heart cardioplegia is delivered under constant infusion Mohl (1988a).

5.1.1.1 Synchronized retroperfusion

Faxon (2015) wrote that a renewed interest in coronary sinus techniques occurred in the 1970s when Meerbaum *et al.* (1976) and Farcot *et al.* (1978) demonstrated that diastolic retroperfusion of arterial blood through a coronary sinus catheter reduced myocardial ischemia and associated wall motion abnormalities in experimental studies. The advantage of the technique was that the retroperfusion only occurred during diastole, allowing drainage of the venous system during systole. Subsequent studies have shown it to be effective for retrograde delivery of drugs and stem cells. Boekstegers *et al.* (1998) used a modified technique with selective suction and pressure regulated retroinfusion. In a study of 45 patients, retroperfusion reduced myocardial ischemia during PCI.

Mohl (1988a) stated that the synchronized retroperfusion technique, that temporary support acutely jeopardized ischemic myocardium, defined a new application for coronary sinus intervention and then Mohl *et al.* (2003b) that in the synchronized retroperfusion system, blood from a suitable arterial site is pumped during cardiac diastole into the regional coronary veins adjoining the experimentally obstructed coronary arteries. Coronary venous drainage during cardiac systole is therefore provided by this method and minimizes vascular congestion, myocardial edema and hemorrhage. SRP significantly improved acutely ischemic myocardial function and significantly decreased infarct size. Evidence and interpretation of SRP data suggest that oxygen delivery in combination with improved retrograde perfusion as well as washout from acutely ischemic zones are the primary mechanism of this coronary venous intervention.

Meerbaum (1990) stated that SRP was to obstruct the coronary vein and retroperfuse arterial blood only in diastole, when venous efflux is minimal and the heart is most receptive to safe coronary venous intervention. SRP was also designed to facilitate normal systolic drainage via the coronary sinus, when ventricular contraction causes a spontaneous 'milking' or 'squeezing out' of the coronary venous blood. The systolic drainage, as well as the arterial blood retroinfusion with simultaneously timed coronary vein occlusion, were synchronized in SRP by means of the electrocardiogram and usually accomplished by means of an intervascular balloon at the tip of the retroperfusion catheter. One variation of this concept (possibly of interest for very short retrograde intervention) is to maintain a steady retrograde blood infusion, but appropriately synchronize and diastolically occlude the coronary sinus or great cardiac vein. Conversely, the coronary vein could be scheduled to remain obstructed for short periods, while the retroinfusate flow is phased to occur only in diastole. The terms of retroperfusion and retroinfusion are really equivalent, but the former is generally associated with arterialization of the coronary veins, while retroinfusion has been largely reserved to characterize retrograde delivery of pharmacologic agents.
Furthermore, SRP has been experimentally shown to have potential in treating acute myocardial ischemia due to coronary artery occlusion. Clinical trials were under way, using upgraded SRP systems. In general, safety and feasibility seem to be well established through studies of Gore *et al.* (1986), Berland *et al.* (1988), Kar *et al.* (1988), and other human trials. Much effort appeared to center on treatment if ischemia associated with single-vessel occlusions during percutaneous transluminal angioplasty (PTCA) balloon inflations. Clinical SRP effectiveness in the setting which was extensively studied and found successful in animals, i.e. during evolving acute myocardial infarction, has not as yet been adequately demonstrated. There are clearly important differences between the experiments and clinical applications. One known factor is the different coronary venous anatomy, which may make it more difficult in the human to develop sufficient coronary venous pressures unless one uses greater than anticipated retroinfusion flows. Catheters, pumps and protocols must all be reexamined in terms of reliability and

optimal SRP application. Nonetheless, it is expected that the clinical efforts will succeed in pinpointing patient subsets and conditions in which SRP or modified SRP treatment can be employed as a useful adjunct support in the area of interventional cardiology. The International Group on Coronary Sinus Interventions , through its biannual symposia and quarterly newsletters, provides a useful link between the various investigators and a forum for review of scientific and clinical advances.

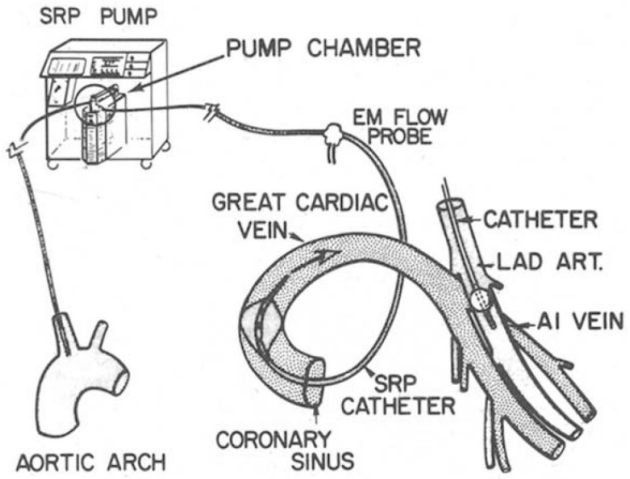

Figure 5.3: Schematic of the synchronized retroperfusion (SRP) system. Arterial blood is shunted from a brachial artery to the pump chamber. During diastole the upward movement of a piston onto the pump chamber displaces blood through an auto inflatable balloon catheter into the coronary sinus. AI = anterior interventricular; EM = electromagnetic; LAD ART. = left anterior descending coronary artery [Drury *et al.* (1985)].

5.1.1.2 Pressure-controlled intermittent coronary sinus occlusion

Faxon (2015) also wrote that in 1984, Mohl (1984a) took another approach by intermittently occluding the coronary sinus. The occlusion was timed until the pressure reached a plateau usually over 3 to 4 cardiac cycle followed by deflation to allow venous drainage and washout. Experimental animal studies by Jacobs *et al.* (1991), Lazar *et al.* (1995) and Mohl *et al.* (1985a) showed reduced ischemia in some studies but not all. Clinical trials by Mohl *et al.* (1988b) and (2008) of these techniques have been limited but positive results have been reported during cardiac surgery and in patients with acute coronary syndrome.

Furthermore, Mohl *et al.* (2003b) wrote that the concept of pressure-controlled intermittent coronary sinus occlusion (PICSO) was developed in the 1970s [Mohl (1984a)], where the idea was to develop a pressure controlled coronary sinus occlusion. That stems from observations which suggested that coronary inflow and distribution could be influenced by coronary venous manipulations, and the assumption that the observed beneficial effects of retroperfusion in the case of myocardial ischemia may largely be due to changes in pressure and flow within the coronary microcirculation. Furthermore, the assumption was that an intermittent balloon blockade of the coronary sinus redistributes blood from non-ischemic zones to underperfused zones, which results in an increase in the venous blood circulation in the ischemic zone and a washout of plasma-like fluid and toxic metabolite from the jeopardized myocardium. Experimental studies have indicated that PICSO significantly reduces infarct size and improves ischemic wall motion.

Additionally the alternate phasing of the coronary sinus occlusion is controlled consistently with the coronary sinus pressure that develops during its occlusion. The systolic blood pressure in the occluded coronary sinus rises beat by beat over a period of a few seconds until it reaches a plateau, which is thought to be an index for optimally controlled coronary sinus occlusion. The coronary sinus balloon is intermittently deflated for a period of 2-5 seconds, which allows for adequate washout. Due to changes occurring in pressure rise, this phased timing has to be controlled throughout the intervention. Because of the brevity of individual coronary sinus occlusion, it is not believed necessary to limit coronary venous pressure to a level consistent with longer periods of coronary venous obstruction or retrograde pumping. On the other hand, it was found to be important to ensure exact monitoring of PICSO timing and phasing, because otherwise this intervention might prove counterproductive and actually limit arterial inflow. Furthermore, it has been found desirable to monitor the coronary sinus pressure with regard to potential diagnostic information derived from coronary sinus pressure-flow relations.

Mohl *et al.* (2015) also wrote that coronary sinus occlusion (CSO) techniques such as ICSO/PICSO and the Banai stent (2007) are based on changes in the pressure and flow relations in the normal and ischemic heart. During coronary sinus occlusion, redistribution of flow within the venous compartment allows access to deprived perfusion zones. During temporal occlusion as seen in ICSO/PICSO procedures, a phase of washout follows the filling of the venous compartment. In contrast, the Banai stent results in a chronic elevation of coronary venous pressure and may lead to severe side effects on coronary circulation including restrictions in venous flow and permanent reorganization of the venous outflow pattern.
Next, during ICSO, the temporary occlusion of the coronary sinus (which collects about 70% of the myocardial outflow) induces a redistribution of venous blood and plasma-dense fluid from normally perfused territories into underperfused areas, such as severe atherosclerotic coronary arteries and in ACS with additional thrombus burden. The temporary increase of venous pressure in the coronary sinus induces a continuous rise and fall of pressure gradients in the microcirculatory bed, clearing debris and eliminating metabolic waste. Reactive buffer systems and the action of osmotic, ionic and, most importantly, mechanical forces squeezing blood into the occluded microcirculation, reduce the area of the no reflow zones. Coronary sinus occlusion pressure reaches a systolic plateau resulting from the squeezing action of myocardial contraction. Since redistributed blood flow needs time to fill the venous compartment, these systolic pressure peaks rise constantly, reaching a plateau after several seconds. During pICSO and PICSO, this plateau level signals the reopening of venous drainage and enables optimal redistribution of venous blood (Fig.5.4). The pressure in the occluded coronary artery fluctuates according to the pressure in the coronary sinus, and the arterial pressure decreases during coronary sinus release. Furthermore, applications of PICSO have focused on ACS. In an experimental animal study, Jacobs *et al.* (2003b) found that PICSO performed during reperfusion significantly enhanced myocardial salvage and postulated that PICSO may decrease heart rate by a reflex mechanism that is mediated by vagal afferents. A clinical study by van de Hoef *et al.* (2015), the Prepare RAMSES trial (reperfusion after acute PCI in myocardial infarction and coronary syndromes: efficacy and clinical significance), which aimed to further analyze the salvage potential of this method, has been completed. This study followed the first-in-man study using new technology. Prepare PICSO by van de Hoef *et al.* (2012) included 15 patients with stable angina scheduled for PCI of the left anterior descending artery (LAD). Balloon occlusion of the LAD was performed twice, once with and once without PICSO and lasting maximally 3 minutes each, to document the effect of PICSO on coronary sinus pressure and LAD wedge pressure. PICSO resulted in a marked increase in coronary sinus pressure with no device related adverse events reported. In a study by Mohl *et al.* (2014) of 32 heart failure patients undergoing resynchronization therapy, PICSO was

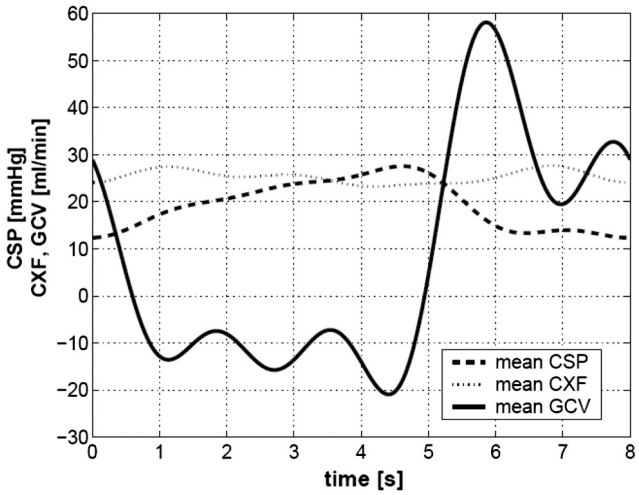

Figure 5.4: Mean arterial inflow (CXF) and great cardiac vein flow (GCV) in relation to coronary sinus pressure during CS occlusion. Note the hyperemic venous flow indicates a surplus of washout. The negative flow during occlusion depicts retroperfusion. Note that pressure control in the coronary sinus is necessary to prevent permanent coronary inflow reduction. With pressure control mean coronary flow remains unchanged due to the "hyperemic response" during coronary sinus occlusion release [Mohl *et al.* (2015)].

performed on 8 patients for 20 minutes versus 24 controls. At 5 year follow-up, the metabolic, biochemical and molecular changes induced indicated that PICSO has regenerative potential beyond its acute effect on myocardial ischemia.

Mohl *et al.* (2015) continued that in order to realize the full potential of this intervention, questions remain regarding the application of PICSO in ACS. There is also need for additional data to optimize the time window of PICSO to prevent/reverse reperfusion injury, to explore the potential to treat different ischemic perfusion territories and reduce the volume of obstructed microcirculation. Although early and recent clinical results are promising, there is also a need for long-term data from a propensity matched trial to establish clinical significance.
However, there are major limitations associated with analyzing myocardial salvage in PICSO. It is known that PICSO interferes with edema formation and increases the energy in border zones by vasodilatation of the microcirculation. These findings demonstrate a reduction in the perfusion deficit and therefore reduce the evidence measured by magnetic resonance imaging (MRI), since it detects edema, which is claimed to be washed out, and positively influenced by PICSO. Myocardial salvage is assessed by MRI several days after the acute event and therefore includes PICSO effects on the area at risk, since deprived perfusion zones are normally measured experimentally before therapy starts. Therefore MRI data in PICSO research might blunt positive PICSO effects, reducing the perfusion deficit and enhancing washout. These effects of PICSO should be taken into account since recent data emphasize the importance and prognostic values of early changes in ischemic/reperfused microcirculation.

Stoller *et al.* (2013) reported that the reduction of ischemia in patients treated with brief ICSO periods depends on collateral flow. Variable levels of effectiveness of ICSO have been observed and seem to be dependent on the location of the balloon within the coronary sinus and therefore the amount of redistributed blood as well as the

optimization of the pressure increase and cycling. A 2004 study by Mohl *et al.* (2005) on a sheep model showed that optimal timing significantly improves the effectiveness of the method. However, the fixed timings in ICSO occlusion/release cycle pattern prohibit optimal redistribution of blood, a limitation that has been demonstrated in several studies like by Ikeoka *et al.* (1990), Matsuhashi *et al.* (1992) and Toggart *et al.* (1987).
Inadequate duration of the coronary sinus occlusion release leads to an insufficient retroperfusion/drainage of the coronary sinus and hence decreases coronary artery inflow rather than resulting in washout and hyperemic response. The unadjusted fixed ICSO approach is unable to correct according to changes in CSP dynamics. Therefore an automatic closed loop method adapting to the dynamics of individuals was developed. In the majority of studies, pressure control was achieved by continuous observation and immediate, but observer controlled adjustment of pressure dynamics by the investigator (pICSO). A closed loop system for coronary sinus occlusion has been established that optimizes the beneficial effects of PICSO. The PICSO cycle adapts instantly (beat to beat) according to the physiologic state of the heart. Several parameters must be optimized in a PICSO intervention. In order to ensure sufficient coronary drainage, the release phase must be long enough to allow the next occlusion phase to be triggered by the end of the peak of hyperemic coronary arterial flow, which can be detected by observing venous flow. In addition, the occlusion phase must be set to ensure that the systolic coronary sinus time of release of the balloon occlusion according to the coronary sinus pressure dynamics sensed over the fluid-filled line of the catheter.

Mohl *et al.* (2003b) stated that pressure-controlled intermittent coronary sinus occlusion is achieved through a balloon occlusion systems, which is driven pneumatically with a pressure-dependent control of the occlusion and release cycles. A balloon catheter is inserted percutaneously or intraoperatively through the right atrium into the coronary sinus. The coronary sinus pressure is monitored through a central lumen of the catheter. As compared to synchronized retroperfusion, PICSO is a simpler device and more convenient to handle.

5.1.1.3 Retroinfusion techniques

Mohl *et al.* (2003b) found that retroinfusion of pharmaceutical agents can be combined with either SRP or PICSO in the beating, ischemic heart or by continuous retrograde infusion such as performed with cardioplegic solutions during open heart surgery. In its latter applications, a cannulation of the coronary sinus with a purse-string suture is easily accomplished through the right atrium near the inferior vena cava, and retrograde cardioplegia is delivered without disturbing the operating field. The special anatomy of the venous vasculature permits a more uniform protection of the heart, especially in the presence of hypertrophic or atherosclerotic coronary lesions. In several experimental and clinical studies retrograde cardioplegia has been beneficial in the presence of the myocardial edema and has been associated with a postoperative increase in left ventricular function.
Retroinfusion of cardioplegic solutions is distinguishable from SRP or PICSO in that it is performed in the nonworking heart. Its specific advantages include minimal interference with the surgical procedure, avoidance of trauma to the coronary arteries, and a more uniform distribution of cardioplegia. Furthermore, monitoring of flow rates and pressures during cardioplegic arrest should enhance prevention of damage to endothelial cells Mohl (1988a).

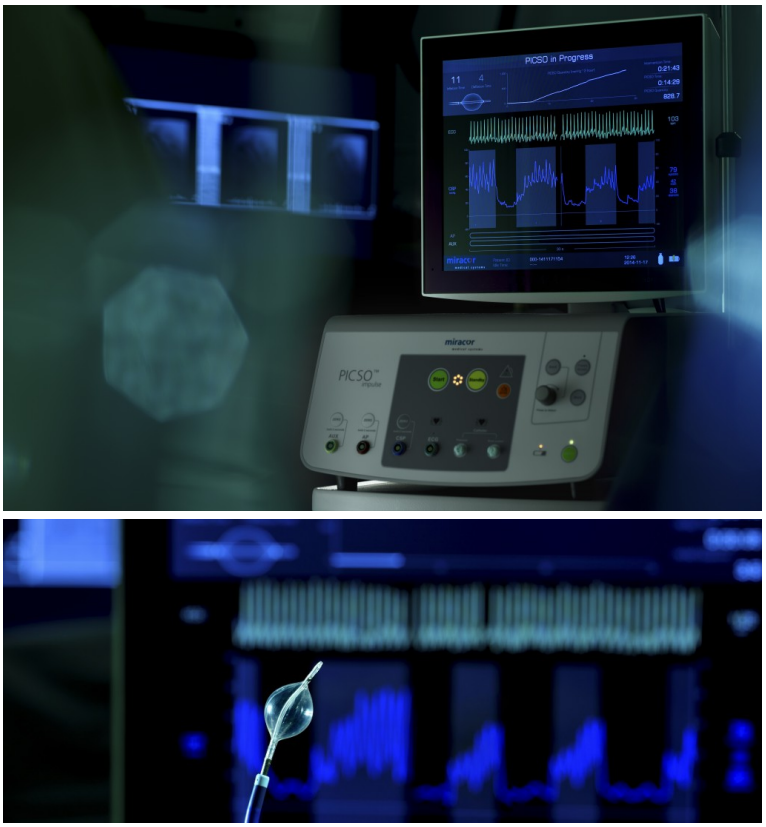

Figure 5.5: PiCSO^{AMI} Impulse Console (above): The monitor displays the inflation / deflation state of the balloon, as well as trend graphs and time counters; Live graphs display curves and numeric values of ECG, CSP, AP and auxiliary input. PiCSO Impulse Catheter (below): 8 French triple-lumen catheter with a low profile, semi-compliant balloon and an atraumatic distal tip. It is inserted in a standard over-the-wire technique via the femoral vein and placed in the coronary sinus using a steerable guide sheath. Two marker bands show the extension of the balloon in the coronary sinus [Miracor Medical SA (2018)].

5.1.2 Advantages and disadvantages

Jacobs (2003a) stated the following advantages and disadvantages:
The advantages of retroinfusion of cardioplegic solutions are

- avoidance of trauma to the coronary arteries especially in patients with ostial left main coronary disease,
- minimal interference with the surgical procedure in
- more uniform distribution of cardioplegia in patients with proximal coronary artery stenosis.

Major disadvantages include

- potential for inadequate protection of the right ventricle,
- longer time to diastolic arrest,
- potential for coronary venous injury and
- an extra right atrial incision.

Advantages of SRP include

- retroperfusion during diastole with normal venous flow during systole and
- potential to deliver pharmacologic agents to an ischemic microcirculation.

Disadvantages include

- need for arterial access and
- potential for hemolysis.

PICSO has similar advantages like SRP but in addition to the fact that PICSO is a simple system without the need for arterial access. Furthermore also probably facilitates washout of edema and ischemic metabolites. Major disadvantages of PICSO is that it may not be effective for acute myocardial ischemia, i.e. in acute coronary insufficiency.

5.2 Pros and cons of CSIs vs. conventional therapy

	Antegrade **vs.**	**Retrograde**
Pros	Proven effective	More uniform delivery
	Quicker diastolic arrest	Better visualization during aortic surgery
Cons	Potentially inadequate in hypertrophy	Slower diastolic arrest
	or severe coronary artery disease	Coronary sinus damage
	Coronary artery damage	May be inadequate in right
		coronary artery disease

	SRP **vs.**	**PICSO**
Pros	Reduces infarct size	Same
	Improves left ventricle function	Same
	Beneficial during reperfusion	Same
	Direct delivery of drugs	-
		Hemodynamic monitoring
Cons	Coronary sinus selective cannulation	Same
	Arterial access necessary	-
	Potential hemolysis	-
	Potentially less effective in ischemia	Same
	Potentially less effective in right	Same
	coronary artery disease	

	CSI **vs.**	**Thrombolysis**
Pros	Reduces infarct size	A more effective means of reducing infarct size
	Improves regional left ventricle function	Same
	Is complementary to reperfusion	-
	Can deliver drugs (SRP)	-
	Hemodynamic monitoring (PICSO)	-
Cons	Invasive	Not necessarily invasive
	Coronary sinus damage	Significant risk of bleeding

Table 5.1: Top table: Retroinfusion of cardioplegia: Antegrade vs. retrograde cardioplegia. Next tables: Coronary sinus interventions - SRP and PICSO in acute myocardial infarction: Coronary sinus interventions (CSI): Synchronized retroperfusion (SRP) vs. pressure-controlled intermittent coronary sinus occlusion (PICSO) and Acute myocardial infarction [Faxon (2003)].

Chapter 6

Mathematical Modelling Of Coronary Sinus Interventions

6.1 Introduction

Schreiner *et al.* (1990b) introduced two basic approaches that are open to mathematical modeling of coronary sinus interventions: phenomenological and mechanistic modeling.
In phenomenological modeling, parameterized mathematical functions are fitted to systolic and diastolic coronary sinus pressure (CSP) envelopes in order to characterize numerically specific parameters of shape of CSP pressure rise. The mathematical procedures yield numerical results which resemble those features of CSP envelopes, e.g. height of plateau and rise time. The modeling results are objective and reproducible substitutes for diagnostic information visually obtained from CSP tracings and in a further step may be used as input of a closed loop regulation of coronary sinus intervention modalities, e.g. occlusion/release time for pressure-controlled intermittent coronary sinus occlusion (PICSO), synchronized retroperfusion (SRP) flow rate and timing.
Mechanistic modeling is achieved by coupled differential equations which describes flows, pressures and volume changes in a mechanical model which was developed to resemble the key features of the coronary circulation in the presence of CSIs. The results comprise pulsatile time courses of all calculated quantities, e.g. the forward and backward flow between capillaries and coronary veins, CSP, which then can be used to address three main issues.
Firstly the modeling is an estimation of intramyocardial hemodynamics which are essentially inaccessible to experimental measurements.
Secondly, insights into the performance of different modes of CSI, e.g. PICSO, SRP, are provided in the presence of derangements of perfusion and function. The case of moderate global ischemia with maintained coronary inflow but reduced contractile function, representing the reperfusion phase after surgical cardiac arrest were specifically addressed and also the setting of a single coronary artery obstruction associated with a regional loss of contractile function.
Thirdly, this mechanistic model is specifically used to simulate stepwise modifications of CSI patterns, e.g. varying the PICSO occlusion/release timing or the SRP flow rate, in order to approach an optimal coronary venous intervention. The obtained results demonstrate that phenomenological modeling is a suitable tool to assure precise CSI

operation based on pre-determined intervention criteria, whereas mechanistic modeling is the method of choice in the search for the optimal intervention mode to applied, since model computations may yield results useful to minimize the need for costly and time consuming animal experiments.

6.2 Phenomenological modeling

Phenomenological modeling emphasizes a mathematical description, e.g. of hemodynamic measurements and it is to provide quantitative results. For instance, the rise of the coronary sinus pressure (CSP) after coronary sinus occlusion (CSO) follows a characteristic pattern, from which a selection of occlusion and release periods for one of the interventions can be concluded, namely pressure-controlled intermittent coronary sinus occlusion (PICSO). However, the systolic and diastolic envelopes of CSP may also be subjected to a mathematical fitting procedure, which derives numerical parameters of curve shape, e.g. height of pressure plateau and its rise time. Such results may be used to calculate an optimal occlusion/release timing, which is reproducible and intersubjective. Two basic features apply to phenomenological modeling:

- rather than considering mechanisms, e.g. physiological or hydrodynamic, which are, in a casual sense, responsible for a special form of CSP rise, a quantitative description of the experimental measurements are provided;
- since no mechanisms are involved in the analysis, the functional form of such a phenomenological model remains to some extent arbitrary.

This approach may achieve little compared to visual inspection since, despite being complex, it still involves the arbitrariness of model selection. However, this argument is really not applicable for the following reason: Even if the initial choice of a model function and the mathematical procedure according to which intervention pattern is adapted are just as arbitrary as visual inspection, the results become objective and reproducible due to strict algorithms applied to measured data. Thus, while phenomenological modeling does not pretend to extract information principally unavailable to visual inspection, it adds an important quantitative and reproducible feature to various adjustments that must be made during CSI. Moreover, the 'calculated diagnostics' approach forms a useful basis for system computerization and automatic closed-loop control desired in routine applications.

6.2.1 Model applications

6.2.1.1 PICSO coronary sinus pressure rise

Numerous studies by Chang *et al.* (1987), Guerci *et al.* (1987), Jacobs *et al.* (1985) , Mohl *et al.* (1984b), Mohl *et al.* (1985b), Mohl *et al.* (1988b) and Toggart *et al.* (1987) have been carried out to evaluate the value of PICSO as an intervention to salvage myocardium at risk. Specific applications by Schreiner *et al.* (1988a) envisaged comprise acute infarction settings and open heart surgery support during the reperfusion phase after arrest. Some studies by Mohl *et al.* (1988b) and Schreiner *et al.* (1988b) were carried out with constant occlusion/release timing (intermittent coronary sinus occlusion, ICSO), others used adaptive cycling adjusting according to the visual inspection of the coronary sinus pressure rise (PICSO). Some of these studies [Mohl *et al.* (1988b)] did find a beneficial effect, others by Zalweski *et al.* (1985) and [Toggart *et al.* (1987)] did not. The poor outcome of some of the latter investigations was attributed by the Vienna PICSO working group to 'improper' PICSO cycling, resulting

from inadequate adjustment based on visual inspection of the CSP tracing. To improve the adaption of PICSO cycling, mathematical models have been established, which put the shape of coronary sinus pressure rise on a quantitative basis.

6.2.1.2 Models for coronary sinus pressure rise

Because the beneficial effect of the PICSO interventions appears to be closely linked to exact application, mathematical models have been developed in order to put the estimation of occlusion and release times on a quantitative basis. The Vienna model by Schreiner *et al.* (1987), model 1, is a three parameter double exponential function to describe the coronary sinus pressure rise, (Fig.6.1, Eq.6.1).

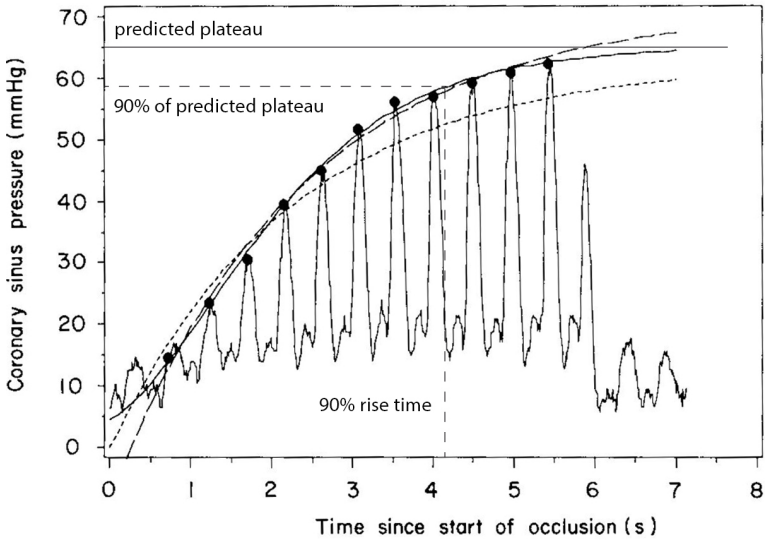

Figure 6.1: Fitting properties of different models for CSP rise and derived diagnostic quantities. CSP data are taken from a representative canine PICSO cycle. Full circles: peak-detected systolic values. Solid curve: model 1, dotted: model 2 (with non-linear fitting), dashed: model 2 with the plateau being forced through the last peak and fitted upon logarithmic transform. Note the differences in onset (near t = 0) and extrapolation properties between the models. Only the systolic envelope is shown. The predicted plateau and T90_SY (dashed reference line) are calculated from model 1 [Schreiner *et al.* (1990b)].

$$P_{CSP}(t) = A \cdot exp(\alpha[1 - e^{-\beta t}] - 1) \tag{6.1}$$

$P_{CSP}(t)$ is the coronary sinus pressure (CSP) in mmHg (systolic or diastolic) at time t and t is the time in seconds since onset of the occlusions and A, α, β are model parameters.
Systolic plateau:

$$P\_SY \equiv P_{CSP}(t = \infty) = A \cdot e^{\alpha - 1} \tag{6.2}$$

Pressure envelope (systolic) at the end of occlusion:

$$ENDP\_SY \equiv P_{CSP}(t = t_0) = A \cdot exp(\alpha[1 - e^{-\beta t_0}] - 1) \tag{6.3}$$

90% rise time (systolic):

$$T90\_SY = \beta^{-1} \cdot ln\left(\frac{-\alpha}{ln(0.9)}\right) \tag{6.4}$$

The same form of function was used for systoles and diastoles, the differences between systolic and diastolic envelopes being reflected in different values for the fitted parameters. An alternative model for the CSP rise, model 2, was developed by the Rhode Island Group by Sun *et al.* (2003), who used a monoexponential function. Mathematical representation of P_{CSP} envelope in model 2:

$$P_{CSP}(t) = A + \alpha(1 - e^{-\beta t}) \tag{6.5}$$

Single point assignments in original version of model 2:
Parameter A:

$$A = P_{CSP}(t = 0) \tag{6.6}$$

Parameter α:

$$\alpha = P_{CSP}(lastpeak) - A \tag{6.7}$$

In the improved version, with A, α and β fitted

$$P\_SY \equiv P_{CSP}(t = \infty) = A + \alpha \tag{6.8}$$

Pressure envelope at the end of occlusion:

$$ENDP\_SY \equiv P_{CSP}(t = t_0) = A + \alpha(1 - e^{-\beta t_0}) \tag{6.9}$$

90% rise time (systolic):

$$T90\_SY = -\beta^{-1} \cdot ln\left(\frac{(A + \alpha) \cdot (1 - 0.9)}{\alpha}\right) \tag{6.10}$$

6.2.2 Derived quantities for model 1

Following the fit, the plateau, P_SY, is calculated as the asymptotic height (mmHg) of the fitted systolic CSP envelope, extrapolated toward $t = \infty$, and may exceed the last systolic peak within the respective PICSO cycle. This extrapolation feature becomes prominent for short occlusion times, there the envelope still rises near $t = t_0$. The diastolic plateau, P_DI, is obtained along the same lines, The systolic pressure at the end of CSO, ENDP_SY, which is defined as the height of the fitted envelope at $t = t_0$, is, particularly for short occlusion times, lower than P_SY and not necessarily identical to the last systolic peak detected. The systolic 90% rise time of coronary sinus pressure, T90_SY, is defined as the time period required, counting from the beginning of the respective PICSO cycle, for the fitted envelope to reach 90% of P_SY. Analog for T90_DI. The rise times, in relation to the coronary sinus occlusion time, t_0, provide information as to the P_{CSP} developed within the occlusion time. Furthermore, the flowing other quantities may be constructed from model 1: mean integral under the envelope, (maximum) slope at the inflection point and rise times to 70% or 80% (or any percentage) of the height plateau.

6.2.3 Derived quantities for model 2

The calculated plateau, P_SY, is set equal to the height of the last systolic peak. This calculation method is fast but fails to account for a rising tendency of P_{CSP} near t_0 (no extrapolation capability). Consequently, ENDP_SY is systematically below the last systolic peak, since ENDP_SY < P_SY = (height of last peak).

6.3 Mechanistic modeling

Whereas phenomenological modeling is mainly applied to measure experimental data, in order to obtain a quantitative assessment or even regulation criteria, mechanistic modeling addresses the important task of achieving an understanding of the influence of principal factors and establishing conditions which will most likely provide optimal therapeutic effects of CSIs.

In vivo studies carried out to evaluate the therapeutic relevance of coronary sinus interventions are based on specific protocols which select the mode of the intervention and also specify the criteria according to which a possible therapeutic effect is to be evaluated. In this context, the broad term 'mode of intervention' describes among others, the occlusion/release phasing of PICSO, the synchronized retroperfusion (SRP) flow rates/pressures and timing within the cardiac cycle, as well as adjustments of these procedures to account for changing physiological needs in the course of the intervention. The characteristic conditions during an experimental investigation are usually kept constant, so that the results, e.g. improvement observed in the treated group, vs control, refers to a particular mode of intervention under the selected circumstances. If the mode of intervention was inappropriately chosen, a positive effect will in all probability not be achieved and the only information which can be derived from the study is that 'this particular mode' of intervention (say a specific mode of PICSO cycling) 'is suboptimal'. In this case the result of a presumably complex and difficult study is quite unsatisfactory. In other words, when an experimental investigation fails to provide evidence of benefits, one might argue that the 'particular mode of intervention' was the reason for the negative result and the intervention could have been beneficial provided 'it had been applied appropriately'. One can then suggest a modification of the intervention and redo the study. Mathematically speaking, such an in vivo study is only a 'point evaluation' and is not by itself capable of indicating the 'direction' toward optimization of the mode of intervention.

It therefore seems desirable to develop a tool capable of anticipating trends or even relations between the mode of intervention and at least certain parameters, e.g. washout or redistribution of venous blood, which may greatly influence the effectiveness of CSIs. It is the purpose of mechanistic modeling to provide such insights which could be very useful in setting up experimental protocols or clinical studies. In contrast to the above in vivo studies, a mathematical model which simulates key feature of the coronary circulation and myocardial physiology in the presence of CSIs, can be run repeatedly to simulate a large number of intervention modalities, at very low cost and expense of time. Those particular conditions, which have already been studied experimentally are very useful as 'reference conditions', according to which the model has to be adjusted so as to reproduce actual study findings. Each set of experimental data constitutes a 'point in a grid of the boundary conditions'. It is the purpose of the model to interpolate between such experimental points and even enable extrapolations to conditions under which the interventions have not yet been experimentally investigated. Moreover, model results are not affected by experimental spread (fully deterministic) and hence very small changes of the intervention's mode can readily be simulated without loosing trace of the changes' effects (due to uncontrolled superimposed physiological changes as seen in vivo). It is possible to derive that combination of changes in parameters which is most promising in terms on increasing the beneficial effects, i.e. the gradient in the direction of a therapeutic optimum.

Obviously, the major drawback of mechanistic modeling is the need to resort to simplifications, e.g. the real coronary circulation, required if one is to arrive at a manageable quantitative and numerical model. Therefore, questions remain as to how close the applied model resembles reality and whether the computational results will be confirmed in subsequent experimental studies.

6.3.1 Coronary circulation during coronary sinus interventions

It is evident that the full complexity of coronary circulation is beyond the scope of mathematical modeling. Therefore, simplifications have to be introduced in any model designed to give mechanistic description of cardiovascular physiology. It is mainly up to the skill of the investigator to introduce these simplifications and at the same time retain those important features of reality which have direct impact on the quantities evaluated from the model. As part of simplifications in the model, parts of detailed structures, say sections of the vascular tree, are lumped together into single volumes, resistors and compliances. Searching for 'the best possible model', one is always tempted to retain as much complexity as possible in order to make the model 'realistic'. However, this approach is prone to involve more and more parameters for which experimental data are simply not available, thus introducing many unknowns to be adjusted 'realistically'. Similar to simple systems of equations, the solution may become arbitrary (or manifold) if there are more unknowns (model parameters) than equations (experimental tests). It was therefore a major aim to restrict a model for the hemodynamics of coronary sinus interventions to a firm if minimal complexity, which is nevertheless still sufficiently realistic to reproduce key features observed in measurements.

6.3.2 Description of compartments

In the following, three models are introduced with their major differences:
Schreiner model *et al* (1990a,1990d): LAD and LXC beds are modeled symmetrically, i.e. with equal parameters
Model Oswald (2004): LAD and LXC beds are modeled asymmetrically
Model Kajgana (2004): LAD and LXC beds are modeled asymmetrically and addition of collaterals.
Since the last two models are based on the first one, the modifications or extensions will be added in the sections when appropriate. A schematic illustration of the models of the coronary circulation and its compartments are shown in Fig.6.2.

LCX and LAD branches are modeled similarly: The main left coronary artery (LCA), which originates from the aortic root is represented by a tube with resistance R_{LCA}, carrying the flow $Q_{LCA}(t)$. The inlet is subjected to a perfusion pressure $p_{LCA}(t)$, which is obtained by Fourier expansion of aortic pressure at a heart rate of 60 bpm, where $p_{LCA}(t)$ represents one driving force in the model. Across the resistance R_{LCA} the pressure drops proportional to flow $Q_{LCA}(t)$ to $p_{bif}(t)$ where flow divide into the beds of the left anterior descending artery (LAD) and the left circumflex artery (LCX). From the bifurcation to the veins, the LAD and LCX beds were modeled symmetrically, i.e. equal parameters in the model and therefore only describe the LCX branch. For model Oswald and Kajgana the symmetry does not apply, since the LAD is usually bigger than the LCX. Crossing the corresponding two major regional coronary resistances from epicardial vessels up to the capillaries, $R_{LCX}^{art\rightarrow cap}$ and $R_{LAD}^{art\rightarrow cap}$, the model shows two distensible capillary compartments, i.e. volumes V_{LCX}^{cap} and V_{LCX}^{cap} and compliances C_{LCX}^{cap} and C_{LCX}^{cap}, which are filled and are subjected to extramural myocardial squeezing pressures. Arteries and arterioles were lumped into the resistances $R_{LCX}^{art\rightarrow cap} = R_{LAD}^{art\rightarrow cap}$ through which flow entered the capillary compartments. The term $capillary$ was used for the sake of simplicity, although in the present lumped parameter approach this term actually represents the entire microcirculatory compartments. These were modeled as inflatable balloons with a linear pressure volume relation, which were additionally exposed to an exterior pressure, $p_{LCX}^{sqz}(t) = p_{LAD}^{sqz}(t)$, representing the squeezing of myocardial contraction, where the squeezing pressure was set proportional to left ventricular pressure $p_{LV}(t)$:

$$p_{LCX}^{sqz}(t) = \gamma_{norm} \cdot p_{LV}(t) \tag{6.11}$$

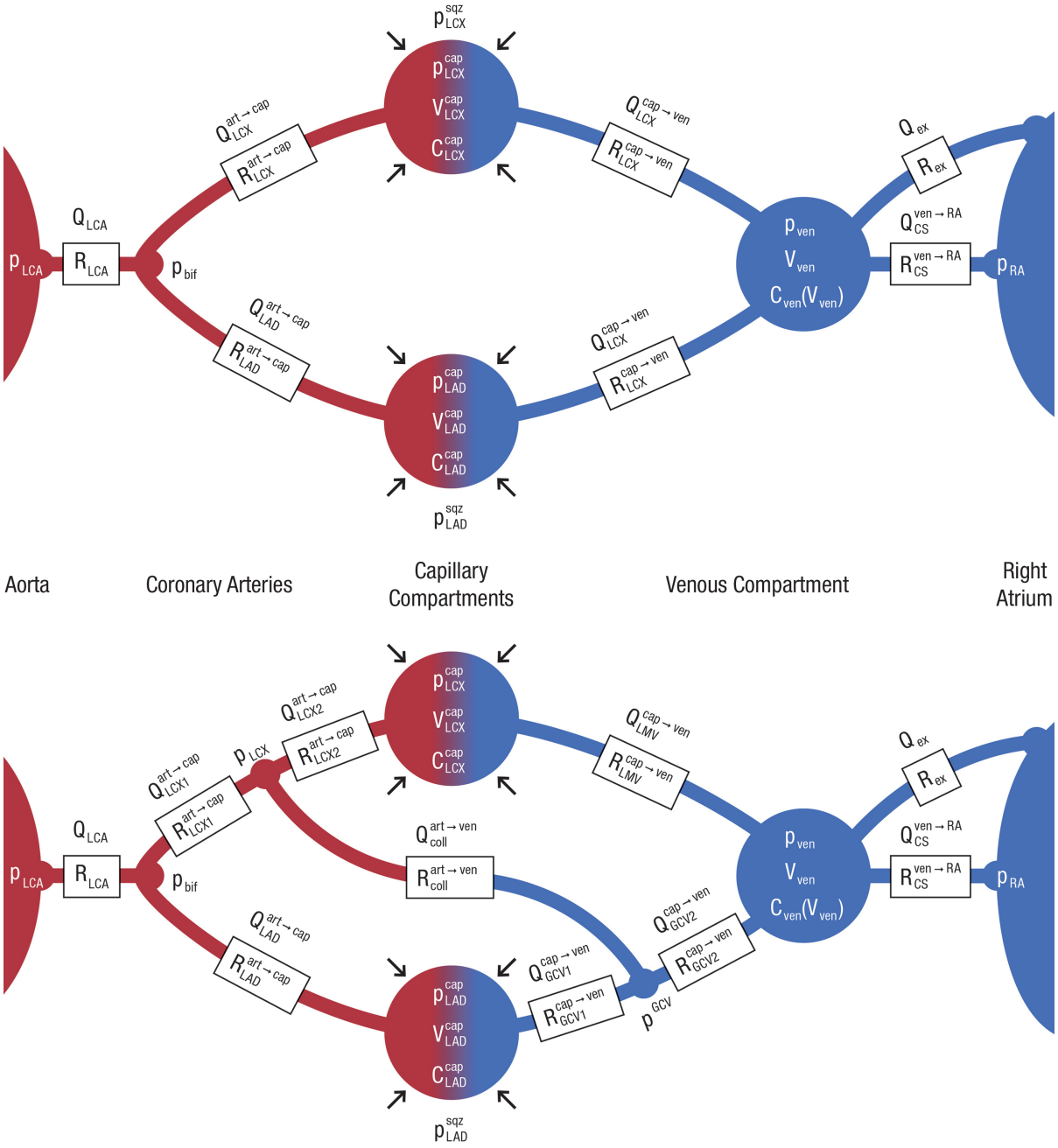

Figure 6.2: Schematics of Schreiner model *et al* (1990a,1990d) and Owasld (top) and model Kajgana (bottom) with the extensions. Note: Oswald model has the same denoation as Kajgana model, just without the extension. From LCA ostium (driving pressure $p_{LCA}(t)$), the left common artery ($R_{LCA}, Q_{LCA}(t)$), leads to the bifurcation $p_{bif}(t)$. LCX ($R^{art \to cap}_{LCX}, Q^{art \to cap}_{LCX}(t)$) leads to $C^{cap}_{LCX}, V^{cap}_{LCX}(t), p^{cap}_{LCX}(t)$, which is subjected to $p^{spz}_{LCX}(t)$. The venules draining the LCX bed ($R^{cap \to ven}_{LCX}, Q^{cap \to ven}_{LCX}(t)$) and the LAD bed ($R^{cap \to ven}_{LAD}, Q^{cap \to ven}_{LAD}(t)$) lead to (volume-dependent compliance $C_{ven}(V_{ven})$, volume $V_{ven}(t), p_{ven}(t)$). Then drains to RA (p_{RA} = constant) via CS ($R^{ven \to RA}_{CS}, Q^{ven \to RA}_{CS}(t)$) and the extra outlet ($R_{ex}, Q_{ex}(t)$).

with $p^{sqz}_{LCX}(t) = p^{sqz}_{LAD}(t)$.
Left ventricular pressure was obtained by Fourier expansion for a heart rate of 60 bpm and represented the second driving force. Experimental studies confirmed that phasic myocardial squeezing runs simultaneous to p_{LV} and that 75% of p_{LV} corresponds to a squeezing pressure. Hence γ_{norm} was set at 0.75 and γ_{norm} can be varied to investigate different degrees of squeezing. From both capillary compartments, blood flows across the resistances $R^{cap\to ven}_{LCX} = R^{cap\to ven}_{LAD}$ into a common venous compartment. Venous pressure was linked to venous volume by a non-linear pressure volume relation, which lets veins become stiffer, resisting distension, as volume increases. The venous compartment empties via the coronary sinus, $R^{ven\to RA}_{CS}, Q^{ven\to RA}_{CS}(t)$, and simultaneously via an extra outlet, $R_{ex}, Q_{ex}(t)$ into the right atrium (RA). The anatomic correlates to the extra outlet are Thebesian veins and small shunting veins draining directly into the right atrium. Coronary sinus occlusion was simulated by setting $R^{ven\to RA}_{CS} = \infty$.
A rather important part of the model is a volume-dependent coronary venous compliance, which decreases as the venous bed is distended. A pressure-volume relation of this kind proved to be mandatory in order to reproduce the CSP rise, with its characteristic shapes of systolic and diastolic envelopes. Further non-standard elements of the model are the volume-dependent resistances governing antegrade or retrogradely induced egress from the capillary compartment. In particular, the total resistance to flow leaving the capillaries was assumed to increase with the inverse square of capillary volume, i.e. effectively becomes infinite as the capillary bed is totally emptied. This assumption mimics the increased resistance during vessel 'collapse' due to systolic squeezing. The rest of the model employs ordinary linear relations between pressure gradients, resistances and flows.
Systolic and diastolic envelopes were fitted to the rise of coronary venous pressure after the onset of CSO, using the very same mathematical function described in the phenomenological modeling section. This offered the possibility to derive analogous diagnostic quantities from the model as those studied in vivo.
Additionally for model Kajgana applies: Coronary veins often run in pairs along the arteries and have interconnections along their course. Those interconnections are called collaterals and can exit between arteries and arteries or arteries and veins. They are individually pronounced in every heart and can be of great importance, if there is stenosis or some other dysfunction of the main vessels, because they can supply myocardium other ways.

6.3.3 Model equations

6.3.3.1 Volumes

In the above described models the **flow balance equations** between compartments have to be satisfied at any time:

$$\frac{d}{dt}V^{cap}_{LCX}(t) = Q^{art\to cap}_{LCX}(t) - Q^{cap\to ven}_{LCX}(t) \tag{6.12}$$

$$\frac{d}{dt}V^{cap}_{LAD}(t) = Q^{art\to cap}_{LAD}(t) - Q^{cap\to ven}_{LAD}(t) \tag{6.13}$$

$$\frac{d}{dt}V_{ven}(t) = Q^{cap\to ven}_{LCX}(t) + Q^{cap\to ven}_{LAD}(t) - Q^{ven\to RA}_{CS}(t) - Q_{ex}(t) \tag{6.14}$$

The right-hand sides of the flow balance equations can be obtained by calculating all pressures, starting from initial conditions for flows and volumes in all compartments. Numerical integration with respect to time can be performed to obtain the courses of all hemodynamic quantities in the model. Therefore it is necessary to know the flows at their corresponding time.

For model Oswald and Kajgana applies:

$$\frac{d}{dt}V_{LCX}^{cap}(t) = Q_{LCX}^{art\rightarrow cap}(t) - Q_{LMV}^{cap\rightarrow ven}(t) \tag{6.15}$$

$$\frac{d}{dt}V_{LAD}^{cap}(t) = Q_{LAD}^{art\rightarrow cap}(t) - Q_{GVC}^{cap\rightarrow ven}(t) \tag{6.16}$$

$$\frac{d}{dt}V_{ven}(t) = Q_{GCV}^{cap\rightarrow ven}(t) + Q_{LMV}^{cap\rightarrow ven}(t) - Q_{CS}^{ven\rightarrow RA}(t) - Q_{ex}(t) \tag{6.17}$$

6.3.3.2 Flows

Flows from the coronary arteries to the capillaries

These flows can be calculated from the resistance and the pressure gradient and represent the flow across the arterial side of microcirculation and not the flow though single capillaries. Depending on the pressure gradient, forward and backward flow can occur in the coronary arteries. Positive gradient between the pressure at the bifurcation point ($p_{bif}(t)$) and the pressure in the LCX capillary bed ($p_{LCX}^{cap}(t)$) is going to lead to forward flow and is given in the following equation:

$$Q_{LCX}^{art\rightarrow cap}(t) = \frac{p_{bif}(t) - p_{LCX}^{cap}(t)}{R_{LCX}^{art\rightarrow cap}} \tag{6.18}$$

for $p_{bif}(t) - p_{LCX}^{cap}(t) \geq 0$. If the gradient becomes negative, p_{LCX}^{cap} exceeds $p_{bif}(t)$, due to too strong myocardial squeezing, retrograde flow must cease as the volume of the capillaries approaches zero, i.e. nothing is left to be squeezed out. Furthermore, when the capillaries are compressed, their resistance increases and they throttle the flow. These circumstances have to be taken into account. This is done by adding a volume dependent flow resistance that reaches infinity when the capillary volume approaches zero. According to Poiseuille's law, resistance increases with the 2nd inverse power of vessel volume. This behavior leads to the following flow equation in its backwards form:

$$Q_{LCX}^{art\rightarrow cap}(t) = \frac{p_{bif}(t) - p_{LCX}^{cap}(t)}{R_{LCX}^{art\rightarrow cap} + \beta(V_{LCX}^{cap}(t))^{-2}} \tag{6.19}$$

with $p_{bif}(t) - p_{LCX}^{cap}(t) < 0$. The constant β = 1 mmHg s ml is parameter for the volume dependent resistance that re-establishes the correct dimensions.

Of importance is that the models switches from Eq.(6.18) to Eq.(6.19) only if both the pressure gradient and the corresponding flow pass through zero. As a result, the integration results, i.e. flows, pressures, volumes, remained continuous although the resistance to forward inflow into the capillary compartment were smaller than the resistance to retrograde outflow towards the coronary arteries. This feature was implemented in this model since it is easier to soak a network of capillaries with blood than to squeeze it totally empty once it has been filled. In this respect this model is different from other approaches, using resistances independent from the direction flow.

Due to the symmetry, the flows for the LAD side can be calculated analog in Schreiner model. For the asymmetry in model Oswald the LAD flow equations results in:

$$Q_{LAD}^{art\rightarrow cap}(t) = \frac{p_{bif}(t) - p_{LAD}^{cap}(t)}{R_{LAD}^{art\rightarrow cap}} \tag{6.20}$$

for $p_{bif}(t) - p_{LAD}^{cap}(t) \geq 0$ for the forward flow and the for the retrograde flow

$$Q_{LAD}^{art\to cap}(t) = \frac{p_{bif}(t) - p_{LAD}^{cap}(t)}{R_{LAD}^{art\to cap} + N \cdot \beta(V_{LAD}^{cap}(t))^{-2}} \tag{6.21}$$

for $p_{bif}(t) - p_{LAD}^{cap}(t) < 0$ with ratio $N = V_{LAD}^{myocard}/V_{LCX}^{myocard}$, where these volumes are not the actual volume of the blood in the corresponding region, but are the volumes of the myocardium that are supplied with blood by their corresponding arteries.

For model Kajgana the LCX side is a little different. The branching point of the collaterals split the LCX in two sections. The flow in the first section is simply given by:

$$Q_{LCX1}^{art\to cap}(t) = \frac{p_{bif}(t) - p_{LCX}^{cap}(t)}{R_{LCX1}^{art\to cap}} \tag{6.22}$$

where p_{LCX} is the pressure at the point where the collaterals leave the LCX. Furthermore, the R_{LCX1} is the flow resistance of the first part of the LCX. The flow in the second section of the LAD is described similar to the flow in the LCX, where the properties just have to be replaced accordingly. By increasing the R_{LAD} value a stenosis in the LAD can be simulated.

The forward flow is given by:

$$Q_{LCX2}^{art\to cap}(t) = \frac{p_{LCX}(t) - p_{LCX}^{cap}(t)}{R_{LCX2}^{art\to cap}} \tag{6.23}$$

for $p_{LCX}(t) - p_{LCX}^{cap}(t) \geq 0$ and the backward flow by:

$$Q_{LCX2}^{art\to cap}(t) = \frac{p_{LCX}(t) - p_{LCX}^{cap}(t)}{R_{LCX2}^{art\to cap} + \beta(V_{LCX}^{cap}(t))^{-2}} \tag{6.24}$$

for $p_{LCX}(t) - p_{LCX}^{cap}(t) < 0$.

Flow from capillaries to veins

The blood of LCX capillary bed drains into the left marginal vein (LMV). The flow equations were obtained similar formulae, where the forward flow is described as:

$$Q_{LCX}^{cap\to ven}(t) = \frac{p_{LCX}^{cap}(t) - p_{ven}(t)}{R_{LCX}^{cap\to ven} + \beta(V_{LCX}^{cap}(t))^{-2}} \tag{6.25}$$

for $p_{LCX}^{cap}(t) - p_{ven}(t) \geq 0$ and for backward flow:

$$Q_{LCX}^{cap\to ven}(t) = \frac{p_{LCX}^{cap}(t) - p_{ven}(t)}{R_{LCX}^{cap\to ven}} \tag{6.26}$$

for $p_{LCX}^{cap}(t) - p_{ven}(t) < 0$

For model Oswald following applies for the flow equations. The forward flows are given by:

$$Q_{LMV}^{cap\to ven}(t) = \frac{p_{LCX}^{cap}(t) - p_{ven}(t)}{R_{LMV}^{cap\to ven} + \beta(V_{LCX}^{cap}(t))^{-2}} \tag{6.27}$$

and

$$Q_{GCV}^{cap\to ven}(t) = \frac{p_{LAD}^{cap}(t) - p_{ven}(t)}{R_{GCV}^{cap\to ven} + N \cdot \beta(V_{LAD}^{cap}(t))^{-2}} \tag{6.28}$$

for$p^{cap}_{LCX}(t) - p_{ven}(t) \geq 0$ and $p^{cap}_{LAD}(t) - p_{ven}(t) \geq 0$, respectively.

The intermittent coronary sinus occlusion during PICSO lead to a pressure elevation in the veins. This can especially lead in the inflation phase to a negative pressure gradient, which then leads to the desired retrograde flow in the capillary beds. The resistance term for an emptied venous compartment is added for the sake of completeness, although this situation will almost never happen. Therefore, the backward flows are given by:

$$Q^{cap\to ven}_{LMV}(t) = \frac{p^{cap}_{LCX}(t) - p_{ven}(t)}{R^{cap\to ven}_{LMV} + \beta(V_{ven}(t))^{-2}} \tag{6.29}$$

and

$$Q^{cap\to ven}_{GCV}(t) = \frac{p^{cap}_{LAD}(t) - p_{ven}(t)}{R^{cap\to ven}_{GCV} + \beta(V_{ven}(t))^{-2}} \tag{6.30}$$

for $p^{cap}_{LCX}(t) - p_{ven}(t) < 0$ and $p^{cap}_{LAD}(t) - p_{ven}(t) < 0$, respectively.

For model Kajgana the great cardiac vein situation is a little different because the GCV is divided into two section in order to allow collateral inflow. In the first section of the GVC, which is near the capillary bed, following equations have to be considered for the forward flow situation:

$$Q^{cap\to ven}_{GCV1}(t) = \frac{p^{cap}_{LAD}(t) - p_{GCV}(t)}{R^{cap\to ven}_{GCV1} + \beta(V_{LAD}(t))^{-2}} \tag{6.31}$$

and for the second section

$$Q^{cap\to ven}_{GCV2}(t) = \frac{p_{GCV}(t) - p_{ven}(t)}{R^{cap\to ven}_{GCV2}} \tag{6.32}$$

for $p^{cap}_{LAD}(t) - p_{GCV}(t) \geq 0$ and $p_{GCV}(t) - p_{ven}(t) \geq 0$, respectively.
The pressure at the point, where the collaterals flow into the GCV is denoted as p_{GCV}. The backward flows are given by:

$$Q^{cap\to ven}_{GCV1}(t) = \frac{p^{cap}_{LAD}(t) - p_{GCV}(t)}{R^{cap\to ven}_{GCV1}} \tag{6.33}$$

for the first section and for the second:

$$Q^{cap\to ven}_{GCV2}(t) = \frac{p_{GCV}(t) - p_{ven}(t)}{R^{cap\to ven}_{GCV2} + \beta(V_{ven}(t))^{-2}} \tag{6.34}$$

for $p^{cap}_{LAD}(t) - p_{GCV}(t) < 0$ and $p_{GCV}(t) - p_{ven}(t) < 0$, respectively.

Balance equations

To set up the above equations Eq.(6.23)(6.24) and Eq.(6.32)(6.34), two quantities are introduced, which represents the pressure at both ends of the collaterals, i.e. p_{LCX} and p_{GCV}. Consequently, two more equations are necessary to determine the system. These are the flow balances at the points where the collaterals branch off the LCX and flow into the GCV, respectively:

$$Q^{art\to cap}_{LCX1}(t) = Q^{art\to cap}_{LCX2}(t) + Q^{art\to ven}_{coll}(t) \tag{6.35}$$

$$Q^{cap\to ven}_{GCV2}(t) = Q^{cap\to ven}_{GCV1}(t) + Q^{art\to ven}_{coll}(t) \tag{6.36}$$

$$\text{with } Q^{art\to ven}_{coll}(t) = \frac{p_{LCX}(t) - p_{GCV}(t)}{R^{art\to ven}_{coll}} \tag{6.37}$$

Flow from the venous bed to the right atrium

As mentioned above, the venous blood empties via the coronary sinus and via an extra outlet, which represents the Thebesian vein, into the right atrium. There is also the possibility to run a simulation with and without PICSO in order to study the effects of the treatment on myocardial arterial and venous flows and pressures. This is possible by setting the coronary resistance very high in the cases of coronary sinus occlusion. The right atrium is considered as an infinite reservoir at constant pressure p_{RA}. The forward flow equation is given by:

$$Q_{CS}^{ven \to RA}(t) = \frac{p_{ven}(t) - p_{RA}(t)}{R_{CS}^{ven \to RA} + \beta(V_{ven}(t))^{-2}} \tag{6.38}$$

for $p_{ven}(t) - p_{RA}(t) \geq 0$ and for backward flow, with no limiting volume, results in:

$$Q_{CS}^{ven \to RA}(t) = \frac{p_{ven}(t) - p_{RA}(t)}{R_{CS}^{ven \to RA}} \tag{6.39}$$

for $p_{ven}(t) - p_{RA}(t) < 0$. Extraordinary venous outflow Q_{ex} was obtained in a similar manner. Additionally, a pressure offset p_{ven}^{off} was included to account for smaller shunting veins which drain directly into both atria rather than via the joint venous compartment. They originate in the venous microcirculation upstream of the large veins. This was modeled by the parameter p_{ven}^{off}, which slightly elevates the pressure gradient for extraordinary flow as compared to coronary sinus flow. The forward flow equation is given by:

$$Q_{ex}(t) = \frac{p_{ven}(t) - p_{RA}(t) + p_{ven}^{off}}{R_{CS}^{ven \to RA} + \beta(V_{ven}(t))^{-2}} \tag{6.40}$$

for $p_{ven}(t) - p_{RA}(t) \geq 0$ and a retrograde is not allowed here and $Q_{ex}(t)$ will be set to zero if $p_{ven}(t) - p_{RA}(t) < 0$.

6.3.3.3 Pressures

Bifurcation pressure

At the beginning the pressure of the left coronary artery $p_{LCA}(t)$ was set equal to the aortic pressure. The pressure at the bifurcation $p_{bif}(t)$ can be calculated with the relation

$$p_{bif}(t) = p_{LCA}(t) - R_{LCA}Q_{LCA} = p_{LCA}(t) - R_{LCA}(Q_{LCX}^{art \to cap}(t) + Q_{LAD}^{art \to cap}(t)) \tag{6.41}$$

For model Kajgana $Q_{LCX}^{art \to cap}(t)$ is adapted to $Q_{LCX1}^{art \to cap}(t)$.

Capillary pressure

The capillary compartments of the LAD and LCX are presented by compliances, C_{cap}^{LAD} and C_{LCX}^{cap}, which hold a certain volume V_{LAD}^{cap} and V_{LCX}^{cap}. Resistance of the compliance is neglected because their overall cross-sectional area is larger than the cross-sectional area of the artery by about three magnitudes. The intravascular pressure in the capillary bed is the sum of the vessels' elastic reaction against distension, i.e. $\frac{V_{cap}}{C_{cap}}$ and a superimposed myocardial squeezing pressure $p_{sqz}(t)$, which is the second driving force in the model.

$$p_{LCX}^{cap}(t) = \frac{V_{LCX}^{cap}(t)}{C_{LCX}^{cap} + p_{LCX}^{sqz}(t)} \tag{6.42}$$

$$p_{LAD}^{cap}(t) = \frac{V_{LAD}^{cap}(t)}{C_{cap}^{LAD} + p_{LAD}^{sqz}(t)} \tag{6.43}$$

As mentioned above, the squeezing pressure can be defined as:

$$p_{LCX}^{sqz}(t) = \gamma_{norm} \cdot p_{LV}(t) \tag{6.44}$$

$$p_{LCX}^{sqz}(t) = \gamma_{sten} \cdot \gamma_{norm} \cdot p_{LV}(t) \tag{6.45}$$

where γ_{sten} is chosen to be one and chosen smaller than one for reduced myocardial function in the LAD dependent region.

Venous pressure

The venous pressure is related to a non-linear relationship, where the compression pressure has not to be considered, since the vessels are on the epicardium. Starting from a volume dependent compliance

$$C_{ven}(V_{ven}(t)) \equiv \frac{dV_{ven}(t)}{dp_{ven}(t)} = \frac{\chi_{ven}}{1+\sigma V_{ven}(t)} \cdot e^{-\sigma(V_{ven}(t)-V^0_{ven}(t))} \tag{6.46}$$

the venous pressure can be calculated by integration:

$$p_{ven}(t) = \frac{V_{ven}(t)}{\chi_{ven}} \cdot e^{\sigma(V_{ven}(t)-V^0_{ven}(t))} \tag{6.47}$$

Chapter 7

PICSO in Myocardial Infarction

Egred *et al.* (2016) stated that a major determinant of morbidity and mortality after STEMI is the extent of myocardial necrosis after PCI, and strategies to limit infarct size may improve prognosis. Numerous mechanical and pharmacological interventions have been studied as potential cardioprotective therapies, with disappointing results. As demonstrated in human studies by Kessels *et al.* (2015), PICSO may enhance myocardial recovery in acute myocardial infarction. The authors assessed the effect of pressure-controlled intermittent coronary sinus occlusion on myocardial salvage in acute MI.

van de Hoef *et al.* (2015) wrote that despite substantial mortality reduction associated with the widespread use of timely primary percutaneous coronary intervention (pPCI) for ST-segment elevation myocardial infarction (STEMI), STEMI survivors remain at high risk for recurrent cardiovascular events.

van de Hoef *et al.* (2012) found that reperfusion therapy in the setting of ST-segment elevation myocardial infarction aims at early restoration of blood flow in the culprit coronary artery by means of primary percutaneous coronary intervention (PCI). Despite a high success rate in restoration of epicardial blood flow by primary PCI, perfusion at the myocardial level is frequently hampered though optimal epicardial reperfusion is achieved. Impaired myocardial reperfusion is considered a consequence of multiple factors and is suboptimal in approximately 40% of patients after primary PCI for STEMI. It is associated with higher mortality, larger infarct size, and reduced left ventricular function at follow-up and reversal of this phenomenon was shown to be associated with a favorable effect on left ventricular remodeling, even without apparent improvement in regional contractile function. Myocardial reperfusion, as well as its improvement during follow-up, is therefore an important determinant of clinical outcome after primary PCI for STEMI and its optimization is considered a target to improve clinical outcomes. Pressure-controlled intermittent coronary sinus occlusion is a novel concept, which aims to improve perfusion at the microvascular level.

Furthermore, Mohl *et al.* (2008) wrote that despite all endeavors to achieve timely reperfusion in acute coronary syndromes (ACS) many efforts fall short to limit myocardial jeopardy in the ischemia - reperfusion complex in a large cohort of patients. Several interesting concepts are investigated to overcome this problem. Coronary sinus interventions (CSI) interfere in the coronary microcirculation using the coronary venous access. Some decades ago, during the pre- primary percutaneous coronary intervention (PCI) era, CSI were a popular concept for re-

ducing myocardial ischemia. There are 2 distinct CSI, each representing a different school of thought. There are proponents of retroperfusion of arterial blood and others proposing the concept of pressure-controlled intermittent coronary sinus occlusion (PICSO) methods. Syeda *et al.* (2004) reported no statistical difference in the salvage potential between these 2 methods in a meta-analysis of both methods, and showed that salvage was related to the developed pressure in the coronary sinus (CS). Although both methods never reached widespread scientific acceptance, clinical data from a few human trials are available for both methods. Retroperfusion was mainly studied in supporting coronary interventions and in cardiac surgery.

In this regard, the extent of myocardial necrosis is an important determinant of post-infarct cardiovascular events. It is well recognized that successful achievement of epicardial vessel patency by pPCI does not imply optimal restoration of perfusion at the microvascular level, which remains impaired in up to 40% of patients and is associated with greater infarct size, reduced left ventricular function, and adverse clinical outcome. Optimization of myocardial perfusion after pPCI is therefore considered an important therapeutic strategy to limit morbidity and mortality in STEMI survivors [van de Hoef *et al.* (2012)].

The mechanism of PICSO in STEMI is based on the following 3 concepts [van de Hoef *et al.* (2012)].

- First, PICSO results in improvement of myocardial perfusion by redistribution of blood from the venous outflow tract of the left anterior descending (LAD) coronary artery to the border zone of the ischemic anterior wall myocardium.
- Second, the periodic increase in pressure resulting from PICSO is transferred onto the venous endothelium, which may improve long-term outcome due to the release of vascular growth factors.
- Third, the intermittent release of pressure is expected to facilitate washout of deleterious agents from the microcirculation.

Pressure-controlled intermittent coronary sinus occlusion aims to improve microvascular perfusion after pPCI for STEMI by intermittently increasing the pressure in the cardiac venous outflow tract using a balloon-tipped catheter introduced in the coronary sinus. PICSO is proposed to redistribute venous blood to the border zone of the ischemic myocardium, to enhance washout of deleterious agents from the microcirculation, and to induce release of vascular growth factors from the venous endothelium, thereby limiting the extent of myocardial necrosis and enhancing infarct healing. Data from large animal models [Syeda *et al.* (2004)] of acute myocardial infarction show that intermittent occlusion of the coronary sinus yields the potential for a marked reduction in infarct size, and the underlying hemodynamic effects of PICSO were confirmed in a clinical study [van de Hoef *et al.* (2012)]. The present study is the first to evaluate the safety and feasibility of PICSO in the setting of acute STEMI, concomitantly exploring its effects on myocardial necrosis and myocardial function [van de Hoef *et al.* (2015].

In contrast to other retroperfusion techniques, the retroperfusion by PICSO is passive of nature. Moreover, the technique claims that not only redistribution of venous flow, and the facilitation of microvascular washout, but also activation of the venous vasculature is an important denominator of its beneficial effects. A meta-analysis of 7 animal studies [Syeda *et al.* (2004)] evaluating the effect of PICSO on infarct size showed a significant reduction in infarct size in the treatment group compared with the control group (mean infarct size 48.7%, and 78.8%, respectively, weighted mean difference -29.3%; 95% confidence interval -40.9% to -11.7%; $p < 0001$). The essential mechanism of action of PICSO is based upon an intermittent increase of pressure in the CS to a plateau pressure

that is transmitted to the microcirculation of the LAD. In the presence of LAD occlusion, and in the absence of microvascular obstruction, this pressure increase will be transmitted to the distal coronary artery, augmenting distal coronary wedge pressure. To document this key intracoronary hemodynamic change induced by PICSO, this first-in-man study evaluated the direct effect of balloon occlusion of the CS on intracoronary pressure parameters distal to an LAD occlusion during elective PCI [van de Hoef *et al.* (2012)].

In advancing the field of broadening the treatment options for ACS, logistic burden again makes it necessary to undo the rigid relationship between the elapsed time and potential salvage, prevent reperfusion injury, to further reduce ischemic sequelae. In addition, new pathophysiologic insight broadens the knowledge on avoidable injury and pathways on the induction of regeneration. Therefore, it seems logical to recall methods that are easily available and effective, in addition to modern revascularization strategies. Reports by Managano *et al.* (2006) and Ota *et al.* (2006) on the application of adenosine or nicorandil in addition to revascularization, or reports by Patel *et al.* (2005) on stem cell-based approaches show the potential of adjunct therapies.
It has been ignored that long-term data exist on PICSO techniques, of which short-term results have been reported. The aim is to re-evaluate this concept and to analyze data on long-term results of patients with a clinically feasible 'adjunct' therapy of PICSO.
Needless to say, this kind of study would never be collected today owing to other therapies, concepts and regimen being en vogue and, therefore, it represents a unique opportunity to evaluate pathophysiologic insight into myocardial ischemia and reperfusion, as well as pathways influencing clinical outcome [Mohl *et al.* (2008)].

Egred *et al.* (2017) continued that the use of pressure-controlled intermittent coronary sinus occlusion has been shown to decrease ischemic damage during coronary occlusions in pre-clinical studies. Whether PICSO reduces infarct size in patients with STEMI undergoing primary PCI and whether coronary sinus occlusion should be established before reperfusion [Kessels *et al.* (2015)] is unknown.

Chapter 8

Material and Methods

8.1 Phenomenological modeling

8.1.1 Testing the models with experimental and clinical data

The in the previous chapter mentioned outlined concepts by Schreiner *et al.* (1990b) were applied to data obtained during both canine and human investigations of PICSO by Mohl *et al.* (1988b), Schreiner *et al.* (1988a) and (1988b). Time courses and mean values of plateaus, end-pressures and rise times were calculated and statistically analyzed. In the dog study, which featured an acute LAD coronary artery occlusion followed by reperfusion, the occlusion/release timing was preset according the particular experimental protocol. Statistical analysis revealed that plateaus and even more so, the rise times are affected by a large spread, despite experimental conditions remaining constant. Thus, to reduce spread to 10% SEM, plateau values form about five successive PICSO cycles have to be averaged; 10 cycles are required for T90_SY and as much 40 cycles for T90_DI. These findings provide essential information regarding computer based closed-loop PICSO control systems. In the human study, PICSO was applied during coronary artery bypass graft surgery in the reperfusion phase. t_0 was initially set to some low value, e.g. 5s, and then gradually increased until systolic P_{CSP} developed something resembling the onset of a plateau. Subsequently, t_0 was readjusted according to visual inspection according to the following criteria: Should an initial setting of t_0 prove insufficient, e.g. due to physiological changes, to produce the onset of a plateau, t_0 was carefully increased, not exceeding an upper limit of 14s which was deemed potentially hazardous. On the other hand, t_0 was reduced immediately if a prolonged systolic CSP plateau appeared. The release time was kept constant at 4s. One physician was entirely occupied with monitoring P_{CSP} tracings and adjusting the PICSO timing. The human study data were mainly used to compare the visually adjusted coronary sinus occlusion time with the rise times calculated from the mathematical model. The postoperative computerized data reduction revealed that visual adjustment did not always properly keep pace with the rapid physiologic changes observed during the surgical procedure. Opening of the grafts entailed an immediate decrease in rise time (T90_SY), calculated from the model. Interestingly, the physician operating the PICSO controller also reduced t_0 (based on visual inspection), however, with a significant delay in time. These findings suggest that modeling results represent useful aids for CSI control. Considering the spread of numerical diagnostics, as investigated in the dog study, one has to be aware, however, that a reliable adjustment of PICSO phasing requires an averaging of rise times over at least 10 PICSO cycles. The question still remains about how rapidly an automatic regulation should follow the changes in

calculated diagnostics, without sacrificing a good deal of regulation security and stability for which time-consuming averaging proved mandatory.

Finally, both phenomenological models were compared using the very same human or canine data. The fitting algorithm of model 2 in its original form proved unstable due to the fact that two out of three parameters, A and α, are derived from single P_{CSP} data points. Therefore, the authors replaced the model 2 fitting method by a true non-linear least squares procedure for all three parameters. Mean derived quantities then turned out to be quite similar for both models, and model 2 thereby additionally gained extrapolation capability. Another criterion of model performance is the numerical stability in the presence of certain artifacts in real data measurements, e.g. extrasystoles, temporary loss of data, insufficient coronary sinus balloon occlusion, poorly calibrated signals. Model 2, with the improved fitting algorithm, proved slightly superior when calculating the fraction of PICSO cycles which could be evaluated without numerical difficulties. The authors concluded that the improved model 2 is to be preferred to model 1 for closed-loop regulation of PICSO. Due it its analytical form, however, model 2 cannot properly represent the early part of a PICSO cycle. For theoretical investigations, they therefore recommend model 1, since it is more realistic and the 'drop-out' rate is only slightly higher.

8.1.2 Interpretation of quantities derived from phenomenological modeling

Derived diagnostic quantities can provide information on the state of the myocardium. For instance, the systolic plateau is closely related to contractile function which, during systole, is largely responsible for the squeezing of blood into the venous bed. During the coronary sinus occlusion, blood accumulates and distend the coronary veins. Thus, the systolic rise and plateau of venous pressure directly reflect the elastic recoil of the venous bed against the input of additional volume, the latter being directly linked to myocardial contraction. Similar arguments apply to the mean integrals (systolic, diastolic) and even more to their difference (INTM_SY - INTM_DI). Statistically, estimate for P_SY are affected by larger spread than those for INTM_SY. In fact, during experimental LAD ligation in dogs [Schreiner *et al.* (1988a)], P_SY declined in one dog while practically no reaction could be found in another animal. The difference INTM_SY - INTM_DY declined in all cases. In the human study [Schreiner *et al.* (1988b)] it was the 90% rise time which showed a remarkable decline following enhanced coronary artery perfusion after opening of the bypass grafts. The detailed mechanisms governing these processes have to be investigated by the use of mechanistic modeling techniques, as described in the subsequent section.

8.1.3 Modes of adaption

Three principal modes of adaption may be envisaged, which differ in concept and complexity:

- fixed adaptation schemes for t_0 and t_r;
- disease-related adaptation schemes;
- disease- and recovery-related adaptation schemes.

A fixed adaption scheme derives t_0 and t_r from calculated diagnostics along fixed lines, i.e. inserts T90_SY, P_SY, etc. into fixed mathematical formulas to get t_0 and t_r. As P_SY, T90_SY, etc. change with changing physiological states, t_0 and t_r will track these changes and may thus be called adaptive, following a fixed adaption mechanism.

The authors speculated that an acute regional infarction actually requires an algorithm, for deriving optimal t_0 and t_r, which is different from the algorithm for moderate global ischemia, i.e. disease-related adaptation. It is not clear whether, or which mode of adaptation is most effective for the above mentioned two main types of ischemia.

Finally, with either type of ischemia, even a disease-related adaptation does not account for the fact that the adaptation most favorable during the initial phase of treatment, e.g. set t_0 = T90_SY, could be suboptimal and should therefore be changed, e.g. to set t_0 = T70_SY, in an advanced state of recovery. Such a 'disease-and-recovery-related' adaption scheme additionally has to incorporate criteria for switching algorithms during recovery.

It is important to point out that experimental studies are only useful to validate (evaluate) the efficacy of a given adaptation scheme, they are an inappropriate tool however, in the search for an adaptation scheme.

8.1.4 Relationship between coronary sinus pressure and coronary artery flow

In modeling the release time regulation of PICSO, the authors assume that peak flow in the coronary sinus during its release occurs well before a maximum of the antegrade flow (reactive hyperemia) can be observed in the coronary arteries. Therefore, the occurrence of peak arterial flow is believed to be a suitably conservative indicator of the duration of the coronary sinus release phase in order to achieve sufficient reduction of overall coronary perfusion, and to allow for toxic metabolites to be washed out from jeopardized regions of the myocardium. In humans arterial flow cannot as yet to be measured directly and CSP is the only quantity generally inferred. They investigated in an experimental study the relationship between CSP and arterial flow and tried to predict the occurrence of the reactive hyperemic response from CSP measurements.

8.1.5 Methods

In three dogs, left ventricular pressure (LVP), CSP and arterial flow in the left anterior descending (LAD) and in the circumflex artery (CX) were monitored continuously. PICSO was applied during normal perfusion, LAD-infarction and reperfusion (1 h each), in 3 x 9 different series, each consisting of 20 - 25 uniform occlusion and release cycles, characterized by systematically varied values of cycle length and occlusion/release ratio. Fourier analysis was applied to averages of 10 superimposed PICSO cycles of each series. CX and LAD flows were added to yield the total left coronary blood flow.

Fourier coefficients for 40 frequencies of total arterial flow, $\Phi(t)$, and of the LVP-CSP pressure difference, i.e. pressure gradient, $\Delta p(t)$, were calculated for all such averages of PICSO cycles.

Complex Fourier coefficients:

$$\hat{\Phi}_n = \frac{1}{T}\int_0^T dt e^{-i\omega_n t}\Phi(t)\Delta p_n = \frac{1}{T}\int_0^T dt e^{-i\omega_n t}\Delta p(t) \tag{8.1}$$

$$\Delta p_n = \frac{1}{T}\int_0^T dt e^{-i\omega_n t}\Delta p(t) \tag{8.2}$$

where T is the total length of a PICSO cycle and $\omega_n = \frac{2\pi n}{T}$; n = 0, $\pm$ 1, $\pm$ 2,... is the discrete set of frequencies compatible with the cycle length T.

It was evident from the spectra that 4 - 5 frequencies are sufficient to study the pressure-flow relationship in the low-frequency range. Assuming, as a first approximation, a generalized linear relationship between arterial flow and pressure gradient, i.e. assuming that for each frequency the respective Fourier coefficients of pressure and flow are proportional to each other, $\hat{\Phi}_n$ is given by:

$$\hat{\Phi}_n = \begin{cases} \hat{y}_0 \Delta p_0 & + \quad \hat{\Phi}_0^{res} \quad n = 0 \\ \hat{y}_n \Delta p_n & \qquad\qquad\quad n \neq 0 \end{cases} \tag{8.3}$$

Since the average flow was found to be almost constant, probably due to a non-coronary sinus flow $\hat{\Phi}_0^{res}$, such as Thebesian flow, lymphatic flow, or collateral venous flow, and independent of the average pressure gradient, proportionality holds for non-zero frequencies only. Experimental proportionality coefficients $\hat{y}'_n$, were calculated by dividing the five lowest flow Fourier coefficients obtained from each series of 10 superimposed PICSO cycles by the corresponding pressure Fourier coefficient, i.e.

$$\hat{y}'_n = \frac{\hat{\Phi}_n}{\Delta p_n}; n = 0, 1, ..., 4. \tag{8.4}$$

Inspection of the experimental $\hat{y}'_n$ shows that for n $\neq$ 0 the transfer function can be roughly approximated by

$$\hat{y}(\omega) = \frac{A}{1 + i\omega\tau} \tag{8.5}$$

i.e. arterial flow is essentially the convolution in the time domain of the pressure gradient with an exponential $A \cdot e^{-\frac{t}{\tau}}$. The parameters can be determined by minimizing the mean square difference between predicted and observed arterial flow.
Minimizing criterium:

$$\frac{1}{T} \int_0^T dt \Big\{ \sum_{n \neq 0} \hat{y}(\omega_0) \Delta p_n e^{i\omega_n t} - [\bar{\Phi}(t) - \hat{\Phi}_0] \Big\}^2 = 2 \Big\{ \sum_{n=1}^{n_{max}} |\Delta p_n|^2 |\hat{y}(\omega_n) - \hat{y}'_n|^2 \Big\} \rightarrow min. \tag{8.6}$$

For reasons to be discussed later, the average (= net) flow $\hat{\Phi}_0 = T^{-1} \int dt \Phi(t)$ is subtracted from the observed flow values, i.e. it is only the deviation of flow from its average value or the shape of the low curve and not the net amount of flow, which is optimized.

Multiplying the experimental CSP Fourier coefficients of any PICSO cycle by $\hat{y}(\omega)$ and inserting the resulting coefficients into the Fourier transform, yields the predicted estimate of the flow curve for that PICSO cycle. The time lag between balloon deflation (at the end of the occlusion period) and the occurrence of the predicted flow maximum can then be used to regulate the length of the release period of the following PICSO cycle.

In their study the transfer function was only fitted to the experimental data of two dogs and applied to the pressure data of the third dog, thus trying a first validation if their method by predicting the occurrence of reactive hyperemia for a third dog from its CSP data and comparing the prediction with the experimental data.

8.2 Mechanistic modeling

8.2.1 Simulation of PICSO under normal conditions, global loss of contractility and reduced perfusion pressure

Schreiner *et al.* (1990b) reported that PICSO is simulated by forcing coronary sinus flow to zero during the balloon inflation periods. Mathematically, this is a boundary condition to the differential equations.

Of all the quantities calculated form the model, e.g. pressures and volumes in each compartment, flows between compartments, the quantity of most interest with regard to CSI effectiveness is the retrograde flow delivered from the coronary venous bed to the capillaries. This computed delivery directly characterizes the retrograde access of the myocardium. For the normal state, following Figure 8.1 displays the time course of the LCX flow from arteries to capillaries (dashed) and from capillaries to veins (solid curve) over a whole PICSO cycle (panel a) and in single beat resolution for CSO (panel b) and CSR conditions (panel c). The area between the baseline and the negative portion if the solid curve reflects the volume of blood redistributed from the coronary venous system toward the capillaries within each heartbeat and may be considered an important quantity characterizing the degree of PICSO 'washout' of toxic metabolites. Just like any other quantity obtained from the mathematical model, the redistributed blood volume may be investigated as a function of any other model parameter(s) to mimic the effects observed under pathological condition. For the sake of briefness only the effects of globally reduced myocardial contractility and changes in arterial perfusion pressure will be illustrated here.

The joint variation of myocardial squeezing (parameter γ_{norm}) and of arterial perfusion pressure (p_{LCA}) was simulated on a grid defined by $0 \leq \gamma_{norm} \leq 1$ and $10 \leq p_{LCA} \leq 140$ mmHg. The mean retrograde flow per heartbeat form veins to capillaries was calculated in each of these simulations during a reference beat under CSO and CSR conditions, respectively. The results were displayed as surface charts. During CSO maximum redistribution is found around a rather linear relation between γ_{norm} and p_{LCA}, where the valley extending from γ_{norm} = 0.25 and p_{LCA} = 40 mmHg to γ_{norm} = 0.95 and p_{LCA} = 120 mmHg. Moreover, it becomes evident that no redistribution is observed in the absence of squeezing (γ_{norm} = 0). This seems to be an important result since one may conclude that severely ischemic areas or arrested myocardium, in which myocardial contraction has ceased, are inaccessible to assistance by PICSO.

During CSR, no redistribution is found in the vicinity of ordinary parameter conditions. Only for very faint squeezing does redistribution occur. In a similar way, the derived diagnostic quantities, systolic and diastolic 90% rise times can be obtained for every combination of squeezing and perfusion pressure.

Physiologically, the line along p_{LCA} = const = 100 mmHg may be interpreted as showing the effect of PICSO under moderate global ischemia, as seen, for instance, during the reperfusion phase after open heart surgery.

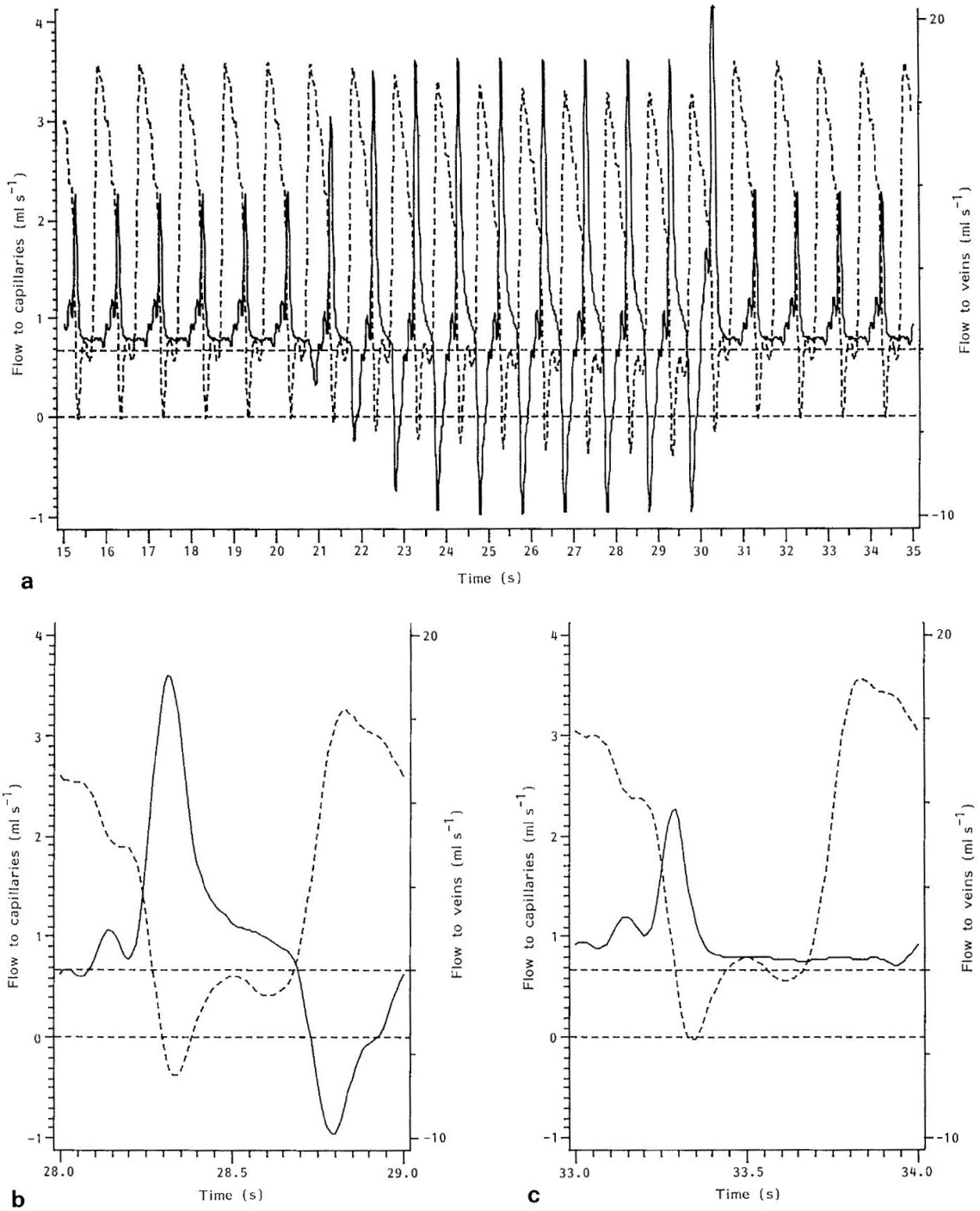

Figure 8.1: Flow dynamics: a) Full time course of flow from the coronary arteries to the capillaries, ($Q_{LCX}^{art \to cap}$, dashed curve) and of flow form the capillaries to the venous compartment ($Q_{LCX}^{cap \to ven}$, solid curve). b) Single beat resolution during coronary sinus occlusion; c) Single beat resolution during coronary sinus release [Schreiner *et al.* (1990b)].

8.2.2 Simulation of PICSO during LAD stenosis and infarction

The retrograde flow from coronary veins to the capillary bed can also be investigated under the joint variation of R_{LAD}^{sten} and p_{LAD}^{sqz}. R_{LAD}^{sten} was varied between 0 (= normal perfusion) and 5000 mmHg (total LAD obstruction),

extramural squeezing in the LAD was varied between 0% and 100% of the normal value ($0 \leq \gamma_{sten}^{LAD} \leq 1$).

Whereas every combination of R_{LAD}^{sten} and γ_{sten}^{LAD} can be simulated in the model, an LAD infarction event in a patient will run only through characteristic combinations of R_{LAD}^{sten} and γ_{sten}^{LAD}, since the loss of contractility is a physiological consequence of low reduction, thus forming an 'infarction trace' over $R_{LAD}^{sten} - \gamma_{sten}^{LAD}$ - plane. To model this trace, mean LAD flow, $Q_{LAD}^{art \rightarrow cap}$, was calculated for each step of R_{LAD}^{sten} increase and expressed as fraction of normal LAD flow. Results reported in literature by Sabbah *et al.* (1982), Stein *et al.* (1980) and Vatner *et al.* (1980) were used to estimate the corresponding reduction in myocardial squeezing (γ_{sten}^{LAD}). Then the simulation was repeated using this particular combination of R_{LAD}^{sten} and γ_{sten}^{LAD} to yield one point on the trace shown. Repeating this procedure for $0 \leq R_{LAD}^{sten} \leq$ 5000 mmHg · s/ml adds up to the full trace. An infarction episode would run from location 1 (healthy) via locations 2 to 5 toward the 68% end (zero flow) of the full heavy trace.

The relation between R_{LAD}^{sten} and γ_{sten}^{LAD} inferred from Stein *et al.* (1980) and Vatner *et al.* (1980) terminates at γ_{sten}^{LAD} = 0.68, since experimental measurements [Sabbah *et al.* (1982)] indicate that even in the case of total loss of regional contractility, intramyocardial pressure is maintained around 68% of normal values, due to the wall tension within the bulging segment. However, since measurements of intramyocardial pressure are very controversial [Sabbah *et al.* (1982)] two other assumptions for the reduction in squeezing, to 30% and to 0% of normal values, have additionally been investigated in the model. Obviously, these lead to combinations of R_{LAD}^{sten} and γ_{sten}^{LAD} much less favorable for retrograde redistribution during PICSO.

Since R_{LAD}^{sten} and γ_{sten}^{LAD} refer to the LAD bed, the model results are non-symmetric for the LAD and LCX beds, Besides drastic changes in the LAD region, LCX-hemodynamics are also slightly affected, due to redistribution phenomena. For reasons of briefness, only the more important LAD results are shown here.

8.2.3 Assessment of model parameters

Schreiner *et al.* (1990d) stated that the values for the model parameters were determined in a two-pass multistep procedure. First, primary estimates were assigned to the parameters. Then, in pass 1 of the adaption process, different boundary conditions were applied and the model results were compared with experimental data referring to the same conditions. Each boundary condition made the model results particularly sensitive to a specific (subset of) model parameter(s) and thus allowed for an assessment of these parameters. Referring to the notation used in the preceeding section and in Fig. 6.2, they briefly outline this process:

Pass 1: R_{LCA} was calculated from anatomical data and Poiseuille's law. For the study, R_{LCA} proved to have negligible importance, cf., also the sensitivity analysis below. One would obtain almost identical results by omitting Eq.(6.41) and substituting $p_{LCA}(t)$ for $p_{bif}(t)$ in Eq.(6.18) and Eq.(6.19). However, the formulation including R_{LCA} keeps the model open to study a main left stenosis and/or an LAD stenosis without changing the differential equations and reassessing all parameters.

The resistance ratio between arteries and veins $R_{LCX}^{art \rightarrow cap}$ / $R_{LCX}^{cap \rightarrow ven}$ was set at 10 in accordance with experimental data. The following parameters were set only on a preliminary basis during the first pass: the sum of resistances $R_{LCX}^{art \rightarrow cap}$ / $R_{LCX}^{cap \rightarrow ven}$ = 57 mmHg s / mL was estimated from the gradient between mean aortic and

right atrial pressure; capillary compliance C^{cap}_{LCX} = C^{cap}_{LAD} = 0.05 mL/mmHg and venous reference volume V^0_{ven} = 25 mL were taken from experimental data; venous compliance was set constant (σ = 0 m/L) at $\chi_{ven} = C_{ven}$ = 0.25 mL / mmHg, which is five times the capillary value; outflow resistances were set at $R^{ven \to RA}_{CS}$ = 2 mmHg s / mL, and R_{ex} = 50 mmHg s / mL.

In a next step the model was run with the boundary condition of an open coronary sinus, and $R^{art \to cap}_{LCX}$ + $R^{cap \to ven}_{LCX}$ was adjusted to yield the correct mean flow (200 mL /min) while the ratio $R^{art \to cap}_{LCX}$ / $R^{cap \to ven}_{LCX}$ was kept constant. Moreover, they checked that changes in the preliminary settings of compliance did not substantially influence the estimate of $R^{art \to cap}_{LCX}$ + $R^{cap \to ven}_{LCX}$. Next, the transition from coronary sinus occlusion to release (CSR) was simulated, during which $R^{ven \to RA}_{CS}$ determines the drainage speed of volume stored in the veins during CSO. $R^{ven \to RA}_{CS}$ was adjusted to allow $p_{ven}(t)$ to decay within 1 to 2 cardiac cycles, in accordance with experimental recordings during PICSO.

For permanent coronary sinus occlusion, R_{ex} was then adjusted to yield a 20% decline in mean total coronary flow, according to experimental evidence. The result (20 mmHg s / mL) is consistent with the fact that extra outflow amounts to 10% of total flow when the coronary sinus is open. Finally, the capillary compliance was adjusted together with the two parameters for venous compliance (χ_{ven}, σ_{ven}) to yield a phasic rise in venous pressure after onset of CSO which matches experimental findings according to the following criteria:

- venous pressure should reach plateau values within several cardiac cycles after the onset of coronary sinus occlusion;
- the plateau pressures should range between 80 and 100 mmHg for systole and around 20 mmHg for diastole;
- systolic and diastolic envelopes of coronary venous pressure should rise such that the developed pressure increases, showing the typical form described earlier in phenomenological models [Schreiner *et al.* (1987)].

These three simultaneous conditions allowed for assessment of the three parameters (C^{cap}_{LCX} = C^{cap}_{LAD}, χ_{ven}, σ_{ven}). Fig.8.2 displays a comparison between experimentally measured values and the model result for $p_{ven}(t)$, which are in satisfactory agreement.

Pass 2: All preliminary estimates of parameters (as used at the start of pass 1) were replaced by adjusted estimates obtained at the end of pass 1. Then each adjustment to experimental data, as described in pass 1, was repeated in pass 2, yielding the final estimates for the parameters, which are listed in Table 9.1 and were labelled "default parameter set" in the following. Inserting the final estimates for the parameters χ_{ven}, σ_{ven} and $V_{ven}(t)$ = V^0_{ven} into Eq.6.46 yielded a venous compliance of 0.12 mL / mmHg / 200 g, which is only 25% below the value compiled if small and large coronary veins are lumped together.

In the present work, myocardial squeezing (γ_{norm}) was varied over a wide range around its default value (0.75). For the remaining model parameters a sensitivity analysis is given in section 9.2.2.4 Sensitivity Analysis, to display their impact on calculated hemodynamics.

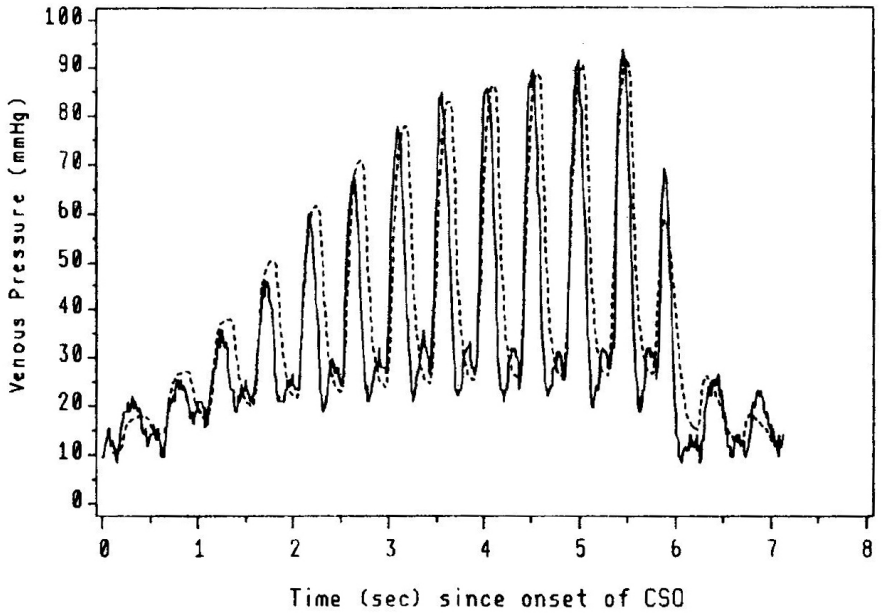

Figure 8.2: Phasic rise of venous pressure: model result versus experimentally determined values. The solid curve represents venous pressure measured during a PICSO cycle in a canine study. From this recording (average) heart rate was determined (92 bpm) and the model was run on the same heart rate and occlusion time, yielding the dashed curve [Schreiner *et al.* (1990d)].

8.2.4 Modifications of Schreiner model for model Oswald

Most of the found values of various parameters from Schreiner model was used for model Oswald. Only the aortic pressure and left ventricle pressure, however, was taken from the experiment. Whereas, the aortic pressure will be set equal to the pressure at the beginning of the left coronary artery and the left ventricle pressure will proceed to the intramyocardial pressure. The gained results was compared with the measured values of its corresponding experiment (p_{ven} correspondent to CSP), which show the typical pressure elevation of the coronary sinus during the inflation phase, but the systolic plateau pressure of the coronary sinus was a little bit lower than of the experiment and the diastolic plateau of the calculated CSP was too high. The calculated CSP without PICSO was too low as well. The total flow through LCA was correspondent to the value of Schreiner model, i.e. 200 ml / min, but the measured LCX-flow was significantly lower than its calculated value.

In this model an asymmetry of LCA and LCX was taken into account, which then lead to that the LAD was supplied during normal perfusion, where its volume is proportional to the volume of the myocardium, which supplied the LCX.

$$N = \frac{V_{LAD}^{myocard}}{V_{LCX}^{myocard}} \tag{8.7}$$

Additionally, it was assumed that the ratio of the quantity of the supplied vessels corresponds to the ratio of the volumes. Which lead to the following equation:

$$C_{LAD}^{cap} = N \cdot C_{LCX}^{cap} \tag{8.8}$$

Furthermore, it was assumed that the antegrade and retrograde blood flow of each volume should be equal when the pressure gradient is equal. Which lead to the conclusion that the resistance of the LAD has to be proportional to the resistance of the LCX:

$$R_{LAD}^{art\rightarrow cap} = \frac{R_{LCX}^{art\rightarrow cap}}{N} \tag{8.9}$$

Since the blood flow through LAD should be n-times the LCX-flow at n-times the LCX-volume, the volume-dependent part of the resistance has to be modified to:

$$\beta \cdot (V_{cap}^{LAD})^{-2} \rightarrow N \cdot \beta \cdot (V_{cap}^{LAD})^{-2} \tag{8.10}$$

The ratio N was varied until the calculated and measured values of the mean LCX flow without PICSO matched.

8.3 Study oversight

The study by Mohl *et al.* (2008) is a long-term follow up of a randomized study of patients, who underwent thrombolysis with PICSO as an adjunct therapy. Some patients in the acute phase of their disease have been reported and are included in this evaluation using data collected in the late 1980s. Evaluation of data was performed in 2006.

The Prepare PICSO Study by van de Hoef *et al.* (2012) was a non-randomized single-center study to evaluate the direct effect of balloon occlusion of the CS on intracoronary hemodynamic parameters in presence of LAD occlusion during elective PCI.

Prepare RAMSES by van de Hoef *et al.* (2015) was a prospective, multicentre, non-randomized safety and feasibility evaluation of adjuvant PICSO treatment in patients with anterior wall STEMI treated by pPCI, concomitantly exploring its effects on myocardial function and infarct size by cardiovascular magnetic resonance (CMR) compared with a historical control group.

8.4 Patient population

Mohl *et al.* (2008) reported that enrolment began in November 1985 and ended in July 1989, in Osaka Police Hospital, Osaka, Japan. During this period, 133 patients with acute myocardial infarction (AMI) underwent thrombolysis therapy, as described elsewhere. These consecutive patients were allocated randomly to 2 groups. Of 67 patients who were assigned to thrombolysis and PICSO therapy, successful catheter insertion into the CS was done in 54 patients; and 79 patients underwent thrombolysis therapy alone. Of these, a group of 34 patients who underwent successful thrombolysis with a culprit lesion in the proximal left anterior descending artery (LAD) was enrolled in the study. The long-term outcome of 17 patients who underwent thrombolysis plus PICSO (PICSO group) was compared with that of 17 patients who underwent thrombolysis only (control group). All patients received aspirin orally (660 mg/day), isosorbide dinitrate (10 mg/day) and diltiazem (90 mg/day) after thrombolysis therapy. In addition, clinofibrate (600 mg/day) was given to patients with hyperlipidemia. All patients were seen every month at the hospital's outpatient clinic.
The primary endpoint was time from discharge to first occurrence of major adverse cardiovascular events (MACE), which was defined as one of the following: reinfarction, unstable angina, PCI, coronary artery bypass grafting

(CABG) or cardiac death. Secondary analyses were myocardial salvage and myocardial lactate metabolism after thrombolysis in the acute phase. The study was approved by the hospital's ethics committee, and informed consent was obtained by all patients to include their data in the database. Demographic variables and clinical characteristics were recorded continuously in the department database and were extracted by retrospective review of all medical records.

van de Hoef *et al.* (2012) prospectively selected a total of 15 consecutive patients of at least 18 years of age with stable coronary artery disease, scheduled for elective PCI of the LAD. They excluded patients with severely impaired left ventricular function (left ventricular ejection fraction <35%), significant valvular abnormalities, severe anemia at screening (hemoglobin <10 g/dL or <6.2 mmol/L), severe renal function impairment (estimated glomerular filtration rate <30 mL/min/1.73m^2), acute myocardial infarction within 72 hours prior to screening, history of coronary artery bypass graft surgery, history of stroke or transient ischemic attack within 6 months before screening, or the presence of pacemaker or other electrodes in the CS. Furthermore, they excluded patients with cardiac arrhythmias or conduction disorders on routine electrocardiography.

van de Hoef *et al.* (2015) wrote that patients aged $\geq$18 years with a first STEMI, defined by symptoms consistent with STEMI >30 minutes duration but <12 hours, and $\geq$1 mm of ST-segment elevation in two or more contiguous leads in V1-V4, who underwent uncomplicated pPCI of a single-vessel left anterior descending coronary artery (LAD) culprit lesion were eligible for enrolment. Uncomplicated pPCI was defined as angioplasty followed by stent placement or direct stenting without the occurrence of adverse events, such as major bleeding, coronary perforation, hypotension, pulmonary edema, or hemodynamic instability. Exclusion criteria included: the presence of a left main coronary artery culprit lesion; previous coronary artery bypass graft surgery; known contraindication to CMR; known creatinine clearance less than 30 mL/min/1.73 m^2 or dialysis; hemoglobin level less than 10 g/dL, platelet count less than 100,000 cells/mm^3, known coagulopathy or bleeding diathesis; history of stroke, transient ischemic attack or reversible ischemic neurological disease within the previous six months; the presence of any lead in the coronary sinus; cardiogenic shock or cardiopulmonary resuscitation; and any comorbid condition likely to interfere with protocol compliance or associated with less than one-year survival.
Included patients were matched with a historical control group from the VU University Medical Center CMR database with a CMR scan date between January 2005 and December 2012, which was performed independently by the core laboratory. The control group consisted of patients who met the inclusion and exclusion criteria of Prepare RAMSES, and who underwent CMR scanning according to the Prepare RAMSES protocol. All control patients were matched for age, body mass index, coronary segment of the LAD culprit vessel, symptom-to-balloon time, and days from pPCI to CMR scan.

Egred *et al.* (2016) enrolled 63 patients with a first anterior MI in a prospective, parallel controlled study at 4 centers. All patients received ACE inhibitors or ARBs, beta-blockers, atorvastatin and dual antiplatelet medication. Antegrade blood flow (TIMI 2 or 3) was first restored in the culprit coronary artery using balloon angioplasty, followed by initiation of PICSO treatment, during which stenting was performed. Consecutive parallel control patients, arriving at the ER on days that a non-PICSO trained physician was on call, received standard treatment. Microvascular obstruction (MVO), infarct size (IS) and left ventricular (LV) function were assessed by cMRI at 5-days post MI.

In the parallel-arm non-randomized UK PICSO in adjunct to PCI study by Egred *et al.* (2017), patients with a

first anterior infarct underwent PICSO treatment after TIMI 3 flow was established in the infarct related artery. Infarct size was assessed by cardiac MRI on day 5, and was compared to control patients without PICSO from the INFUSE-AMI with day 5 cardiac MRI. A statistician, blinded to infarct size, balanced the PICSO and INFUSE-AMI cohorts on sex, age, pre-PCI TIMI flow (0/1 vs 2/3), post-PCI TIMI flow (2 vs 3), diabetes mellitus, culprit lesion location (proximal vs mid LAD), and symptom to balloon time with a propensity score adjusted ~1:3 match. A second statistician compared the infarct size between PICSO and INFUSE-AMI patients.

8.5 Study procedures

Mohl *et al.* (2008) stated that the PICSO system consisted of an electrocardiogram and pressure monitor; pump controller; position-driven pump and a CS balloon catheter. PICSO was initiated immediately after patients were carried to the catheter laboratory, and ended after successful reperfusion was documented by angiography. Balloon inflation for 10 s and deflation for 5 s were repeated, as described elsewhere. CS pressure was monitored continuously and gas volume in the CS balloon was optimized not to exceed 50 mmHg, according to then valid predictions about avoiding damage of coronary venous system.

After successful left coronary artery catheterization, van de Hoef *et al.* (2012) visualized the anatomy of the CS by fluoroscopic evaluation of the venous return phase of a standard coronary angiogram. Subsequently, the PICSO Impulse catheter was introduced into the ostium of the CS, using the right femoral venous route and a 9-French (inner diameter) steerable sheath. Wiring of the CS was then performed, followed by over-the-wire delivery of the catheter. After secure positioning of the Impulse catheter was achieved, the guidewire was removed and the steerable sheath was retracted into the right atrium for support. A 0.014" pressure sensor equipped guidewire was then introduced into the LAD, over which a standard PCI balloon was introduced. Patients underwent 2 low-pressure LAD balloon occlusions, lasting a maximum of 3 minutes each or until the occurrence of subjective severe angina. Complete occlusion of the LAD was verified by angiography. LAD occlusion was performed once with PICSO and once without PICSO.
PICSO in concert with the LAD inflation/deflation cycle was continued until a total of 10 minutes of PICSO treatment was provided. CS pressure was measured continuously through the PICSO Impulse catheter, and intracoronary pressure was measured continuously with the sensor-equipped guidewire. All hemodynamic information was recorded simultaneously on the PICSO Impulse console. A12-lead surface electrocardiogram (ECG) was monitored continuously and recorded every minute during LAD occlusion for evaluation of the ST-segment deviation score. After completion of the study procedure, PCI of the target lesion was completed according to standard of care.
Initially, PICSO was provided during the second LAD occlusion. After documentation of a clear difference in ST-segment deviation between the LAD occlusion with, and the LAD occlusion without PICSO in the first 6 patients, the order was reversed in the final 4 patients to discriminate the effect of PICSO from the effect of sequential coronary artery balloon occlusions on ST-segment deviation and to correct for the effect of postconditioning. Follow-up for adverse events was performed before hospital discharge and at 30 days after the procedure by means of a telephone survey.

van de Hoef *et al.* (2015) reported that emergency angiography and pPCI were performed using standard techniques, and according to clinical practice guidelines. Immediately after successful PCI of the LAD culprit lesion,

a 9 Fr compatible steerable guide sheath was used to engage the ostium of the coronary sinus using the right femoral venous route, guided by the venous return phase of a left coronary angiogram. The coronary sinus was wired using a 0.032-inch guidewire, after which the PICSO Impulse catheter was advanced into the coronary sinus over-the-wire. Subsequently, the guidewire was exchanged for a 0.014-inch wire, which was left in situ for support, while the guide sheath was retracted into the right atrium. Procedural anticoagulation was provided to maintain a target activated clotting time of 200-250 seconds for unfractionated heparin. The guide sheath was flushed continuously with heparinised saline (5,000 units in 500 cc 0.9% NaCl at 3 cc/hour). The first 30 minutes of PICSO therapy were provided in the catheterization laboratory, after which the patient could be transferred to the coronary care unit at the discretion of the operator. Therapy was provided for a maximum of 90 minutes in total, after which the Impulse catheter was removed. CMR was scheduled in all patients at two to five days after pPCI, as well as at four-month follow-up. All patients were treated with aspirin indefinitely and with a P2Y12 inhibitor for at least one year.

8.6 Data analysis

Evaluation for myocardial salvage and myocardial lactate metabolism

Mohl *et al.* (2008) performed every 1 min during thrombolysis therapy to detect reperfusion time electrocardiogram analysis and scoring of chest symptoms. Angiograms of the infarct-related artery were obtained to confirm reperfusion immediately. The perfusion grade of the infarct-related artery at pre-treatment and 30 days after treatment were assessed according to the Thrombolysis In Myocardial Infarction (TIMI) study classification.

Blood samples were collected before and just after thrombolysis. Enzymatic activity of creatine kinase (CK) was measured and total CK release was determined using the integrated appearance function curve with the individual disappearance constant.

Abnormality in wall motion was calculated by abnormally contracting segments, global ejection fraction and regional ejection fraction, using the area method, from the left ventriculogram at 30 days after onset of symptoms (i.e., before hospital discharge). To assess myocardial infarct size, 32 projections of single photoemission computerized tomography (SPECT), 3 h after intravenous administration of 3 mCi of thallium-201 (201 Tl), were obtained over 180°. The volume of defects was weighted for the average value of counts in the defect area, and this was defined as the extent of damaged myocardium in the total left ventricle or 'defect severity'. The QRS score was also calculated as a parameter to estimate residual infarct size during the follow-up period.

To assess lactate extraction, blood sampling was taken from the aorta and CS before and after thrombolysis was performed; and every 6 h for up to 24 h from the onset of symptoms.

van de Hoef *et al.* (2012) evaluated changes in distal LAD wedge pressure during LAD occlusion both with and without PICSO after adjustment for the baseline wedge pressure. Furthermore, to appropriately address the pulsatile nature of the technique, they evaluated the direct effect of balloon occlusion of the CS on LAD wedge pressure by comparing the CS occlusion phase (inflated PICSO Impulse balloon) with the non-occlusion phase (deflated PICSO Impulse balloon) during the LAD occlusion with PICSO. They evaluated both differences in mean pressure, as well as pulse pressure, which was defined as the increase in pressure from diastole to systole per heartbeat. All analyses were performed based on per beat averages of the hemodynamic data, which were extracted using Acknowledge software. Data are presented as mean ($\pm$ standard deviation), frequency, (percentage) or median (interquartile range [IQR]). Standard crossover analysis was performed for the ECG deviation score,

which was defined as the sum of ST-segment deviation on a standard 12-lead surface ECG, to evaluate the presence of a period effect or treatment-period interaction. A paired Student's t-test was used to test for differences between groups. Correlation between parameters was tested using Pearson's correlation coefficient. A 2-sided alpha level of 0.05 was considered statistically significant.

Cardiovascular magnetic resonance protocol and data analyses

van de Hoef *et al.* (2015) acquired cine images for measurement of global left ventricular (LV) volumes and function, and segmental wall thickness. Delayed-enhancement (DE) images were acquired for measurement of the size and extent of infarction and microvascular obstruction (MVO), and to delineate the infarct endocardial surface area (ESA). The area at risk was measured using the ESA. Myocardial salvage index (MSI) was calculated as the difference between the area at risk and the total infarct size, normalised for area at risk. All CMR data were analysed by the core laboratory on a separate workstation using validated software, blinded to patient identity and clinical information.

Coronary sinus pressure data analysis

van de Hoef *et al.* (2015) analyzed offline the coronary sinus pressure data to calculate PICSO quantity, defined as: balloon inflation hold time $*$ (mean systolic coronary sinus pressure plateau - mean coronary sinus pressure during deflation) $*$ (mean systolic coronary sinus pressure plateau - mean diastolic coronary sinus pressure plateau), summed over the complete PICSO procedure and expressed in (mmHg). PICSO quantity reflects the magnitude of coronary sinus pressure modulation during the PICSO procedure, and is a marker of PICSO therapy performance.

8.7 Endpoints and definitions

van de Hoef *et al.* (2015), the primary endpoint was feasibility of PICSO in STEMI, defined as successful delivery of the PICSO Impulse catheter and successful administration of PICSO treatment for 90 minutes. Safety of PICSO was assessed as the rate of serious adverse device events, defined as any major complications or death caused by the implantation procedure or the presence or performance of the device. Additionally, the occurrence of major adverse cardiac events (MACE) was documented, defined as the composite of all-cause death, myocardial reinfarction not clearly attributable to a non-target vessel, or new onset of severe heart failure or hospitalisation for heart failure. Exploratory CMR endpoints included infarct size, MSI and MVO, as well as LV volumes and function at two to five days post pPCI, and at four-month follow-up.

8.8 Statistical methods

Mohl *et al.* (2008) presented continuous data as the mean value $\pm$ standard deviation. Baseline data were compared by means of the chi-squared test for categorical variables and t-test for continuous variables. Cardiac event-free survival curves were constructed by the Kaplan - Meier method. Statistical differences between curves were assessed using an exact log-rank test, adjusting for potentially unequal follow-up periods in the groups. Changes in lactate extraction ratio (LER) after reperfusion were compared between the PICSO and control groups by means of repeated measures analysis of covariance (ANCOVA), including the baseline LER as a covariate.

The effect of PICSO on cardiac event-free survival was assessed by means of a Cox regression model, stating relative risk estimates and 95% confidence intervals (CI).
Despite randomization, the crude effect of PICSO on event-free survival could be the result of different exposure to risk factors in the 2 groups. Hence, ideally, one would use a multivariable model that included all potential risk factors at the same time, which would adjust for such different exposure; however, because of the low total number of events in our data, such a model could not be used. Therefore, separate bivariable Cox regression models, each including group (i.e., PICSO or control) and one of the risk factors (i.e., age ($\geq$65 years or <65 years), gender, hypertension, hyperlipidemia, diabetes mellitus, smoking, family history, pain-to-admission time and TIMI flow), were estimated. We also estimated bivariable Cox models, including group (i.e., PICSO or control) and stenosis value at Day 30 to obtain an estimate of the effect of PICSO on long-term outcome that is independent of PICSO's effect on restenosis. A p-value of <0.05 was considered statistically significant.
Stenosis values at Day 30 were compared between the groups, using ANCOVA, adjusting for differences in the baseline stenosis value at Day 0 by including the individual baseline values as a covariate. ANCOVA was also used to adjust for differences in the LER between groups for baseline differences. This analysis was repeated, replacing stenosis values by their ranks to obtain a confirmative non-parametric p-value.

van de Hoef *et al.* (2015), enrolment was planned for 40 patients to obtain meaningful safety and feasibility information, while minimizing unnecessary patient exposure. Considering the small sample size, parametric testing was used for the principal analysis of the exploratory CMR endpoints. Continuous descriptive variables are presented as mean and standard deviation, or median and first and third quartiles, and are compared by Student's t-test or Wilcoxon rank-sum test, as appropriate. For segmental wall thickening analyses, a linear mixed-effects model with robust standard errors was used to account for clustering of LV segments within patients. All statistical tests were two-sided, and a p-value <0.05 was considered significant.

8.9 Optimization of PICSO therapy

Mohl *et al.* (2015) stated that in order to optimize PICSO therapy, the position of the occluding balloon redirecting blood in relation to side branches of the coronary sinus is of outmost importance. Exact positioning in an optimal region of the coronary sinus not only requires expertise, but is also a prerequisite of the effectiveness of the PICSO procedure. The easiest way to access the coronary sinus is the left jugular, subclavian or brachial vein. Since a routine anticoagulation regimen is used in ACS and to minimize the risk of bleeding, central venous punctures are avoided in several centers endorsing peripheral veins. The femoral approach has been extensively used and results in favorable catheterization times. The balloon catheter is positioned into the so-called "silent zone" of the coronary sinus. Infrequently, an obstructing valve at the coronary sinus orifice hampers the positioning of the catheter within the silent zone of the great cardiac vein.
It is also important to stabilize the catheter system against the force of the outflowing blood, especially during the hyperemic response increasing the venous velocity. The pressure within the pneumatic balloon catheter is monitored, avoiding any excessive force on the vessel wall and allowing maximal safety. Since the orifice of the coronary sinus is covered by endocardium and contains nerve endings, reflexes such as hypotension and bradycardia have been observed in animals. The squeezing action of the heart creates the pressure increase and forces the blood backwards into deprived zones; it is therefore important to collect as much inflow as possible from veins draining into the occluded section of the coronary sinus. The rate of rise gives an estimate of the capacity to

be filled by retroperfused blood and is a summation of the venous compartment and the coronary microcirculation deprived from normal circulation. Epicardial flow into the deprived coronary vasculature and subsequent washout during the release phase therefore reduces the so-called ’no reflow’ zones that are present in patients with ACS and allows a shift of blood towards the endocardium.

Chapter 9

Results

9.1 Phenomenological modeling

Results by Schreiner *et al.* (1990b) show the real and imaginary parts of the proportionality coefficients $\hat{y}'_n$ at the five lowest frequencies $\omega_0, \ldots, \omega_4$ for all types of PICSO cycles applied in the two dogs during normal perfusion, LAD-infarction and reperfusion. While the $\hat{y}'_n$ -coefficients at $\omega \neq 0$ show a common trend toward zero, a tremendous spread of the data was found at $\omega = 0$. The reason for this is that for each set of experimental conditions (normal perfusion, LAD-infarction, reperfusion) the average total flow was found to remain relatively stable, irrespective of the type of PICSO cycle applied. Obviously, slow processes corresponding to $\omega \to 0$, allow for compensatory reactions of the heart to the intermittent flow depression, so that a certain level of flow can be sustained by non-coronary sinus pathways. Therefore, it is not possible to maintain that the average value of flow $\hat{\Phi}_0$ is proportional to the average LVP-CSP pressure gradient Δp_0, when PICSO cycles with different occlusion periods are used. Formally, this is indicated in Eq.(8.3) by adding to $\hat{y}_0, \Delta p_0$ a quantity $\hat{\Phi}_0^{res}$, which is supposed to account for the cycle type, the experimental condition and the dog under consideration.

Within the experimental error the $\hat{y}'_n$ - coefficients for non-zero frequencies of both dogs appear to be lying on a single curve, regardless of cycle type and experimental condition. Therefore, when fitting the function $\hat{y}(\omega)$ to $\hat{y}'_n$, $n = 1, \ldots, 4$, (thus excluding $\omega = 0$) they summed Eq.(8.4) over all PICSO cycles of both dogs to obtain a single transfer function, representative of the data of both dogs. The parameter estimates for the transfer function were A = 0.50 ml / (min x mmHg) and $\tau = 0.86s$. The RMS-deviation of the fit was 0.985 ml / min. By means of this function it was possible to predict flow curves for the third dog using only its measured CSP and to determine the points of maximum flow on these curves. Result shows to what extent this prediction is in agreement with the actual experimental data of one PICSO cycle.

9.2 Mechanistic modeling

9.2.1 Overview of the model parameters

Parameter	Unit	Schreiner	Oswald	Kajgana
R_{LCA}	mmHg s / ml	0.05	0.05	0.05
$R_{LCX}^{art\to cap} = R_{art\to cap}^{LAD}$	mmHg s / ml	27.0	-	27.0
$R_{LCX}^{cap\to ven} = R_{LAD}^{cap\to ven}$	mmHg s / ml	2.7	-	2.7
$R_{LCX}^{cap\to ven}/R_{LCX}^{art\to cap}$	none	0.1	-	-
$R_{CS}^{ven\to RA}$	mmHg s / ml	0.6	6.0	0.6
$R_{LCX}^{art\to cap}/R_{LMV}^{cap\to ven}$	none	-	10.0	-
$R_{LAD}^{art\to cap}/R_{GCV}^{cap\to ven}$	none	-	10.0	-
$R_{LCX1}^{art\to cap}/R_{LCX2}^{art\to cap}$	none	-	-	5:22
$R_{GCV1}^{cap\to ven}/R_{GCV2}^{cap\to ven}$	none	-	-	17:10
R_{ex}	mmHg s / ml	20.0	10.5	20.0
R_{tot}	mmHg s / ml	14.85	17.0	-
$N = R_{LCX}^{art\to cap}/R_{LAD}^{art\to cap}$	none	1.0	2.83	-
p_{ven}^{off}	mmHg	5.0	5.0	5.0
γ_{norm}	none	0.75	0.75	0.75
$C_{LCX}^{cap} = C_{LAD}^{cap}$	ml / mmHg	0.2	0.7	0.2
β	mmHg s ml	1.0	1.0	1.0
χ_{ven}	ml / mmHg	1.0	1.0	1.0
σ_{ven}	1 / ml	0.3	1.5	0.3 ,
V_{ven}^{0}	ml	25.0	25.0	25.0
HR	bpm	60	-	-

Table 9.1: Overview of the used values in Schreiner model *et al.* (1990d), Oswald (2004) and Kajgana (2004).

9.2.2 Schreiner Model

9.2.2.1 The impact of squeezing on phasic flows

Fig.9.1 by Schreiner *et al.* (1990d) displays single beat resolutions of intramyocardial flow for different values of γ_{norm}, ranging from $\gamma_{norm} = 0$ (no squeezing, long dashes) to $\gamma_{norm} = 0.75$ (default value, solid curve). The right panels [(b) and (d)] correspond to a cardiac cycle during coronary sinus release (CSR). The left panels correspond to a cardiac cycle near the end of a 10 s period of coronary sinus occlusion (CSO). In the absence of squeezing, the flow from coronary arteries to the capillary bed [$Q_{LCX}^{art\to cap}(t), Q_{LCX}^{art\to cap}(t)$ long dashed curves in Fig.9.1, panels (a) and (b)] essentially paralleled aortic perfusion pressure and showed a distinct global maximum during late systole (ejection phase). This was true for both CSR and CSO conditions.

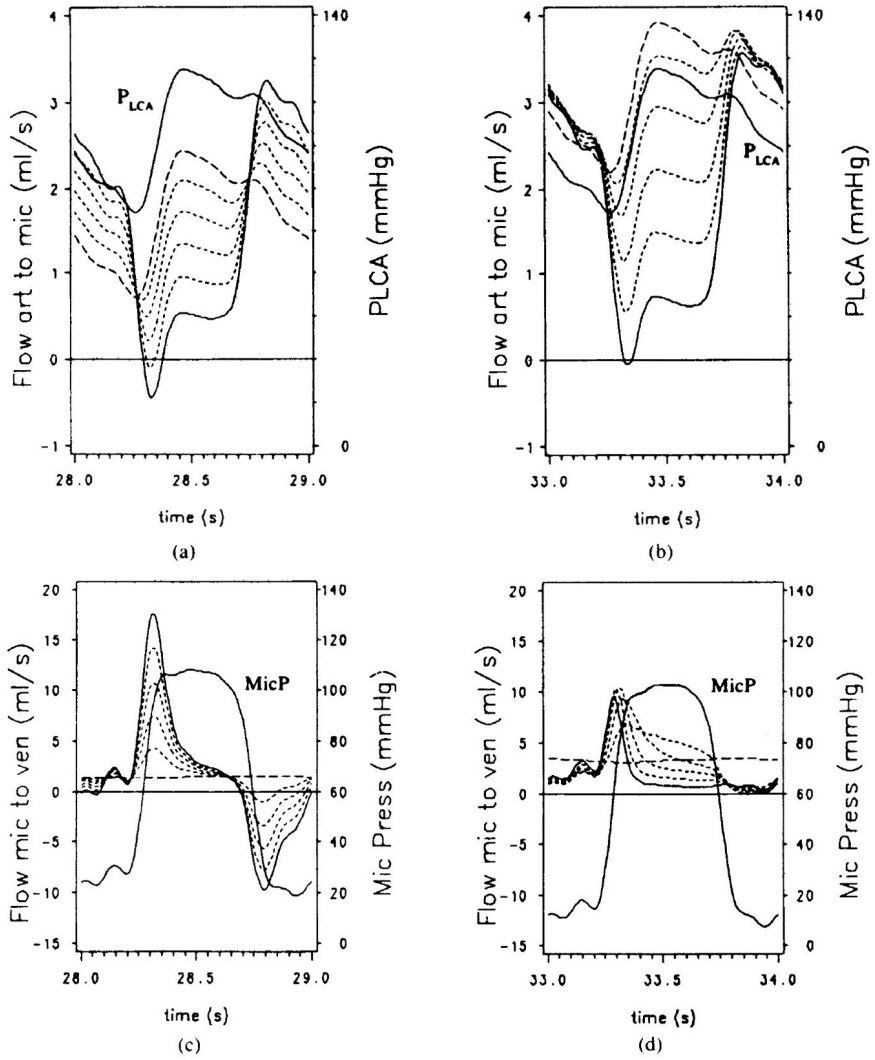

Figure 9.1: Pulsatile flows under variation of squeezing γ_{norm} is varied from 0 (long dashes) to 0.75 (solid curve) in increments of 0.15. All other parameters have their default values. Flows are given in mL / s, which is equivalent to units of milliliters per heartbeat for HR = 60. (a) Flow from coronary arteries to the capillary bed, $Q_{LCX}^{art\rightarrow cap}(t)$, during a cardiac cycle near the end of a 10 s period of coronary sinus occlusion (CSO). The full curve (labeled p_{LCA}) gives the aortic perfusion pressure (right scale). Note that total arterial inflow [$Q_{LCA}(t)$] is exactly twice the inflow to the LCX bed [$Q_{LCX}^{art\rightarrow cap}(t)$]. (b) $Q_{LCX}^{art\rightarrow cap}(t)$ under coronary sinus release (CSR). Perfusion pressure shown on right scale, similar to (a). (c) Flow from the capillary bed to the venous compartment, $Q_{LCX}^{cap\rightarrow ven}(t)$, under CSO. Additionally, microvascular pressure (p_{mic}) is shown on the right scale. (d) $Q_{LCX}^{cap\rightarrow ven}(t)$ under CSR [Schreiner *et al.* (1990d)].

With increasing squeezing, however, flow was progressively depressed throughout systole and showed a distinct global minimum in early systole (isovolumetric contraction) followed by a small relative maximum (within systole), corresponding to peak aortic pressure. In other words: without squeezing, flow was maximum during systole (simultaneously with perfusion pressure), whereas with squeezing flow was maximum during diastole. Hence myocardial squeezing was seen to invert the phasic shape of coronary inflow, in agreement with physiological

findings. In the model, the mechanism works as follows: the squeezable part of capillary volume decreases during systole as a consequence of squeezing, thereby increasing the volume-dependent part of resistance [Eq.(6.19) and (6.25)]. With CSR the latter reaches 100 mmHg s / mL, which equals about three times the static component of inflow resistance ($R_{LAD}^{art\rightarrow cap}$) and 30 x the static component of the outflow resistance ($R_{LAD}^{cap\rightarrow ven}$).
Conversely, CSO lead to larger capillary volumes (vasodistention). Even during systole the volume-dependent part of the resistance did not exceed 1.56 mmHg s / mL, and thus amounted to 6% of static inflow- and to 57% of static outflow resistance.
However, the effect of increased squeezing on diastolic flow was different for CSR and CSO. Because during CSR (Fig.9.1(b)), variations in squeezing produced little changes in diastolic flow. Whereas during CSO (Fig.9.1(a)), diastolic flow increased with squeezing, cf., the solid line corresponding to $\gamma_{norm} = 0.75$. A possible explanation is as follows: elevated venous pressure during CSO caused a back pressure toward the capillary compartment, such that for $\gamma_{norm} = 0$ distension pressure alone did not achieve a complete emptying of the capillaries. Therefore, with $\gamma_{norm} = 0$, a substantial residual capillary volume (and distension-pressure) was still present at the beginning of diastole, which impeded arterial inflow. Conversely, with maximum squeezing the capillary compartment was almost empty at the onset of diastole, thus allowing free inflow. In summary, under CSO conditions the systolic depression of $Q_{LCX}^{art\rightarrow cap}(t)$ caused by squeezing was compensated by increased diastolic flows, leaving the mean coronary artery flow nearly unaffected by squeezing. Conversely, during CSR the systolic depression was not compensated in diastole, yielding a decline of approximately 1 mL / s in mean flow as γ_{norm} was increased from 0 to 0.75, cf., Fig.9.2(a) and (b).
The phasic form of flow from capillaries to veins ($Q_{LCX}^{cap\rightarrow ven}(t), Q_{LAD}^{cap\rightarrow ven}(t)$, Fig.9.1(c) and (d)) was markedly influenced by squeezing. During CSR (panel (d)) even minimal squeezing ($\gamma_{norm} = 0.15$) sufficed to distinctly enhance systolic flow, characterized by a maximum in mid systole and an almost linear decline throughout the duration of systole. For larger values of γ_{norm} the flow maximum became more distinct, shifted toward the beginning of systole and was followed by a rapid decline to near zero flow for the rest of systole and the following diastole. This change in shape of $Q_{LCX}^{cap\rightarrow ven}(t)$ was due to an almost total emptying of the "squeezable portion" of the capillary compartment under heavy compression, which, well before the end of systole, left no residual volume to be squeezed out. However, even minimal squeezing sufficed to displace the major portion of capillary volume toward the venous compartment during systole.
Subsequently, in diastole, the capillary volume was small and little distension pressure remained to drive forward flow. Hence $Q_{LCX}^{cap\rightarrow ven}(t)$ was reduced during diastole. During CSO (lower left panel, Fig.9.1(c)) increasing squeezing produced positive (forward) maxima of $Q_{LCX}^{cap\rightarrow ven}(t)$ during early systole and retrograde maxima during diastole. The phasic shape of $Q_{LCX}^{cap\rightarrow ven}(t)$ remained almost unchanged (in contrast to during CSR) and merely increased in amplitude as γ_{norm} increased. The retrograde flow during diastole is driven by elevated venous pressure near the end of a CSO period. This represents the central and most important quantity calculated from the model as far as the therapeutic effects of coronary sinus interventions are concerned. It provides retrograde access to the capillary bed. Therefore, values for forward and LCX backward components of $Q_{LCX}^{cap\rightarrow ven}(t)$ have been separately averaged and displayed as functions of γ_{norm} in Fig.9.2(a) and (b). Note that retrograde flows are given as negative values throughout the current work.

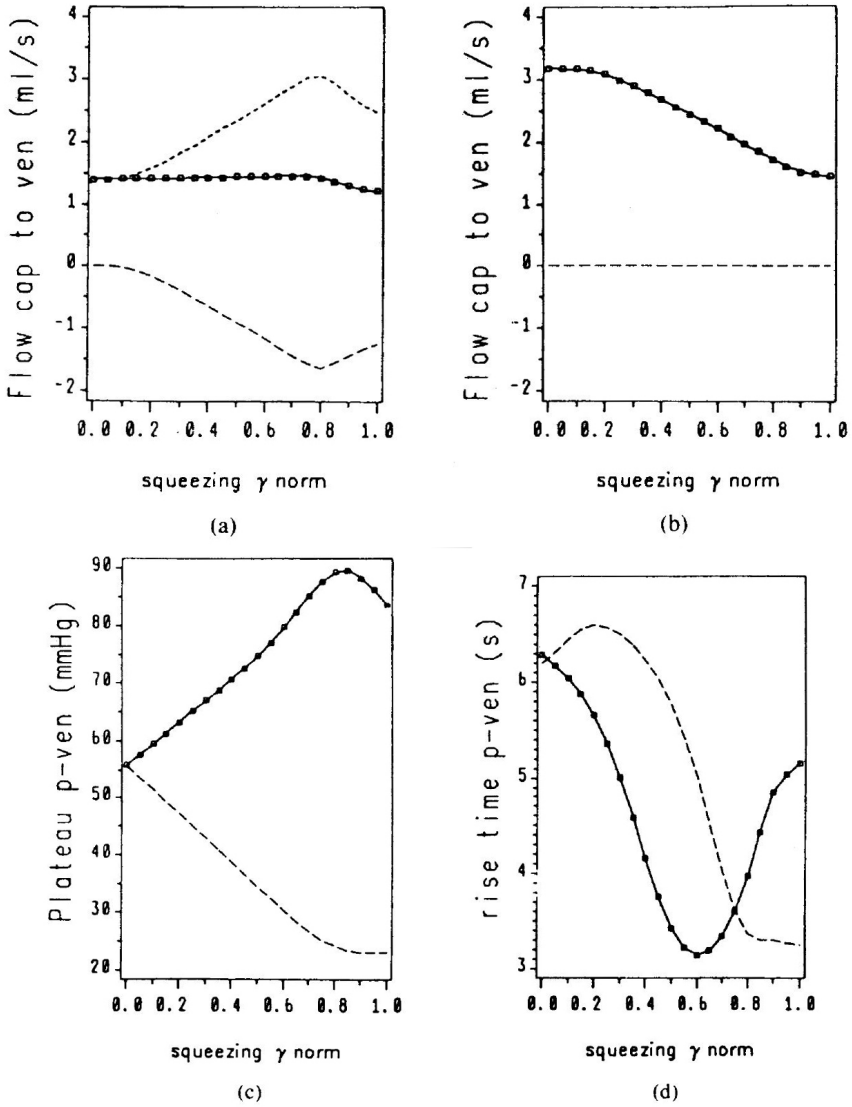

Figure 9.2: Impact of squeezing on mean flows and venous pressure. Each square symbol represents a separate simulation for the respective value of γ_{norm}. Although all quantities displayed are obtained at each value of γ_{norm} square symbols are only shown for one of the quantities. Flows in mL / s. (a) Flow from capillaries to veins under CSO. Total mean flow (squares. Solid curve), forward component (short dashes) and retrograde component (long dashes). (b) Like (a), however under CSR conditions. (c) Plateau of venous pressure (mmHg) calculated from a 10 s occlusion of the coronary sinus. Systolic plateau (squares. solid curve) and diastolic plateau (dashed). (d) 90% rise times of venous pressure calculated from a 10 s CSO period. Systolic (squares, solid curve) and diastolic (dashed) [Schreiner *et al.* (1990d)].

9.2.2.2 Forward, retrograde and mean flows

Mean arterial flow ($Q_{LCX}^{art\rightarrow cap}(t)$) ran parallel to the mean flow from capillaries to veins ($Q_{LCX}^{cap\rightarrow ven}(t)$) since obviously volume must not be lost or accumulated during stationary conditions with solutions periodic from beat to beat. Moreover, except for a small retrograde component in early systole under CSO [Fig.9.1(a)], $Q_{LCX}^{art\rightarrow cap}(t)$

was always forward and hence mean forward $Q_{LCX}^{art\rightarrow cap}(t)$ coincided with mean $Q_{LCX}^{cap\rightarrow ven}(t)$. Therefore, only ($Q_{LCX}^{cap\rightarrow ven}(t)$) together with its pronounced mean forward and retrograde components were shown as functions of γ_{norm} in Fig.9.2(a) for CSO and in Fig.9.2(b) for CSR conditions.

Simulations were carried out for increments of 0.05 in γ_{norm}, ranging between zero and 1 (the result of each simulation corresponds to a square symbol in Fig.9.2). Under CSR (panel (b)) the retrograde component was zero (long dashes), and hence mean forward- and mean-total flows coincided. There was a decrease from about 3 mL / s to 1.5 mL / s with increasing γ_{norm}. Conversely, during CSO conditions (panel 9.2(a)), total mean flow remained virtually unchanged despite the increase in squeezing ($0 \leq \gamma_{norm} \leq 0.8$). At the same time, forward components (short dashes) and backward components (long dashes) increased symmetrically (yielding approximately constant mean flow). For $\gamma_{norm} > 0.8$ a decrease in forward, backward and mean $Q_{LCX}^{cap\rightarrow ven}(t)$ was observed. Note that the values displayed in Fig.9.2(a) and (b) correspond to areas above and below the abscissa in Fig.9.1(c) and (d).

9.2.2.3 Impact of squeezing on plateau and rise time of venous pressure

In experimental investigations, the systolic and diastolic envelopes, $p_{ven}|_{sys}(t)$ and $p_{ven}|_{dia}(t)$, of the rise of coronary venous pressure following the onset of CSO have been modeled by a mathematical function in order to describe important features, such as rise times and extrapolated plateaus, on a quantitative basis [Schreiner *et al.* (1988b,1988a), (1987)]. The following function was fitted to the systolic envelope:

$$p_{ven}|_{sys}(t) = A_{sys} \cdot exp(\alpha_{sys}(1 - e^{-\beta_{sys} \cdot t}) - 1) \tag{9.1}$$

where t is the time from onset of coronary sinus occlusion, and A, α and β_{sys} are parameters of fit. From Eq.(9.1) the height of the asymptotic plateau for large t can be calculated as

$$P\_SY \equiv p_{ven}|_{sys}(t = \infty) = A_{sys} \cdot e^{\alpha_{sys} - 1} \tag{9.2}$$

The fitted envelope reaches 90% of P_SY after a period called 90% rise time (systolic):

$$T90\_SY = \beta_{sys}^{-1} \cdot ln\left(\frac{-\alpha_{sys}}{ln(0.9)}\right) \tag{9.3}$$

For diastole the same form of equations applies, with different numerical values for the parameters. In the current work, envelopes of $p_{ven}(t)$ were generated for different values of squeezing. Equation (9.1) was fitted by a non-linear algorithm, and plateaus and rise times were then calculated. One can thus study within the model, which changes can be expected for the "calculated diagnostic quantities" P_SY and T90_SY, if all parameters retain their values except for myocardial squeezing ("net impact of squeezing"), see Fig.9.2(c) and (d).
Without squeezing, the systolic and diastolic plateaus, P_SY and P_DI, coincided at 56 mmHg, reflecting that pulsatile pressure from the ostium of the left common artery never penetrates to the venous side, being heavily damped by intramyocardial resistances and compliances. As squeezing was increased, an increasing gap emerged between P_SY and P_DI (Fig.9.2(c)). Of note, this finding quantitatively confirms a hypothesis put forward in previous investigations [Schreiner *et al.* (1988b,1988a)], namely that the systolic and diastolic plateaus of $p_{ven}(t)$ and particularly their difference, may provide a computed diagnostic quantity reflecting myocardial contractility. The changes in P_SY and P_DI were very close to linear as functions of squeezing. However, around $\gamma_{norm} = 0.9$ the trends of P_SY and P_DI changed directions.

The rise times T90_SY and T90_DI, when seen as functions of squeezing, exhibited a behavior much more complex than that of P_SY and P_DI. P_SY decreased steadily for $0 \leq \gamma_{norm} \leq 0.6$ but increased for $\gamma_{norm} > 0.6$ (full line with square symbols in Fig.9.2(d)). Conversely, T90_DI increased for $0 \leq \gamma_{norm} \leq 0.2$ and then decreased steadily. The physiologic explanation for this behavior of rise times is unclear.

9.2.2.4 Sensitivity analysis

It is important to see how changes in each model parameter affects hemodynamic quantities calculated from the model. The authors investigated those calculated quantities which are physiologically most important ("target quantities"):

- the mean forward component of flow between capillaries and veins during coronary sinus occlusion,
- the mean backward component of flow between capillaries and veins during coronary sinus occlusion, and
- the mean coronary flow during coronary sinus release.

For each of these quantities (η) they estimated the percent change following a 100% increase in each single model parameter ξ above its default value listed in Table 9.1: $(\eta(2\xi) - \eta(\xi))/\eta(\xi)$. These calculated percent changes, while providing information similar to that of partial derivatives $\partial\eta/\partial\xi$, all have the same dimension (% change / 100% change) and hence are more easily comparable among different parameters. Some parameters, e.g., $R_{CS}^{ven \to RA}$ failed to show impact on any of the three target quantities. This is reasonable since the latter represent only a selection from a large variety of hemodynamic quantities calculated within the model, and hence, cannot reflect changes in each feature (and parameter) of the model. For example, during coronary sinus occlusion, the choice of $R_{CS}^{ven \to RA}$ was irrelevant since flow through the coronary sinus was forced to zero by definition. However, $R_{CS}^{ven \to RA}$ drastically affected the transients of coronary venous pressure and of the flow to the right atrium immediately after the release of coronary sinus obstruction.

9.2.3 Comparison of experiment-model Oswald

In this model by Oswald (2004) Q_{LCA} was set to 200 ml / min and the LAD and LCX beds are asymmetric. To reach this goal, only small adaptation of the other parameters were necessary. However, a phase shift between the measured values and calculated flows could be detected.
A look at the LCX-flow show that the height and a similar course outside the deflation phase can be found, but the measured value vary more significantly than the calculated value. The depression of the flow during the inflation phase is weak, which can also be seen in the gained results of the modeling. The hyperemic reaction of the LCX-flow in the deflation phase cannot reproduce this behavior.
By increasing the resistance of the coronary sinus it was possible to reproduce the CSP in the phase without PICSO. The model can also reproduce the experimentally found rise of the CSP at the beginning of the inflation phase. However, the systolic plateau of the CSP was at ca. 80 mmHg in the experiment, but in the model only at ca. 60 mmHg. The phase shift that occurred in the flows is also reflected in the CSP.

9.2.3.1 Variation of ratio N

Since this model assumed an asymmetry of the LAD and LCX beds, the ratio N of volume of the myocardium that supplies the LAD and the myocardium volume that supplies the LCX was introduced. To reach the parameters

from Schreiner model, N was set to 2.83. By varying the value to 20%, the height of the systolic flow changes, and with increased N the flow decreases, however the curve and the diastolic value hardly change.
A variation of N of $\pm$ 20% will not show significant changes of the CSP. Only by decreasing the pressure during the beginning of the deflation phase and with a low N the pressure falls quicker.

9.2.3.2 Variation of the coronary sinus resistance

The coronary sinus resistance $R_{CS}^{ven \rightarrow RA}$ was optimized, to reproduce the CSP during the phase without PICSO. Also considered was that the deflated balloon catheter counteracts the blood flow that leads to a relative high resistance, which resulted in 6 mmHg s / ml. The behavior of the CSP after inflation can be reproduced well. Varying the coronary sinus resistance to $\pm$ 20% shows only little impact to the fall time of the CSP, but the impact of the CSP without PICSO was therefore distinctive. $R_{CS}^{ven \rightarrow RA}$ plays no important role during the inflation phase and for the LCX-flow.

9.2.3.3 Variation of the total resistance

The total resistance $R_{tot} = \frac{(R_{LCX}+R_{LMV})(R_{LAD}+R_{GCV})}{R_{LCX}+R_{LMV}+R_{LAD}+R_{GCV}}$ is the parameter that was used by variation to get the value for the flow Q_{LCA} = 200 ml / min. The found resistance has a value of 17 mmHg s / ml. Varying the resistance R_{tot} by $\pm$ 20% had an impact on the CSP, whereas a decrease of R_{tot} lead to a systolic CSP increase. That dependence also occur during inflation and deflation of the balloon, so that the systolic CSP plateau of 50 mmHg ($R_{tot} = 20.4$) rises to 70 mmHg ($R_{tot} = 13.6$).
The variation of R_{tot} also has great impact to the fall of the CSP at the beginning of the deflation phase. A decrease of 20% the systolic CSP stays at a high level for a few heart beats and only sinks slowly, but an increase of 20% the CSP reaches after only two heart beats the normal value for an open coronary sinus.

9.2.3.4 Variation of the capillary compliance

The systolic CSP plateau during the inflation phase was the only parameter in this model that could not be reached. Measured value of the experiment was about 80 mmHg, but the model only gave about 60 mmHg. To reach the plateau the capillary compliance C_{LCX}^{cap} was changed and the found value was 0.7 ml / mmHg. By setting the value to 0.05 ml / mmHg only lead to a lower value for the systolic CSP plateau. An increase to 1.35 ml / mmHg was also unsatisfying.

9.2.4 Model Kajgana

Kajgana (2004), in order to compare different states which are representing normal perfusion, infarction and reperfusion, one can vary stenosis resistance, as well as squeezing power. $R_{LAD}^{art \rightarrow cap}$ can be varied between 27 (normal perfusion) and 5000 mmHg s/ ml (total obstruction of LAD). Extramural squeezing in the LAD area can be varied between 0% and 100% of the normal value ($0 \leq \gamma_{sten} \leq 1$). Since $R_{LAD}^{art \rightarrow cap}$ and p_{LAD}^{sqz} refer to the LAD bed the model results are different for LCX and LAD capillary beds due to redistribution phenomena.
However, flow, pressure or volume in various regions (arterial, capillary and venous) with special regard on their state during different stenosis degrees and under influence of different collateral resistances will be described.

$R_{coll}^{art \to ven}$	$Q_{GCV1}^{cap \to ven}$ [ml / min]		$Q_{GCV2}^{cap \to ven}$ [ml / min]	
[mmHg s / ml]	PICSO on	PICSO off	PICSO on	PICSO off
30	57.5	-24.6	150	45
90	36	-16.2	67	16.8
300	24.5	-11.8	46.66	0

Table 9.2: Shift of the flow caused by the collaterals.

9.2.4.1 Arterial flow

The flow in the LCX1, LCX2 and in the collaterals can be influenced by changing the collateral resistance, which seems logical and will occur during interventions, see Fig.9.3. By increase of the collateral resistance, there is, as expected, decrease of the collateral flow. That means that the entire flow is draining over LCX capillary bed. This has influence on the GCV flow and does not support flow over the ischemic zone. Two extreme examples were compared; once the collateral resistance was set to 30 mmHg s/ ml and other time to 300 mmHg s / ml. In Fig.9.4 one can see the shift of the flow caused by collaterals. Further variations of the collateral resistance revealed distribution of flow in the GCV region, see table 9.2. Flow in the LAD branch is very similar to the case of the LCX flow with very high collateral resistance.

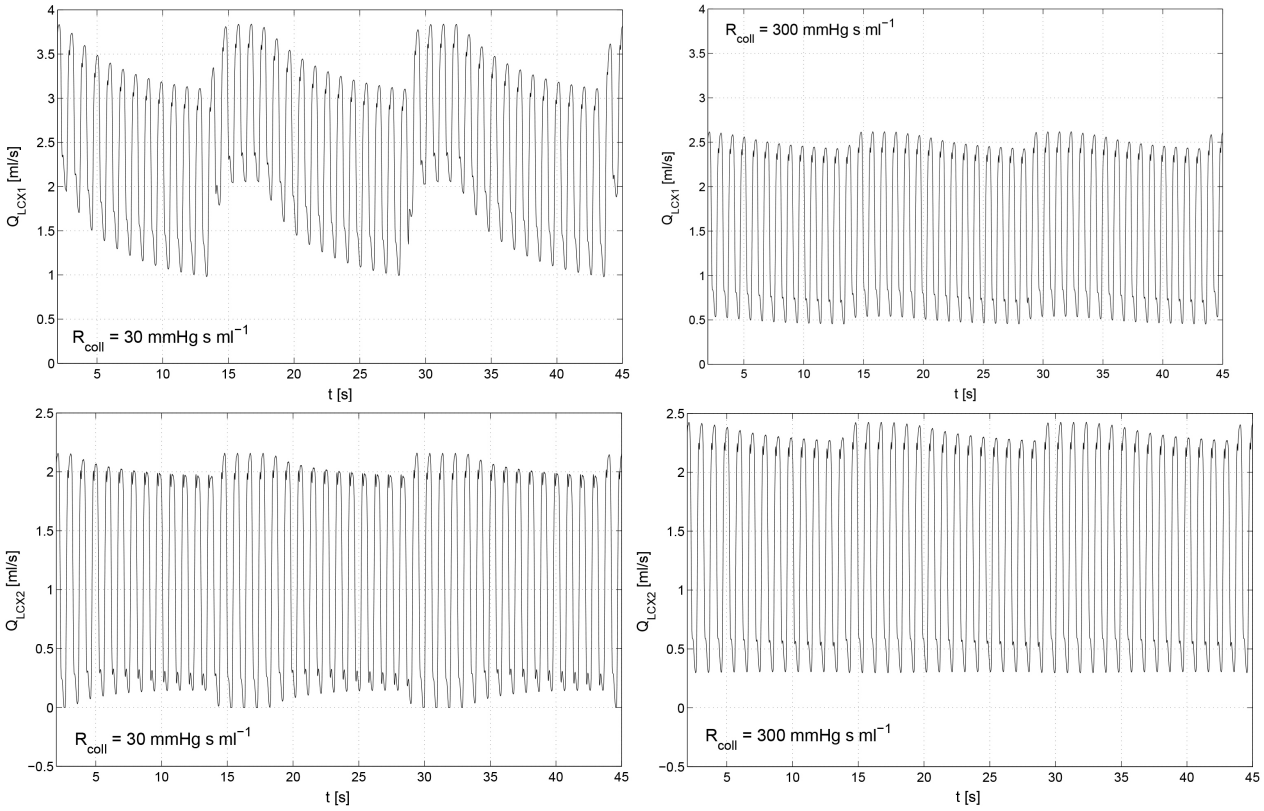

Figure 9.3: Changes of the flow in the LCX1 and LCX2 under influence of modified collateral resistance. It is important to consider different collateral resistances because every heart has differently expressed collaterals. Note, the differences between LCX1 and LCX2.

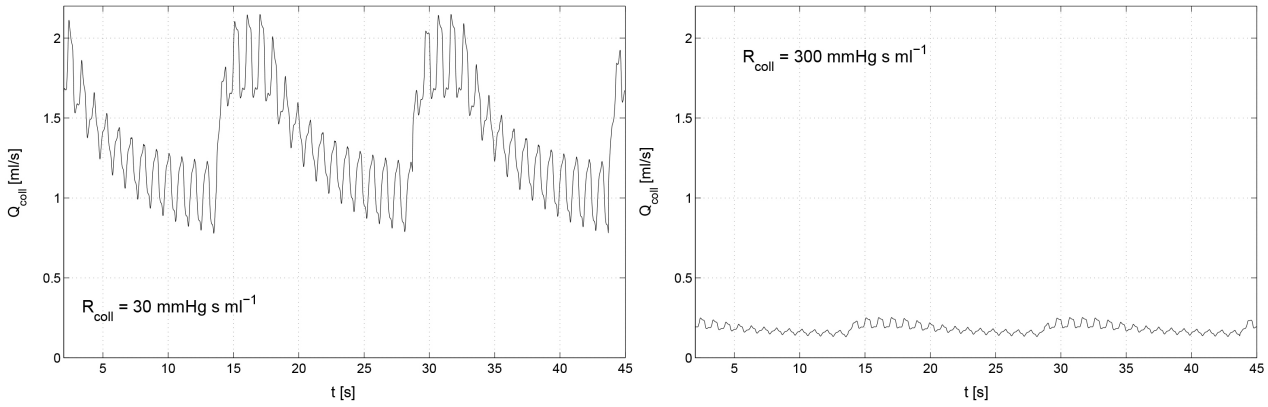

Figure 9.4: Differences in the collateral flow caused by different resistances. The difference in the resistance causes, as expected, great quantitative changes in the collateral flow, which again causes differences in the vein flow.

9.2.4.2 Capillary volume

With coronary sinus occlusion capillary volume can be distended up to 5 ml. During coronary sinus release, capillary volume oscillates between 0.1 and 1 ml. The lower limit of capillary volume is related to V_{LCX}^{cap} and constant β, see Eq.(6.24) and (6.27). Capillary volume is on one hand dependent on arterial input and on the other hand on retrograde flow caused by venous pressure elevation. During systole major part of the capillary volume is squeezed out, despite coronary sinus occlusion.
Interestingly, the capillary distension is dependent on reduced myocardial function, where the influence of different γ_{sten} on capillary volume and pressure were evaluated. With reduced myocardial function ($\gamma_{sten} < 1$) capillary volume is increasing and this effect allows retrograde filling.
Besides, capillary volume is also dependent on the collateral resistance. With the increase in the collateral resistance, capillary volume, as well as the capillary pressure, are decreasing. Collateral resistance of 30 mmHg s / ml distension of capillary volume up to 5 ml and capillary pressure up to 37 mmHg was observed. On contrary, by collateral resistance of 300 mmHg s / ml capillary volume distension was only 2.5 seconds and pressures reached 50 mmHg.

9.2.4.3 GCV1 and GCV2

In this model great cardiac vein is simulated by two resistances connected in the series. Between these two resistances there is collateral inflow. The GCV1 is closer to the capillary bed of the LAD and in the model one can observe retrograde and antegrade flow in this part of the LAD. Antegrade flow was calculated for the period of the coronary sinus release, and the retrograde flow is present during coronary sinus occlusion. The most outflow happens during the first heartbeat, which has been well studied. However, retrograde flow increases continuously during the occlusion phase of the coronary sinus.
In the second part of the great cardiac vein (GCV2), one can notice only antegrade flow during both: occlusion and release of the coronary sinus. The flow, however, differs during those two phases. The most remarkable aspect of the modeling was, however, variation of the collateral resistance, and its influence on antegrade and retrograde flow in the region of the LAD and the great cardiac vein (Table 9.2).

This should be especially taken into account when myocardial squeezing is varying. It is natural that if the squeezing power of myocardium is getting better (that means γ_{sten} is increasing) at the same time, despite PICSO, there will be less retrograde flow in the capillary region, because myocardial squeezing is going to pump out the blood more powerful. This observation let the author conclude that with the improvement of the myocardial squeezing function, there will be less retrograde flow. According to this result it would be contraproductive to apply longer occlusions. Possibly, one should reduce inflation period in order to support newly approved myocardial function.

9.2.4.4 Venous volume and pressure

Venous volume oscillates between 21 and 26 ml during PICSO treatment and this value does not changes if the myocardial function is reduced or improved (Fig.9.5). However, p_{ven} shows very characteristic form during coronary sinus occlusion, which is well known from the animal experiment. On contrary to venous volume, the pressure in the venous system is dependent on reduced myocardial function, as well as on the collateral resistance. The small amplitude of the venous volume during coronary sinus release is due to the small pressure gradient between CS and the right atrium. During coronary sinus occlusion V_{ven} is distended up to 29 ml in the systole. In the diastole, a part of the volume is draining retrograde towards capillaries and the smaller amount drains via Thebesian veins.

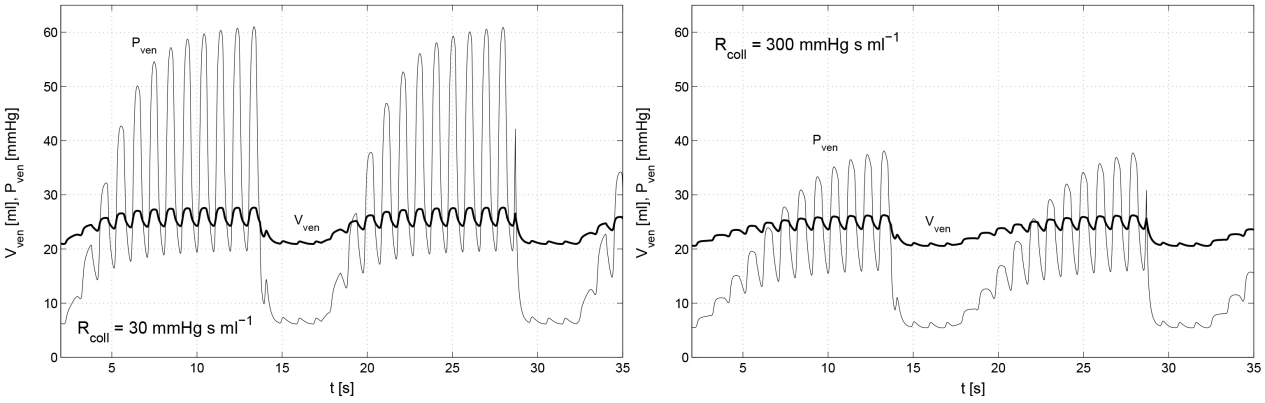

Figure 9.5: The pressure in the venous system is dependent on the degree of the stenoses, as well as on the collateral resistance.

9.3 Effects of PICSO in myocardial infarction

9.3.1 Myocardial protection via the coronary sinus

Following results are by Mohl *et al.* (2008):

9.3.1.1 Baseline patient characteristics

Baseline clinical characteristics of the 2 groups were recorded. No significant difference was observed in the baseline patient characteristics and in angiographical findings just after reperfusion. The PICSO and control group were comparable in age, gender, risk factors, site of thrombus, residual stenosis just after thrombolysis, and extent of coronary artery disease.

9.3.1.2 Hemodynamic effect

The hemodynamic effects of PICSO were recorded. Heart rate, aortic pressure, pulmonary pressure and cardiac index were not significantly affected by PICSO. There was no adverse effect on hemodynamics. Mean systolic CS pressure significantly increased from 8.3 mmHg to 47.4 mmHg when the CS was occluded.

9.3.1.3 Reperfusion time

The mean time to insert a balloon catheter into the CS was 11$\pm$4 min. The time interval to completion of reperfusion in the infarct-related artery from the initial administration of thrombolysis agents was significantly shorter for the PICSO group (28$\pm$12 min) than for the control group (41$\pm$18 min, p=0.014). The difference of the time interval from the onset of symptoms to reperfusion was not significant between the 2 groups.

9.3.1.4 Enzymatic infarct size

The PICSO group showed significantly less total CK release than that of the control group. The peak CK activity value was slightly smaller and the peak time of CK was slightly earlier for the PICSO group than those for the control group (p=0.16, 0.09, respectively).

9.3.1.5 Cardiac function analysis

A left ventriculogram done at 30 days after myocardial infarction (MI) showed that the PICSO group had significantly smaller abnormally contracting segments (21.4$\pm$16.5%) than the control group (31.9$\pm$10.6%; p<0.05).
Global and regional ejection fractions, which were measured for each group, failed to show any differences between the PICSO group (41.3$\pm$17.1, 23.2$\pm$17.1, respectively) and control group (49.6$\pm$10, 22.8$\pm$17, respectively). One patient in the PICSO group, who had a very severe course and had a delayed reperfusion, which is demonstrated by his value for total CK release, had a very low ejection fraction of 8%, and he was among those who needed further intervention. Otherwise, median values showed no difference between groups (51%), with regional ejection fraction values being 31% for the PICSO group compared with 26% for the control group.
The value for defect severity, which was assessed using 201 TI SPECT perfusion at 30 days after onset of symptoms, was significantly smaller for the PICSO group compared with the control group, indicating that PICSO contributed to reducing infarct size. The QRS score for the PICSO group (6.7$\pm$6.7) was also significantly smaller than that for the control group (11$\pm$4.3, p=0.038).

9.3.1.6 Myocardial lactate metabolism after thrombolysis

Lactate extraction became positive within 6 h from the onset of symptoms in the PICSO group. Conversely, lactate extraction in the control group was still negative or around zero 24 h after the onset. Baseline-adjusted reference (PICSO - control) demonstrated that there was almost a statistical difference between the groups at 24 h after reperfusion.

9.3.1.7 Restenosis

After adjusting for baseline differences, the PICSO group had a lower stenosis value at Day 30. Average baseline-adjusted stenosis at Day 30 was 65.5% for the PICSO group but 73.5% for the control group (p=0.0126). In other

words, the incidence of stenosis was about 8% less (SE, 3.02%) after PICSO compared with the control group. Non-parametric analysis confirmed this result with a p-value of 0.044.

9.3.1.8 Time to MACE

The median follow-up time was 67 months (25th percentile, 58 months; 75th percentile, 81 months). They observed major adverse cardiovascular events (MACE) in 15 patients (44%; 3 patients in the PICSO group, 12 patients in the control group). Progression of the culprit lesion of the proximal LAD was observed in all 15 patients. Four patients in the control group developed reinfarction that was fatal, resulting in 3 cardiac deaths. Recurrence of unstable angina was observed in 8 control patients compared with 3 PICSO patients. In the control group, this resulted in PCI (7 patients) and, because of multivessel involvement in 1 patient, in CABG. Three PICSO patients had PCI only. Cardiac event-free survival was significantly longer in the PICSO group compared with the control group ($p<0.0001$). The cardiac event-free survival rate at 48 months was 82% for the PICSO group but only 23% for the control group. The relative risk for cardiac events (95% CI) of PICSO compared with control was 0.12 (0.03, 0.42), meaning that the risk for cardiac events was 8.4 times higher for the control group than for the PICSO group. Adjusting for reperfusion time, the relative risk for PICSO compared with control is 0.14 (0.04-0.52). Adjusting for pain-to-admission time changes, the relative risk for PICSO compared with control only was 0.19 (0.05-0.59). The relative risk estimate did not change by more than 0.02 when any of the other risk factors were included in the analysis, suggesting that the minor differences in risk factor exposure in the 2 groups do not affect their conclusions. There is a strong relationship between restenosis and MACE, the Hazards ratio is 24 (per 25% stenosis), and confidence limits are 1.86-312 ($p=0.0149$). Adjusting for restenosis, the relative risk of PICSO compared with control was 0.11 (0.03, 0.40), meaning that the risk for MACE was 9 times higher for the control group than for the PICSO group.

9.3.1.9 Time to reinfarction

Time to re-MI was significantly longer in the PICSO group compared with the control group ($p=0.0152$). After 48 months, 100% (95% CI, 81-100%) of patients in the PICSO group but only 55.6% (95% CI, 20.4-80.4%) in the control group were free from re-MI. The relative risk for re-MI (95% CI) of PICSO compared with control was 0.058 (0.0004, 0.55), meaning that the risk for re-MI was 17 times higher for the control group than for the PICSO group. Adjusting for reperfusion time, the relative risk for PICSO compared with control was 0.039 (0.0003-0.39).
Adjusting for pain-to-admission time changes, the relative risk for PICSO compared with control was 0.06 (0.0005-0.62). The relative risk estimate did not change by more than 0.02 when any of the other risk factors were included in the analysis. Particularly, after adjusting for restenosis, the relative risk of PICSO compared with control was 0.035 (0.0002, 0.45), meaning that the risk for reinfarction was 29 times higher for the control group than for the PICSO group.

9.3.2 Intracoronary hemodynamic effects of PICSO

Following results are by van de Hoef *et al.* (2012):

9.3.2.1 Patients and procedural characteristics

A total of 15 patients (mean age: 62 $\pm$ 7 years) with stable angina pectoris were included in the study. CS catheterization and delivery of the PICSO Impulse catheter was successful in all patients. Median duration from insertion of the steerable sheath until successful delivery of the PICSO Impulse catheter into the CS was 12 minutes (IQR: 9-18 minutes). Initial console calibration difficulties occurred in the first 3 patients, precluding conduction of the study protocol. In addition, the study protocol was not completed in 2 patients, one because of a vagal response at the start of the procedure, and another in whom the pressure sensor guidewire could not be positioned in the distal LAD. These 5 patients were excluded from hemodynamic analysis. Therefore, the study population consisted of 10 patients. Optimal positioning of the PICSO Impulse catheter, enabling adequate elevation of the CS pressure, was achieved in all 10 study patients.

9.3.2.2 Hemodynamic impact of PICSO

Figure 9.6 shows a typical recording of aortic pressure, distal LAD wedge pressure, and CS pressure during a low-pressure balloon occlusion of the LAD without (Fig.9.6A) and with PICSO (Fig.9.6B). Concomitant intermittent occlusion of the CS resulted in an intermittent obstruction of venous outflow, which increased the CS pressure. As highlighted in Figure 9.7, this pressure increase in the coronary venous system due to PICSO correlated with a simultaneous increase in distal LAD wedge pressure. Initial wedge pressures were not significantly different between the 2 LAD occlusions (31$\pm$14 mmHg without PICSO vs. 29$\pm$13 mmHg with PICSO; p=0.34). The difference in mean LAD wedge pressure compared to the initial wedge pressure was higher during LAD occlusion with PICSO than without PICSO (2$\pm$4 mmHg without PICSO vs. 5$\pm$4 mmHg with PICSO; p<0.001). Subsequently, they compared the occlusion phase of PICSO (inflated balloon) with the non-occlusion phase (deflated balloon) to evaluate the pulsatile nature of PICSO. Results of the absolute values of CS pressure and distal LAD wedge

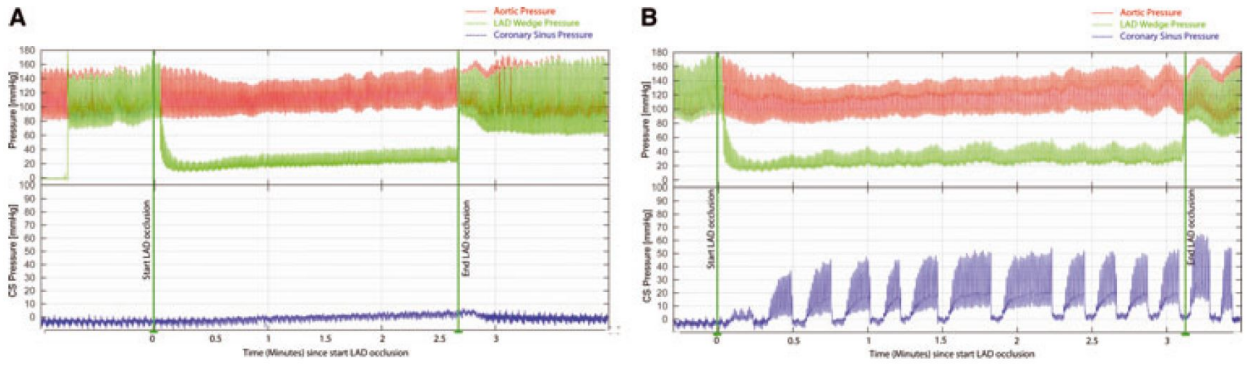

Figure 9.6: Hemodynamic measurements during a low pressure balloon occlusion in the left anterior descending artery (LAD). (A) LAD occlusion without PICSO. (B) LAD occlusion with PICSO. Of note: the coronary sinus pressure plateau is higher when the LAD occlusion has ended.

pressure during LAD occlusion and PICSO were also shown. Occlusion of the CS resulted in a significant increase in mean CS pressure. Concomitantly, CS pulse pressure increased significantly when the CS was occluded. Simultaneously, mean coronary wedge pressure in the LAD increased 10% on average when the CS was occluded, and pulse pressure in the distal LAD increased 17% on average during the occlusion phase of PICSO. Notably, the increase in mean and pulse pressure in the CS was enhanced in those patients with a high initial coronary wedge

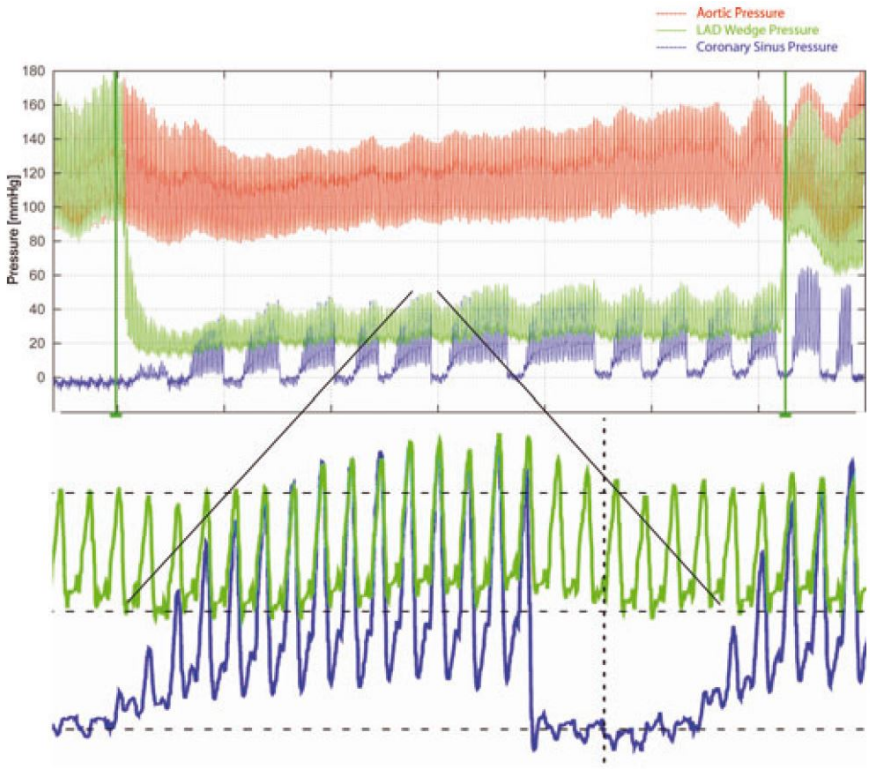

Figure 9.7: Coronary sinus and LAD wedge pressure measurements. Elevation of coronary sinus pressure results in a simultaneous increase in distal LAD pressure.

pressure; high coronary wedge pressures correlated with a high increase in CS pressure during CS occlusion (r=0.806; p=0.005). Furthermore, the mean CS pressure, averaged over 2 PICSO cycles, increased significantly after LAD balloon deflation (22.3$\pm$5.6 mmHg with LAD occluded vs. 26.9$\pm$6.8 mmHg with LAD not occluded; p=0.003).

9.3.2.3 Myocardial ischemia: ST-Segment deviation score

No period effect or treatment-period interaction in ST-segment deviation was found (p=0.34 and p=0.35, respectively). When PICSO was performed during the first LAD occlusion, ST-segment deviation was similar to the second LAD occlusion without PICSO. When the order was reversed, and PICSO was provided during the second LAD occlusion, ST-segment deviation was numerically lower during the LAD occlusion with PICSO, but the difference did not reach statistical significance. Overall, electrocardiographic measures of ischemia during LAD occlusion with PICSO were numerically lower when compared to the LAD occlusion without PICSO, but did not reach statistical significance (13$\pm$6 mm vs. 11$\pm$ 6mm; p=0.26).

9.3.2.4 Follow-up

No CS perforation, dissection or thrombosis occurred. Two adverse events occurred during 30-day follow-up. A periprocedural myocardial infarction developed in 1 patient from compromise of a small diagonal side branch after LAD stent implantation performed after PICSO. The second patient required repeat revascularization of a

non-target vessel because of residual angina. No other adverse events were observed during the follow-up period.

9.3.3 Safety and feasibility

Following results of the safety and feasibility were done by van de Hoef *et al.* (2015)

9.3.3.1 PICSO feasibility

PICSO therapy was initiated in 19 out of 30 patients (63%), and was provided for the intended 90 ($\pm$2) minutes in 12 patients (63% of patients in whom PICSO could be initiated, 40% of all included patients). In the 11 patients in whom PICSO therapy was not initiated, this resulted from the inability to engage the coronary sinus in one patient (3%), from a user error in one patient (3%), from an unstable PICSO catheter position prohibiting catheter calibration in six patients (20%), and from exceeded PICSO console safety limits in one patient (3%). A serious adverse event during PICSO catheter calibration precluded initiation of PICSO therapy in one patient (3%). Additionally, the study protocol was aborted prior to PICSO initiation in one patient (3%) as a result of catheterization laboratory logistics.
In the seven patients in whom maintenance of PICSO therapy for 90 ($\pm$2) minutes was unsuccessful, this resulted from catheter instability in two patients (7%), and from exceeded PICSO console safety limits in four patients (13%). Additionally, PICSO therapy was aborted in one patient (3%) as a result of catheterization laboratory logistics.

9.3.3.2 PICSO quantity

In those patients in whom PICSO was initiated, PICSO therapy was provided for a median of 88.8 minutes (Q1, Q3: 72.0, 89.6 minutes). Median PICSO quantity in these patients was 494 mmHg (Q1, Q3: 160, 1,171 mmHg). PICSO quantity was substantially higher in the centre with previous experience with the PICSO Impulse System, as compared to the other centres (852 mmHg [Q1, Q3: 572, 1,347 mmHg] vs. 160 mmHg [Q1, Q3: 82, 282 mmHg], respectively; p=0.007), despite equivalent PICSO therapy duration across centres (88.9 minutes [Q1, Q3: 81.3, 90.6 minutes] vs. 88.8 minutes [Q1, Q3: 72.0, 89.2 minutes], respectively; p=0.46).

9.3.3.3 PICSO safety

One serious adverse device event was reported during the study. In this patient, cardiac tamponade occurred immediately after starting PICSO calibration, in retrospect originating from guidewire-induced coronary sinus perforation during wiring of the coronary sinus. As such, the adverse event was attributed to the implantation procedure. The tamponade was successfully managed with pericardiocentesis. Nonetheless, the patient developed segmental pulmonary embolism during hospitalization, for which oral anticoagulation was prescribed for six months post discharge without further clinical sequelae.
Three patients were transferred to the coronary care unit to receive the final 60 minutes of PICSO therapy without the occurrence of adverse events. During follow-up, two episodes of MACE occurred. One patient in whom PICSO could not be initiated died seven months after the procedure without documented cause, and one patient in whom only low PICSO quantity was achieved died nine months after the procedure due to a major stroke.

9.3.3.4 Efficacy analysis of PICSO versus historical control patients

Evaluable CMR data were available in 13 PICSO patients for global and segmental LV function, and in 11 PICSO patients for infarct size analyses. Global and segmental LV function at baseline and follow-up CMR were not significantly different in PICSO patients compared with their matched controls. Similarly, infarct size at baseline and follow-up, the extent of MVO, and the reduction in infarct size from baseline to follow-up were not significantly different between the groups.

9.3.3.5 CMR analyses according to high or low PICSO quantity versus matched control patients

Since efficacy of PICSO conceivably depends on effective modulation of coronary sinus pressure, and is probably negligible when pressure modulation is minimal, additional CMR analyses were performed according to the magnitude of PICSO quantity. In the absence of clinical cut-off values for PICSO quantity, patients were stratified into a high and low PICSO quantity group based on the median PICSO quantity (494 mmHg).
Myocardial function tended to be preserved to a greater extent in patients with high as compared to low PICSO quantity. Moreover, high PICSO quantity was generally associated with favorable trends in the magnitude of infarct size, MVO, and MSI. Even in this small patient cohort, infarct size reduction from baseline to follow-up MRI was significantly higher for high PICSO quantity patients compared with those patients in whom PICSO quantity was low (41.6±8.2% vs. 21.1±14.1%, respectively; p=0.02), where the reduction in infarct size from baseline to follow-up CMR showed a significant dose dependency (r2=0.70, p=0.008) (Fig.9.8). These favorable trends for patients

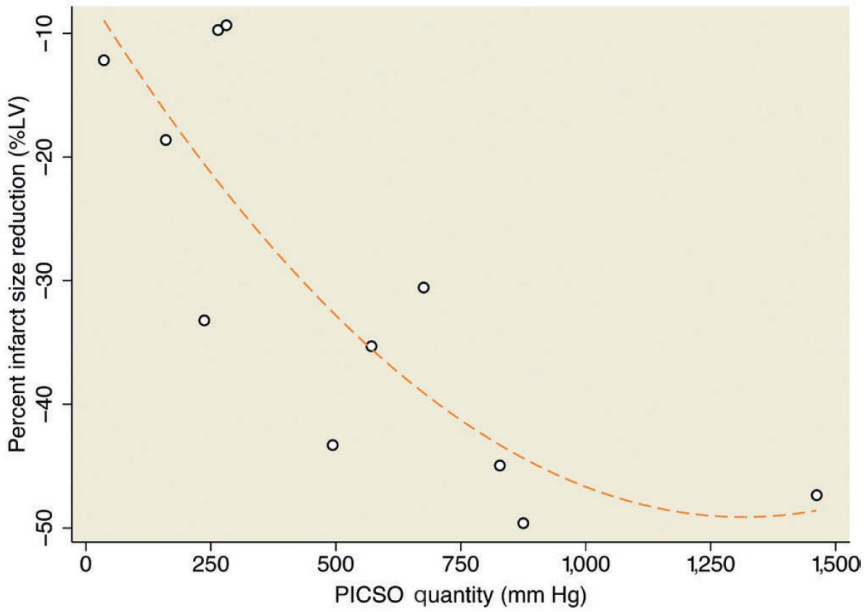

Figure 9.8: Relationship between PICSO quantity and infarct size reduction expressed as the percent change in infarct size (% of the left ventricle) from baseline (day 2-5) to four-month follow-up.

with high PICSO quantity were confirmed as compared to their matched control patients. Notably, infarct size reduction from baseline to follow-up CMR was significantly greater in the high PICSO quantity group compared with its matched controls (41.6±8.2% vs. 27.7±9.9%, respectively; p=0.04).
MVO tended to be reduced in the high PICSO quantity group compared to the matched control group, although

this difference did not reach statistical significance (2.0±3.0% versus 6.7±6.6% of total infarct size, respectively; p=0.18). In contrast, the low PICSO quantity patients demonstrated similar LV function and volumes at baseline and follow-up, and similar MVO and infarct size reduction over time compared to their matched control patients.

9.3.4 From myocardial salvage to tissue regeneration

Following results are by Mohl *et al.* (2015):

9.3.4.1 The salvage potential of PICSO

The significance of myocardial salvage by ICSO has been established in a meta-analysis of 7 experimental trials comprising 125 test animals that showed an inverse relationship between achieved (developed) coronary sinus systolic pressure, (i.e. occlusion duration and elevation of the coronary venous systolic pressure per minute multiplied by the application times of ICSO) and infarct size. The so-called "dose dependence" between optimized ICSO therapy and salvage has been documented in different species and different durations of ischemia [Syeda *et al.* (2004)].

Syeda *et al.* (2004) reported a significant reduction in infarct size of 29.3% in the PICSO group compared to the control group (p<0.001; 95% confidence interval, -40.9 to -17.7), which correlated to the achieved (developed) coronary sinus pressure increase per minute (r=- 0.92; p<0.007) [Syeda *et al.* (2004)]. This dose-dependency has been recently confirmed by the Prepare RAMSES study, which showed a significant correlation (r=0.70, p=0.008) in reduction in infarct size and the cumulated coronary sinus pressure modulation over time [van de Hoef *et al.* (2015)]. This has led to the development of an algorithm by Miracor Medical Systems that automatically calculates the PICSO quantity applied. The quantity is calculated as:

$$\text{PICSO Quantity} = \sum_{n=1}^{n=total\ PICSO\ cycles} ((sCSPP_n - dCSPP_n) * (sCSPP_n - CSPDA_n) * IHT_n) \tag{9.4}$$

(mean systolic coronary sinus pressure plateau - mean coronary sinus pressure during deflation) $*$ (mean systolic coronary sinus pressure plateau - mean diastolic coronary sinus pressure plateau) $*$ (Balloon inflation hold time), summed over the complete PICSO procedure and expressed in [mmHg]. It therefore reflects the magnitude of coronary sinus pressure modulation during the complete PICSO procedure. The meta-analysis [Syeda *et al.* (2004)] analyzing different experimental ischemia protocols showed that additional retroperfusion of arterial blood during ISCO was found to increase salvage by around 10%, but dose dependence data showed that the amount of blood retroperfused had an inverse correlation to salvage (r=-0.97; p<0.004), indicating a counterproductive engorgement of the coronary vasculature. Therefore, redistribution of venous flow together with periodic washout of metabolites, rather than additional arterial infusion and perfusion, is responsible for myocardial salvage [Mohl *et al.* (1984b), (1985b)].

The relationship between the hemodynamic force of periodic elevation of coronary venous pressure on jeopardized myocardium and salvage has only recently been appreciated because historically, the scientific mainstream associated beneficial effects of CSI and myocardial salvage with delivery of oxygenated blood. Salvage never occurs in Krogh-like diffusion cylinders around major "arterialized" retroperfused cardiac veins, but rather in border zones of deprived myocardium, therefore it is very unlikely that retroperfused oxygen is the benefactor in CSI. On the contrary, it is believed that redistribution of venous blood into the center of ischemia and washout, thus maintaining basal metabolism as well as vasodilation, collateral flow and improved perfusion of the border zone

leading to increased energy storage is the main factor of salvage in CSI. Clinical data on myocardial salvage and PICSO are limited to applications combined with lysis therapy and date back to the early clinical trials of CSI. However, long term clinical trial data are available, which should be corroborated during reperfusion by pPCI in clinical trials [Mohl *et al.* (2008)]. Although these historical studies have employed primitive technology and observer limited PICSO, clinical experience has supported the findings of animal studies [Komamura *et al.* (1989), Mohl *et al.* (2008)]. Enzymatic infarct measurements in patients with a lysis protocol with and without PICSO showed significantly less total creatine kinase (CK) release than that of the control group, an important finding since CK is a prognostic indicator following acute myocardial infarction (MI). Infarct size assessed at 30 days after onset of symptoms was significantly smaller for the PICSO group compared with the control group [Mohl *et al.* (2008)]. Although CS catheter placement required additional treatment time (mean time to insert a balloon catheter into the CS was 11$\pm$4 min) the period to the completion of reperfusion in the infarct-related artery from the initial administration of thrombolysis agents was significantly shorter for the PICSO group (28$\pm$12 min) than for the control group (41$\pm$18 min, p=0.014). The reduced procedure time in the PICSO group resulted from enhanced clearing of the microcirculation and even the site of coronary occlusion from thrombus (as seen by Meerbaum in animal models [Meerbaum *et. al* (1983)). A left ventriculogram at 30 days after MI showed that the PICSO group had significantly smaller abnormally contracting segments (21.4$\pm$16.5%) than the control group (31.9$\pm$10.6%; p<0.05). The global ejection fraction, however, did not differ significantly among groups.

Surprisingly, 5-year follow up showed results on risk reduction to suffer from re-infarction or major cardiac events: 96% risk reduction for re-infarction (95% CI: 61%-99%), 86% risk reduction for major adverse cardiac events (MACE) (95% CI: 48%-96%) after PICSO. Freedom from major adverse cardiac events was 82% for the PICSO group but only 23% for the control group. These results are noteworthy since they show superiority even against analysis of STEMI by Pedersen *et al.* (2014) even after risk adjustments for differences in times to reperfusion and correcting for residual stenosis in the culprit vessel after 30 days. In context with the findings by Weigel *et al.* (2007) on upregulation of vasoactive and cardioprotective molecules in experimental studies applying PICSO and recent clinical findings by Kusmic *et al.* (2014) supporting the clinical effectiveness of upregulation of HO-hemeoxygenase, PICSO unfolds a second important mechanism, namely support of regenerative efforts of the myocardium in jeopardy. These discoveries have been a turning point in the knowledge of the basic mechanism of PICSO and have led to the development of the hypothesis "embryonic recall", claiming that PICSO interferes with molecular cascades during infarct healing and might initiate structural recovery beyond salvage.

Historical data by Mohl *et al.* (1988b) for PICSO in ACS are only available for intervention in the late ischemic time, but before reperfusion. Advances enable intervention in the early reperfusion period. It may be possible to commence PICSO when passing the guide wire to reopen the coronary occlusion before treating the residual stenosis. Furthermore, the existing relationship between cellular damage and enzyme leakage during PICSO and intensified washout relates to better preservation of regional function.

van de Hoef *et al.* (2015) compared matched controls with 30 patients with acute coronary syndromes treated with pPCI and additional 90 minutes of PICSO in the reperfusion period. They confirmed additional salvage (baseline versus 4 months) in the PICSO group compared to matched controls measured by MRI (41.6$\pm$8.2% vs. 27.7$\pm$9.9%, p<0.04).

9.3.5 Early PICSO preserves LVEF in porcine acute myocardial infarction

Kessels *et al.* (2015) results showed that the histologic and MRI group mean values for percent infarct size were numerically lowest in Group A when compared to Group B and Group C, albeit not reaching significance (13.5%±5.8% vs. 16.6%±3.6% vs. 16.2%±4.2% respectively, p=0.31). The same was true for MVO (3.2%±3.5% vs. 6.4%±7.7% vs. 8.8%±7.1% respectively, p=0.16). However, left ventricular ejection fraction (LVEF) was greatest in the Early PICSO group (61.0±7.0% vs. 50.2±9.8% vs. 52.3±7.3% respectively, p=0.02), as was wall thickening (49.7±15.0 vs. 33.7±15.1 vs. 39.5±7.0 respectively, p=0.045). Compared to control, group A animals had 3-fold greater expression of VEGF-R1 in the myocardial zone remote from the infarct (median [IQR] 19 [12-24] vs. 9 [6.8-11.5] vs. 5 [3.5-8] respectively, p=0.001). Group B animals had 2-fold greater expression of VEGF-R2 in the border zone of the infarct compared to control (5 [3.5-9], 14.5 [9.5-16], 6 [5-12.5], respectively). No safety issues were noted.

9.3.6 Infarct size reduction and results in functional recovery

Egred *et al.* (2016) established PICSO in 29 patients; 31 patients treated with primary PCI only served as control. Baseline features were well matched between groups except for age, gender, and height. Significantly fewer PICSO-treated patients had evidence of MVO compared to control (18.75% vs. 57.90%, p=0.019). At 5-days post MI patients treated with PICSO had smaller infarct size (IS), in % of LV (7.72±7.50 vs. 19.19±12.56, p=0.002), LV ejection fraction (53.21%±7.94% vs. 46.84%±8.52%, p=0.018), smaller LV end-systolic volume (40.52±12.50 vs. 52.11±14.94, p=0.011) and LV end-diastolic volume (84.99±14.69 vs. 96.61±17.35, p=0.026). After multivariable analysis to adjust for differences in baseline features, PICSO was predicted in absolute IS by 10.57 percent points (95% CI [-17.19%; -3.44%], p=0.005) compared to the control group.

9.3.7 Infarct size reduction after pPCI

Egred *et al.* (2017) enrolled twenty patients in the PICSO study and 80 control patients from INFUSE-AMI were available. After propensity score matching, 15 PICSO patients and 40 INFUSE-AMI remained. Baseline variables were well matched between the groups. Mean infarct size (% total left ventricular mass) in PICSO treated patients was 10.9% (95% CI 5.1%, 16.8%), which was less than that in the INFUSE-AMI control group (20.9% (95% CI 17.33%, 24.48%)); mean difference -10.0% (95% CI -16.8%, -3.2%), p-value = 0.004.

Chapter 10

Discussion/Conclusion

10.1 Phenomenological modeling

Schreiner *et al.* (1990b) concluded that for several reasons, it might be questionable to assume a simple linear relationship between coronary venous pressure and arterial flow:

- Firstly, non-coronary sinus flow sustaining a certain level of total perfusion is thought to become increasingly important as a compensatory mechanism when coronary sinus flow is heavily obstructed;
- Secondly, the distensibility of the vessels and the pressure in the surrounding tissues will change when PICSO is applied, so that the distribution of impedances in the micro-circulation cannot be assumed to remain constant.

The authors believe these mechanism to be responsible for the long-time stability of the flow level observed at a given experimental condition, irrespective of the PICSO cycle length and occlusion time applied. Consequently, they dropped the assumption of linearity for zero frequency. For non-zero frequencies, however, they could show that a suitable transfer function can be found, by means of which it is possible to predict at least the shape of the low curve from CSP measurements.
Flow prediction was possible, even though in this first approach they simply chose the Fourier transform on an exponential for the transfer function. With more experimental data it should be possible to fit more than two parameters and to use a more sophisticated function which could represent the data more accurately. The question remains, however, whether a single transfer function, i.e. a single set of parameters can be applied to different individuals at all. In order to adjust parameters individually, one could try to relate them to other variables, such as heart rate, arterial and venous pressure, etc. and to use these quantities as estimators for the parameters of the transfer function.
Thus, further experiments are needed to validate and improve the low prediction, to fit the parameters of the transfer function to a larger sample and to re-validate the new parameters.

10.2 Mechanistic modeling

10.2.1 Further concepts

Schreiner *et al.* (1990b) stated that the variations of model parameters may be applied in support of the search for a direction toward an optimal intervention mode. However, the parameters investigated do not refer to the intervention pattern itself, i.e. the occlusion/release timing, but rather to prevailing physiological covariables which importantly affect the efficacy of the intervention. Thus, the model may also be used to determine those physiological states which are most favorable for effective CSIs. Different physiological states inevitably occur during experimental studies in different animals, adding variability (intersubjective spread) in any statistical analysis of CSIs efficacy. Yet, knowing the directional impact of the various covariables, from the simulation results, might be helpful in normalizing for the covariables, prior to the statistical evaluation.
In summary, the mechanistic modeling of coronary circulation during CSIs may provide quantitative estimates of myocardial blood redistribution, as well as qualitative insights regarding the direction of changes to be expected whenever certain elements of an experimental CSI design are modified.

10.2.2 Discussion

10.2.2.1 Schreiner model

Several models of the coronary circulation have been proposed in the literature. Mates *et al.* (1983) evaluated networks of capacities, resistances, and inertial elements, which were adjusted to experimental findings by optimization techniques. However, extramural compression and the effects thereof were not explicitly incorporated. Vergroesen *et al.* (1987) applied resistive and capacitive elements to interpret measurements on intramyocardial compliance. Downey *et al.* (1983) modeled systolic impedance to flow in different layers of the myocardium by introducing back pressures as driving forces together with nonlinear elements (diodes). Sun and Gewirtz (1988) have compared the performance of four of these models against canine data and estimated intramyocardial pressure. However, the two models involving diodes produced flow patterns with sharp edges. Before these aforementioned approaches, Arts (1978) had already introduced volume dependent resistances and different myocardial layers. His model was slightly modified and further evaluated by Bruinsma *et al.* (1988). Bayar and Sideman (1987) used zener diodes instead of diodes to reproduce zero flow pressure found experimentally.
All these models focused on the arterial side of the coronary circulation, even if they formally considered the venous section. Wong *et al.* (1984) provided a model which explicitly took experimental data on venous pressure into account. Coronary artery flow was entered as a driving force rather than being calculated. Volume-dependent compliances and resistances were modeled similar to the work of Arts (1978). However, the rise in venous pressure calculated for coronary sinus occlusion in their model did not agree with the typical form found experimentally. Beyar *et al.* (1989) considered the venous section and even CSO. However, they did not show how their model, based on the waterfall concept without volume dependent resistances, reproduced coronary sinus pressure data.
In the present work, three key features of the aforementioned approaches are retained:

- volume-dependent resistances,
- volume-dependent compliances, and
- intramyocardial pressure being proportional to left ventricular pressure.

Resistances were split into "static" and "dynamic" components [Eq.(6.18), (6.19), (6.25), (6.26)]. This has been proposed by Sun and Gewirtz (1988), but is different from Bruinsma *et al.* (1988), who used two fully volume-dependent resistors for each compartment. Using separate equations [(6.18), (6.19), (6.25), (6.26)] to calculate flow, depending on the pressure gradient, may also be interpreted as "gradually closing valves" which softly terminate the egress from a compartment if the volume approaches zero, while avoiding the discontinuous behavior of diodes. Bruinsma *et al.* (1988) used the same functional forms of volume-dependent compliance for the arteriolar, the capillary and the venous compartment with different parameters of shape. They introduced another parameter in order to scale the compliances to the different volumes of arteriolar, capillary, and venous compartments, which were taken from a compilation of experimental estimates. Conversely, in this work capillary and venous compliances are adjusted simultaneously and more directly in a two-pass procedure, exploiting the information of experimental data on venous pressure rise under an additional boundary condition (CSO).

Critique of Methods

Models of coronary circulation must always be simplifications of the real situation. In the present work the simplifications introduced consist of

1. disregarding arterial compliance and inertial elements
2. lumping together epi- and endocardial layers
3. replacing the distributed and frequency-dependent resistances of vascular trees (vessel divisions) by simple resistors
4. considering only one venous compartment
5. neglecting collateral flow
6. using constant capillary compliance
7. disregarding autoregulation.

Some of the above features could be included in the model. However, this would mean adding additional parameters which cannot be accurately assessed and which are of minor importance for venous hemodynamics, on which the present work focuses.

1. The effects of arterial compliance and inertial elements on venous hemodynamics are heavily damped across the high-resistance capillary compartment.

2. Even if the distribution of myocardial pressure across the ventricular wall is known [Heineman *et al.* (1985)] the distributions of all other model parameters remain hard to assess. Bruinsma *et al.* (1988) had to assume an epi /endo ratio even for the compartmental volumes due to a lack of data. Moreover, in their model the flows in different layers were simply added, rather than coupled, and therefore the model provides the same information obtained by simulating one layer with different parameters (e.g., squeezing). In particular, the redistribution of flow between endocardial and epicardial layers can only be simulated using substantial resistances upstream to the branching into layers. In the light of these arguments the authors preferred a single layer. With the computer resources presently at hand, "lumping" seems unavoidable.

4. They have attempted to split the venous compartment in order to simulate "the opening" of additional shunts, pathways and storage areas under venous distension pressure, as suggested by qualitative physiologic arguments. However, the model became drastically under-determined and parameters could no longer be assessed due to lack of sufficient experimental data.

5. Collateral flow varies considerably between individuals and is therefore hard to introduce into a model.
6. Constant capillary compliance was assumed in concordance with other investigators [Mates *et al.* (1983), Downey *et al.* (1983), Sun and Gewirtz (1988)] and proved sufficient to reproduce arterial and venous hemodynamics with the present model.
7. Autoregulation has been explicitly considered by Wong *et al.* (1984). Many models either disregard it or restrict themselves to maximally dilated vascular beds. In any case, a quantitative representation would require all remaining parameters to be expressed as functions of a "vasodilation index", a level of complexity from which we refrained.
Despite the above mentioned simplifications, the present model reproduced experimental results obtained for the phasic pattern of arterial inflow, the mean values for flow [Netter (1983)], the non-coronary sinus flow as well as the reaction of venous pressure [Schreiner *et al.* (1988b, 1988a)] under both normal and CSO conditions. They therefore infer that the calculated intramyocardial flow between capillaries and veins, which is inaccessible to measurement, at least approximated the real situation in its key features.
Another quantity which is reproduced by the model, although not primarily addressed, is zero-flow pressure (p_{zf}). p_{zf}, as a possible cause of underperfusion during diastole, has been discussed and investigated experimentally. In the present model, it turned out that the minimum of $p_{LCX}^{sqz}(t)$ was a lower bound for p_{zf}. Reduction of perfusion pressure showed that p_{zf} was very close to this minimum (10 mmHg) since compliance is large at low volumes and hence only a negligible distension pressure adds to extramural compression shortly before vessel collapse.
The sensitivity analysis revealed that percent changes in calculated flows were smaller than the percent change (100%) applied to the respective parameter. The arterial resistance ($R_{LAD}^{art\rightarrow cap}$) had the largest impact on flow (-49%) during coronary sinus release. For clarity, it must be noted that retrograde flows numerically have negative signs. Hence, e.g., -27.3% means in fact a reduction in absolute value.
The sensitivity analysis also confirmed some aspects of the approach adopted in the two-pass, multistep assessment of parameters (section 8.2.3 Assessment of model parameters). For example, they mention the lack of sensitivity of mean coronary flow during coronary sinus release to changes in χ_{ven}, σ_{ven} and V_{ven}^{0}. It indicates that these parameters can hardly be assessed from experimental data under normal perfusion conditions. Experimental data obtained under a new boundary condition, such as CSO, can provide the necessary information on the venous bed. Incorporating this information, particularly the shape of venous pressure rise [Schreiner *et al.* (1987)], into a model seems to be an advantage of the present, as compared to previous, work [Bruinsma *et al.* (1988)].

10.2.2.2 Model Oswald

With the consideration of the asymmetry of the LAD and LCX beds it was possible to reproduce the LCX-flow by keeping the given value of the LCA-flow from the literature. However, it was not possible to reproduce the hyperemic reaction of the LCX-flow in the deflation phase in this model. Therefore, it would be necessary to refine the model, e.g. regarding the resistance in the arterial area.
The consideration of the residual volume of the balloon catheter by increasing the resistance of the coronary sinus, it was possible to reproduce the coronary sinus pressure without PICSO. The behavior of the CSP after inflation was reproducible, although the adaptation of several parameters were not considered. That shows the consistency of the model. Another trait is the adaptation of the total resistance of both retrograde flows out of the coronary vessels regarding the goal 'CSP without PICSO' and then the variation of the ratio between the two resistances.

Whereas the latter reproduce the LCX-flow in the inflation phase.
Following equation shows a linear relationship between pressure gradient and flow of a catheter in a vessel:

$$Q_{DP} = \frac{\Delta p}{R_{DP}} \tag{10.1}$$

where DP stands for double pipe. However, following equation shows that resistance in the double pipe is higher than the resistance in the hollow pipe HP:

$$R_{DP} = R_{HP}\left[1 - \frac{r_0^4}{R_0^4} - \frac{(R_0^2 - r_0^2)^2}{R_0^4 ln(R_0/r_0)}\right]^{-1} \tag{10.2}$$

Setting the radius of the catheter r_0 to 40% of the radius of the vessel R_0 gives with the equation above Eq. (10.2) a catheter resistance $R_{DP} = 4.9 \cdot R_{HP}$. Setting r_0 to 60% of R_0 results in $R_{DP} = 14.5 \cdot R_{HP}$. The consequence of changing the ratio between the radii to 50% (just a few millimeters) can lead to an increase of 250% of the resistance. That shows the importance of the ratio between r_0 and R_0 if a quick outflow of the dammed blood in the deflation phase is desired.
The systolic plateau of the CSP in the inflation phase was significantly lower than the in the experiment found one and an increase of C_{LCX}^{cap}, which has a value of 0.7 ml / mmHg in the model, has hardly an impact on the calculated CSP-plateau. By varying the total resistance influences the systolic CSP and the systolic plateau in the inflation phase. Since an increase of C_{LCX}^{cap} has nearly no impact on the CSP-plateau, it is assumable that a different parameter limits the LCX-volume and therefore the pressure during systole in the capillaries . This pressure is also crucial for the CSP. A possible limit factor could be the total resistance R_{tot}, where a decrease lead to an increase of the capillary volume and CSP-plateau.
The calculated CSP and LCX-flow are leading ahead the corresponding experimentally found values. In the model a solid pipe wall and a constant blood density was used. Both simplifications lead to an infinite spread of the velocity by changing the pressure according the Hagen-Poiseuille law. Assuming the length of the coronary vessel of 0.1 m would lead to a propagation velocity of the pressure wave of 10 m /s. That results in a pressure change on the arterial side after 0.01 s on the venous side and that corresponds to the phase shift of 0.02 s between the measured and calculated data in the model.

10.2.2.3 Model Kajgana

The data obtained by experiment during PICSO intervention can provide a solid basis for realistic modelling. The model proposed to comprise several compartments (Fig.6.2).
An important part of the model is a volume dependent coronary venous compliance, which decreases as the venous bed is distended. A pressure volume relation of this type proved to be obligatory in order to reproduce the CSP rise with characteristic shape of the systolic and diastolic envelopes.
Further model elements are volume dependent resistances governing outlet from the capillary compartment. The total resistance to the flow leaving the capillaries was assumed to increase with the inverse square of capillary volume (Poiseuilles' law), i.e. effectively becomes infinite as the capillary bed is totally emptied. This approach imitates the increased resistance during vessel collapse which is caused by the systolic squeezing. The rest of the model is based on the ordinary linear relations between pressure gradients, resistances and flows.
This model also supplements previous approaches focused on the arterial and venous coronary circulation with no special regard on collaterals. Nakazawa *et al.* (1978) showed the importance of the venous interconnections, which may allow extensive movement of venous blood when the coronary sinus is occluded. His findings indicated

that one third of the blood supplied to left ventricular myocardium through the anterior descending artery normally drains to the coronary sinus through circumflex venous branches rather than through the great cardiac vein. On the other hand about 5% of the circumflex inflow passed into the great cardiac vein through the venous channels connecting the anterior descending and circumflex beds. In the model an example demonstrates the impact of those interconnections. Therefor the author decided to model collaterals from the circumflex to LAD venous bed and picked out exactly those interconnections, because of the fact that in their earlier experimental studies they measured flow in the GCV and herewith they were able to compare experimental results with the simulation results. Nevertheless, it would be possible to create in the exactly same manner collaterals from the LAD to the circumflex venous bed. The present study highlighted the importance of the venous channels connecting two beds and clarified effects of their variation on capillary support in underperfused myocardial region.
Further, present study showed that the mechanism by which the flow reaches the microcirculation of the ischemic territory is bi-directional and that if there are pronounced interconnections the bi-directional flow can be supported. The degree of the backflow was also estimated by this model (Table 9.2) and it is very well comparable with the results obtained experimentally. Nevertheless, the impact of possibly increased squeezing action has to be taken into account, because with higher collateral inflow (R_{coll} = 90 mmHg s/ ml) the myocardial function is going to be supported and myocardial function is getting higher. This implies again less retrograde flow in the capillary region. That lead to the conclusion that after some prolonged occlusions, if myocardial squeezing action is improved one should possibly start shorter occluding periods in the coronary sinus.
The variation of the model parameters may be applied as a support toward an optimal intervention mode. The model may be used to determine those physiological states which are most favorable for effective coronary sinus intervention. Different physiological states occur unavoidably in different species, however impact of diverse variables can be studied from such a simulation. The mechanistic modeling of the coronary circulation during PICSO may provide quantitative estimation of myocardial blood redistribution, as well as it can give qualitative insight regarding changes that may occur whenever certain experimental elements are modified.

10.2.3 Conclusion

Schreiner *et al.* (1990d) concluded that regarding the scope of the present simulations it must be noted that they assumed equal conditions in the LCX and LAD beds (symmetric case). However, the investigated variations in γ_{norm} may be interpreted in two ways.

1. For a myocardial layer between endo- and epicard, $\gamma_{norm} = 0.75$ represents normal contractility, lower values ($\gamma_{norm} < 0.75$) simulate a state of reduced contractility.
2. Alternatively, simulations for different γ_{norm} may be interpreted to reflect the situations in different myocardial layers for the undiseased state: Subendocardial layers experience much stronger squeezing (which is close to left ventricular pressure, $\gamma_{norm} \simeq 1$) than do subepicardial layers ($\gamma_{norm} \simeq 0$).

Stepwise changes of myocardial squeezing have been used in order to study the reaction of hemodynamic quantities calculated from the model (forward, retrograde and mean flows, systolic, and diastolic plateaus and rise times of venous pressure). Some of the results confirmed well known features of the coronary circulation under normal perfusion conditions (CSR) and, hence, could be used for checking the validity of the model (confirmatory results, CONF). Those effects, however, for which no experimental evidences exist, were virtually predictions drawn from the model (inference results, INF).

1. Under conditions of coronary sinus release, myocardial squeezing was seen to reduce total coronary flow (CONF [Vergroesen *et al.* (1987)]).
2. During coronary sinus occlusion, which by itself reduces total mean flow (CONF [Neumann *et al.* (1989)]), no effect of squeezing on mean flow was found up to $\gamma_{norm} = 0.8$ (INF); larger squeezing reduced coronary flow (INF).
3. Squeezing proved mandatory in order to achieve redistribution of blood from the venous compartment toward the capillaries under CSO (INF). For $0.2 \leq \gamma_{norm} \leq 0.8$, redistribution increased fairly linear with squeezing (INF). Without squeezing, the capillary bed was not emptied, and retrograde filling could not occur. Very strong squeezing again reduced redistribution (INF).
4. Increasing squeezing fairly linearly elevated the systolic and lowered the diastolic plateau of p_{ven} up to $\gamma_{norm} = 0.8$ (CONF [Schreiner *et al.* (1988a)]). This trend was reversed, however, for $\gamma_{norm} > 0.8$ (INF).

10.2.3.1 Physiological considerations

Out of three possible modalities of coronary sinus interventions,

1. pressure controlled intermittent coronary sinus occlusion (PICSO),
2. synchronized retroperfusion (SRP), and
3. the combination of both techniques, only the first (PICSO) has been considered in the present work.

During PICSO, venous blood drained from healthy regions of the myocardium accumulates (approximately 250 mL / min) over periods of about 10 s, pressurizing the venous bed. Synchronized retroperfusion (SRP) injects much smaller volumes (around 60 mL / min) of arterial blood during diastole but does not accumulate this input over successive cardiac cycles. Thus the hemodynamic effect of PICSO can be expected to be much larger than that of SRP. Therefore the authors focused on PICSO in the present work. However, the provision of arterial blood in SRP potentially offers a much higher biological effectiveness than PICSO does. Consequently, the combination of both techniques is most promising. Canine experiments with an acute LAD infarction setting have shown that SRP + PICSO is indeed therapeutically more effective than PICSO or SRP alone.
Based on these developments, the present work may be extended in two aspects:

1. considering an LAD stenosis with concomitant reduction of squeezing while the LCX region is still contracting normally and
2. applying different boundary conditions to venous egress which represent synchronized retroperfusion alone or in combination with pressure controlled coronary sinus occlusion.

10.3 PICSO in myocardial infarction

10.3.1 Myocardial protection via the coronary sinus

Mohl *et al.* (2008) stated following:

10.3.1.1 Discussion

The re-evaluation of a clinical trial, which was published prior to current therapies of MI, is unique in several ways, as it represents a pathophysiologic insight into the ischemic and reperfusion period, which is otherwise unavailable under current clinical standards. Data analyzed should be viewed as an important influx of innovation gained from past experience and as a unique opportunity to view them with today's clinical knowledge and scientific experience.

10.3.1.2 Immediate effects and their influence on clinical outcome

The study's main findings can be differentiated between short- and long-term effects. First, the study showed that PICSO significantly contributed to a reduction in infarct size and to re-establishing myocardial lactate metabolism in the acute phase. Second, reperfusion was achieved earlier in the PICSO group, indicating that the interaction between clot lysis and ischemic microcirculation was more favorable with intermittent pressure elevation in the coronary venous system. The third important finding is the effect of PICSO on the grade of the residual stenosis itself. In terms of the remaining stenosis, the difference between the trends in both groups can be explained by the improved clot lysis and patency of the microcirculation at the time of reperfusion. The results of myocardial infarct size evaluated 30 days after symptom onset also supports the positive effect of PICSO on myocardial salvage. In contrast, there was no indication that global function could be improved with this technique. Whether this technique (i.e., extending the PICSO therapy during the reperfusion phase) and state-of-the-art technology will be able to improve myocardial function globally needs further investigation with a larger number of patients. The principle finding of the present study was that generating an impulse for only about 1 h of PICSO during the ischemic period shortly before reperfusion resulted in a significant reduction in MACE during long-term follow up.

10.3.1.3 PICSO and salvage time

PICSO also has the potential to achieve earlier recanalization as an adjunct to reperfusion therapy. PICSO increased coronary venous system pressure, resulting in augmented retrograde access to the microcirculation and collateral perfusion in the area at risk. It is reported that PICSO improves washout and that there is less pronounced no flow phenomena in the area at risk [Syeda *et al.* (2004)]. Although the potential to resolve a thrombus seems to be similar in both groups, changes in the impedance to coronary flow might be different in the treated group. PICSO may also enhance the thrombolytic agents' lytic effects on any microthrombi occluding the microcirculation in jeopardized areas.
The earlier and more complete reperfusion in the PICSO group may have affected long-term results. Vasodilatation is indicated to be one of the positive effects of PICSO. In addition, washout seems to be a contributor to clearing the ischemic microcirculation and to protecting its structural integrity.

10.3.1.4 PICSO and restenosis after thrombolysis therapy

Clearing the culprit region from residual clots is an important goal in clinical practice. In the pre acute PCI era the residual stenosis after lysis therefore represents also the residual impedance of the reperfused microcirculation. The mean residual infarct artery stenosis in the present study was similar that of the conservative strategies group after thrombolysis in the TIMI phase II-A trial (i.e., 67.2%). The cumulative performance rate of PCI at 1 year was 23.9% in that group. A German study of AMI patients treated with thrombolysis in the MITRA trial showed that MACE in the thrombolysis group was 32.3% during a 17-month follow up. Henriques *et al.* (2006) showed that the

combined endpoint of MACE in the patient group treated by streptokinase was 59% during 8 years of follow up. When compared with those large clinical trials, there might be a higher incidence of MACE in the present study's control group (52.9%) at 17 months, and yet the incidence of MACE tends to be lower in the PICSO group (17.6% at 60 months). As indicated below, there is also a relationship between MACE and the occurrence of restenosis.

10.3.1.5 Regeneration potential

Weigel *et al.* (2007) showed that the pressure increase in the coronary venous circulation generated by PICSO augmented the local expression of heme oxygenase-1 and vascular endothelial growth factor (VEGF) in acute ischemia in porcine myocardium. Seko *et al.* (1999) showed that pulsatile mechanical stretch stimulated VEGF secretion by cultured rat cardiac myocytes. Pulsatile stretch induces mRNA expression of VEGF and VEGF receptors in cardiac myocytes. Yamamoto *et al.* (2003) demonstrated that endothelial progenitor cells (EPCs) were sensitive to shear stress and shear stress stimulated EPC proliferation, suggesting that their vasculogenic activities may be modulated by shear stress.
With this in mind they put forward the following PICSO mechanism: during balloon inflation rising coronary sinus pressure "massages" venous endothelium thus inducing periodic pulsatile stretch whereas deflation of the CS balloon introduces a rapid decrease in CS pressure imposing a powerful shear stress during the PICSO cycle. Although their theory cannot explain whether there are structural changes in the reperfused myocardium induced by PICSO, their data suggest that there is another beneficial mechanism involved, which might be the aforementioned mechanism on vasoactive and neoangiogenetic gene expression. Conducting studies supporting their hypothesis will be the basis of their future research.

10.3.1.6 The context to other 'adjunct therapies'

Although reperfusion strategies are the gold standard in modern interventional cardiology, there is still a place for the protection of damaged myocardium. Recent clinical trials show that adenosine or nicorandil as an adjunct therapy attenuated reperfusion injury. Moreover, postconditioning using the repetition of brief episodes of ischemia/ reperfusion as a 'gentle' temporary reperfusion performed at the time of recanalization after prolonged ischemia, results in significantly reduced infarct size and attenuated reperfusion injury, including the development of oxidants, pro-inflammatory cytokines, neutrophils, and pro-apoptotic regulators. Postconditioning attenuates cardiomyocyte damage and coronary vascular endothelium injury also reduces apoptosis. Focusing on the mechanism of restenosis after AMI, inflammation plays an important role in atherogenesis and atherothrombotic events, and high-sensitivity C-reactive protein (hs-CRP) has been associated with an increased risk of coronary artery disease. A combination of soft plaques and elevated preprocedural hs-CRP levels are associated with a higher incidence of restenosis in bare-metal stent implantation. In this context, PICSO might be a valuable and easily applicable technology.

10.3.1.7 A second window of opportunity, a step towards clinical significance and a new pathophysiologic insight

The mainstream of clinical interest passed CSI and especially PICSO despite obvious improvements since the observational study on PICSO and its technology was published several years ago. Since then clinical focus has changed towards the emergent technology of acute PCI, and the application of CSI was also hindered because

of the problem of how to access the CS securely and rapidly. This hiatus in interest buried the enormous pathophysiologic potential of these interventions. In the present report, they were able to assess the significance of PICSO during the ischemic/reperfusion period far beyond any other adjunct therapy tested clinically. This report also showed convincingly that only 59±30 min of treatment was able to set an impulse for long-lasting clinical improvements. Furthermore, they were able to shed light on an otherwise ignored pathophysiologic consequence of an apparent inflammatory process originating in the previous ischemic reperfused myocardial area setting an atherosclerotic stimulus-inducing restenosis. PICSO seems to have a positive effect in changing the microenvironment in the ischemic/reperfused myocardium.

There is, however, also a major obstacle to using PICSO in an acute setting like AMI, as the CS catheterization is cumbersome and needs special attention. Using the CS as an access route for myocardial protection has been routine practice in cardiac surgery. Biventricular pacing via the CS is also a common remedy for patients with chronic congestive heart failure. Not only cardiac surgeons but also cardiologists use the CS in current clinical practice. In the present study, CS catheter insertion time via the basilic or brachial vein was 11±4 min, without any complications. Present technology and interventional experience must be used to focus on CS access so that the pathophysiologically promised success can be reached.

Presently, they are forced to treat compromised patients (i.e., multi-vessels disease with diffuse atherosclerotic lesions and poor runoff and compromised ventricular function). Needless to say, timely reperfusion is the principal goal in improving the survival of patients with AMI. There is, however ample, evidence that PICSO could take the logistic tension from acute PCI as a present gold standard therapy by widening the window for myocardial salvage, influencing the reperfusion process and thus inducing structural changes, which would result in a significant improvement of the clinical outcome and myocardium protection, salvage and regeneration.

In summary, the clinical potential of this technology can also be demonstrated as an adjunct therapy in complicated and even compromised revascularization procedures. If the results described in this report can be duplicated during the ischemic period prior and after acute PCI, the road towards an efficient adjunctive therapy, as well as a modern alternative in myocardial protection, will be available for patients otherwise beyond the therapeutic window, who are not suitable for standard revascularization procedures.

10.3.2 Intracoronary hemodynamic effects

van de Hoef *et al.* (2012) reported following:

10.3.2.1 Discussion

In this first-in-man study, they have demonstrated that the PICSO catheter can be introduced into the CS, and PICSO treatment can be provided without the occurrence of device-specific adverse events during an elective PCI procedure. PICSO resulted in an immediate increase in CS mean and pulse pressure, which resulted in an increase in distal LAD wedge pressure and wedge pulse pressure. These effects on intracoronary hemodynamics support a potential benefit of PICSO in STEMI, and are concordant with previous findings. These results therefore justify further evaluation of this novel technique in patients with acute LAD occlusion and STEMI.

10.3.2.2 Hemodynamic effect of PICSO

In this study, they have documented that PICSO results in an increase in pressure in the LAD venous outflow tract, resulting in a significant, though modest, increase in coronary wedge pressure. When the CS is occluded in the presence of an LAD occlusion, the pressure build up in the venous outflow tract depends on the inflow of blood through either venous connections proximal to the point of occlusion in the CS, or collateral connections on the arterial side. The correlation between high-baseline wedge pressure and the increase in CS pressure suggests an inflow-dependency of the rise in CS pressure. The significant increase in mean CS pressure observed after opening of the LAD also supports the inflow dependency of CS pressure during PICSO.
PICSO was capable of intermittently increasing CS pressure to a plateau pressure, the level of which is dependent on the magnitude of inflow, and resulted in an increase in LAD wedge pressure, suggesting redistribution of blood from the venous outflow tract into the microcirculation of the culprit coronary artery, though blood flow was not measured directly. These findings are consistent with the anticipated protective mechanism of PICSO in STEMI, which relies on this redistribution to reduce infarct extension, and facilitate washout of harmful agents via the periodic obstruction of venous outflow with subsequent release of pressure. The periodic increase in pressure transferred onto the venous endothelium may also improve long term outcomes due to stimulating release of vascular growth factors.

10.3.2.3 Myocardial ischemia

One of the anticipated effects of PICSO is protection from myocardial ischemia. It is important to note that myocardial ischemia is expected to be attenuated during sequential coronary occlusions, as performed in this study. Thus, in cases in which PICSO was established during the second LAD occlusion, PICSO would be expected to result in a more pronounced reduction of ST-segment deviation, but the effect of PICSO cannot be differentiated from an attenuation effect. Conversely, when PICSO was established during the first LAD occlusion, the reduction in ST-segment deviation from PICSO compared to the second (non-PICSO aided) LAD occlusion would be expected to be diminished. In the present study, when PICSO was performed during the first LAD occlusion, no difference between ST-segment deviation scores was found, which suggests that PICSO may have provided protection from myocardial ischemia.
This finding is supported by the fact that in those patients where the first LAD occlusion was performed without PICSO, ST-segment deviation was 50% higher compared with the patients where the first LAD occlusion was performed with PICSO. Furthermore, when PICSO was performed during the second LAD occlusion, ST-segment deviation was numerically lower than with the first LAD occlusion without PICSO, though an attenuation effect cannot be excluded in this case. Overall, no statistically significant differences in ST-segment deviation scores between the LAD occlusion with and without PICSO was found in this small study population, and thus larger studies with a randomized balloon inflation crossover design are required to determine the extent to which PICSO modulates ischemia.

10.3.3 Safety and feasibility study

van de Hoef *et al.* (2015) reported following:

10.3.3.1 Discussion

In this prospective, non-randomized, multicentre, safety and feasibility study involving patients with anterior STEMI who underwent successful pPCI of a LAD culprit lesion, adjuvant treatment with the PICSO Impulse System was safe, although successful PICSO Impulse catheter positioning, initiation and maintenance of PICSO therapy was limited to 40% of patients. Nonetheless, successful PICSO therapy administration was associated with favorable trends in CMR infarct size and myocardial function parameters, compared both to patients in whom PICSO administration was unsuccessful, as well as to matched control patients. Notably, successful PICSO administration was associated with a significant improvement in myocardial recovery from two to five days to four months post pPCI as compared to patients in whom PICSO administration was unsuccessful, as well as to matched control patients.

10.3.3.2 PICSO safety and feasibility in anterior wall STEMI

The use of the PICSO Impulse System was generally safe, with only one major adverse safety event which was related to the implantation procedure - similar to the implantation-related complications observed in routine electrophysiology procedures. PICSO therapy was not initiated in 37% of included patients, which was largely attributable to technical difficulties with catheter stability, precluding appropriate calibration of the PICSO catheter. In patients in whom PICSO was initiated, PICSO could be provided for the intended 90 ($\pm$2) minutes in 63% of patients, which was largely dictated by the strict PICSO Impulse console safety settings.
These safety limits apply for example to heart rate, as well as to intraluminal and balloon pressures in the PICSO catheter, which preclude safe functioning of the device, and lead to an instant abortion of PICSO therapy or its initiation. The provided PICSO quantity varied markedly from 15 to 2,735 mmHg, and was substantially higher in patients treated within the most experienced centre, despite equivalent PICSO therapy duration across centres, which suggests an important learning curve required for successful application of the technique. The anticipated mechanisms of action of PICSO are based on the mechanical effects of intermittent pressure increase in the cardiac venous outflow tract. Therefore, suboptimal administration of PICSO, as documented by low PICSO quantities, is conceivably associated with limited therapeutic efficacy, which is in line with the dose dependency of PICSO in the present study. The successful modulation of coronary sinus pressure during PICSO is related to both catheter positioning and stability. Catheter positioning near the coronary sinus ostium provides the largest magnitude of venous inflow, and therefore the largest modulation of coronary sinus pressure.
Catheter stability during balloon occlusion is better in more proximal, narrower parts of the coronary sinus, where the distending pressure of the balloon against the coronary sinus wall is larger, securing the catheter to the coronary sinus wall despite substantial backward pressure. The feasibility results of the Prepare RAMSES study indicate that optimal positioning of the catheter is subject to a learning curve, and that current PICSO technology may benefit from improvements to allow reliable and optimal therapeutic efficacy in patients in daily clinical practice.

10.3.3.3 Cardiovascular magnetic resonance analyses

Although by intent-to-treat there was no significant reduction in infarct size with PICSO compared to control, administration of high PICSO quantity was associated with favorable trends in myocardial function and infarct size parameters, when compared both to those patients in whom administered PICSO quantity was limited, as well as to matched historical control patients. Administration of high PICSO quantity was also associated with significantly

greater myocardial recovery during follow-up by both assessments. These favorable trends were not observed in patients treated with low PICSO quantity. Although no definite conclusions can be drawn from these findings in this small, non-randomized study without a concurrent control, overall the magnitude of effect appears comparable to that with cardio protection during pPCI for STEMI in recent randomized trials, warranting further evaluation of PICSO in larger efficacy studies.

10.3.4 Future developments

Mohl *et al.* (2015) reported that although PICSO might be best applied immediately before pPCI, there remains a need to investigate the effects of a longer time window of PICSO application in the early reperfusion period. Reperfused myocardium with cell death, (i.e. apoptosis and necrosis) cell signaling and cell migration is a potential analogue to a lizard's blastema formation combining growth signals with dedifferentiation of cells inducing structural rescue, which cannot be established in mammalian hearts without additional regenerative phenomena. Many species able to regenerate in adulthood use a blastema, which is an epigenetically controlled regeneration zone combining molecular signals from dying and dedifferentiated as well as migrated cells able to reenter the cell cycle producing structural recovery. It may be expected that coronary sinus interventions produce similar effects.
Based on their hypothesis and experimental and early clinical findings, there is a strong rationale for investigating the potential of PICSO in heart failure patients. Future clinical research is mandatory to decipher the regenerative potential of PICSO and to further support the hypothesis that a relatively easy coronary sinus intervention can induce structural regeneration.

10.3.5 Conclusion

van de Hoef *et al.* (2012) demonstrated that the results from this first-in-man study show that introduction of the PICSO Impulse catheter can be performed in a timely manner using the femoral venous route, and that PICSO can be performed without the occurrence of adverse events during elective PCI. PICSO intermittently increases CS pressure, translating into an increase in distal coronary wedge pressure. These findings support the hypothesized mechanism of PICSO, and are concordant with the results from previous experimental studies. These results therefore provide the basis for further research to determine the potential protective benefits of PICSO in patients with STEMI undergoing primary PCI, as well as its effect on long-term clinical outcomes.
Furthermore, van de Hoef *et al.* (2015) reported that pressure-controlled intermittent coronary sinus occlusion using the PICSO Impulse System was safe in patients with anterior STEMI, and exploratory efficacy analyses suggest that PICSO may augment myocardial recovery after primary PCI for LAD infarction in a dose-dependent manner. These results warrant further exploration of the safety and efficacy of adjuvant PICSO therapy.
Mohl *et al.* (2015) stated that clearing microvascular obstruction via cardiac veins has undergone a resurgence in interest in treating patients with complex high risk interventional procedures as well as in ACS. Conceptualized decades ago, access to deprived myocardium has demonstrated benefits during ischemia, which have been corroborated by preliminary studies in the era of pPCI. Clinical results indicated that the salvage potential of PICSO is dose dependent, but that a second threshold dependent effect influencing structural regeneration also influences patient outcome. Activation of venous endothelium by the hemodynamic force of venous blood initiates molecular cascades similar to developmental processes, leading to the possibility that limiting ischemic jeopardy and regaining structural integrity might be a realistic goal for the interventional cardiologist.
Kessels *et al.* (2015) safely applied PICSO in a porcine model of LAD infarction. MRI at day 5 showed greater

LVEF, better wall thickening, and trends toward smaller infarct size and MVO in animals treated with early PICSO, suggesting a cardioprotective effect of PICSO. In addition, PICSO resulted in an increased VEGF-R1 expression in the remote zone and VEGF-R2 in the border zone indicating, increased neo-angiogenic activity. Large trials are underway to demonstrate the benefits of PICSO in humans.
In the study by Egred *et al.* (2016), initiation of PICSO in patients with acute MI immediately after flow restoration but before stenting was associated with evidence of reduced MVO and IS, with improved left ventricular function measured 5 days after reperfusion. And the study shows that after anterior STEMI, adjunctive PICSO therapy during pPCI is safe, feasible and results in:

- Reduced incidence of MVO
- Significantly smaller infarct size
- Significantly reduced end-diastolic volume
- Significantly improved left ventricular function

Egred *et al.* (2017) stated that in the present propensity matched analysis, initiation of PICSO in patients with acute anterior MI immediately after flow restoration but before stenting was associated with a 47% relative reduction in 5-day infarct size. These findings have formed the basis for an upcoming randomized trial to determine the safety and efficacy of PICSO in patients with anterior STEMI undergoing primary PCI.

10.4 Coronary Sinus Intervention

Faxon (2015) concluded that interventions through the coronary veins to treat coronary artery disease was first suggested by Pratt over 100 years ago but were not actively investigated until when Gross *et al.* (1937) demonstrated that retrograde flow into the ventricles after ligation of the coronary sinus in an experimental infarct model. The mortality in these experiments was high because of engorgement of the myocardium over time, so when Beck and Mako (1941) repeated these experiments, they used a partial occlusion rather than complete occlusion. This resulted in a significantly lower acute mortality in an infarct model. Subsequently, others demonstrated that combining a partial ligation of the coronary sinus with arterial cannulation further increased survival from arterial retroperfusion rather than venous. In experimental dog studies, Beck *et al.* (1948) using newly developed vascular surgical techniques showed that arterial bypass with a free carotid artery conduit from the aorta to the partially occluded coronary sinus reduced mortality in an experimental animal study. He subsequently modified the technique for clinical use by using a brachial artery bypass from the aorta to the coronary sinus (the Beck II operation). Beck *et al.* (1955) reported his experience with 102 patients. He showed a reduction in angina or elimination of angina in 90% of patients with an operative mortality of 6.6%. It is important to remember that these studies were done before the introduction of cardiopulmonary bypass and before modern medical treatment of angina. The operation fell out of favor because of loss of effectiveness over time and the introduction of internal mammary implantation into the myocardium (Vineberg operation) in the 1940s and saphenous vein bypass surgery in the 1960s. Nevertheless, these pioneers demonstrate that coronary sinus occlusion and retroperfusion could reduce myocardial ischemia and could be done effectively in man.
Despite, >75 years of experimental studies of coronary venous interventions, only a few small clinical trials have been conducted following the work of Beck *et al.* (1948). Is it finally time to give up this approach since we have not been able to successfully develop a clinically useful technique by now? The author would argue that we should

not. Despite the long history of coronary sinus interventions, we still understand little about the hemodynamic and biological effects of these techniques. Emerging evidence suggests these techniques might provide additional benefit beyond retrograde perfusion and enhanced washout with restoration of vascular function and angiogenesis. The studies of 2 different coronary venous interventions are small and underpowered but they are provocative and should stimulate further study of coronary sinus interventions in the treatment of coronary artery disease. Exploration of other novel coronary venous techniques is also needed to exploit the potential that the coronary venous system has to offer. The author would not rule out coronary sinus techniques as yet. Despite its history, we are still in the infancy of the technique.

Bibliography

Amsterdam, E.A., Wenger, N.K., Brindis, R.G., Casey, D.E., Ganiats, T.G., Holmes Jr., D.R., Jaffe, A.S., Jneid, H., Kelly, R.F., Kontos, M.C., Lveine, G.N., Liebson, P.R., Mukherjee, D., Peterson, E.D., Sabatine, M.S., Smalling, R.W. and Zieman, S.J. 2014 AHA ACC Guideline for the management of patients with non-ST-Elevation acute coronary syndromes. *Circulation*; 130:e344-e426, 2014.

Arts M.G.J. A mathematical model of the dynamics of the left ventricle and the coronary circulation, PhD Thesis, *State University of Limburg*, Maastricht, The Netherlands, 1978.

Banai S, Ben Muvhar S, Parikh KH, et al. Coronary sinus reducer stent for the treatment of chronic refractory angina pectoris: a prospective, open-label, multicenter, safety feasibility first-in-man study. *J Am Coll Cardiol*; 49:1783-9, 2007.

Bassand, J.P., Danchin, N., Filippatos, G., Gitt, A., Hamm, C., Silber, S., Tubaro, M. and Weidinger, F. Implementation of reperfusion therapy in acute myocardial infarction. A policy statement from the European Society of Cardiology. *European Heart Journal*, 26, 2733-2741, 2005.

Beck, C.S. and Mako, A.E. 1941 Venous stasis in coronary circulation. An experimental study. *Amer Heart J.*;21:767-779, 1941.

Beck, C.S., Stanton, E., Batiuchok, W. and Leiter, E. Revascularization of heart by graft of systemic artery into coronary sinus. *J Am Med Assoc.*;137:436-442, 1948.

Beck, C.S. and Leighninger, D.S. Scientific basis for the surgical treatment of coronary artery diease. *J Am Med Assoc.*;159:1264-1271, 1955.

Berland, J., Farcot, J.C., Barrier, A., Derumeaux, G., Cribier, A., Bourdarieas, J.P., Corday, E. and Letac, B. ECG and 2D echo assessment of myocardial protection achieved by diastolic synchronized coronary sinus retroperfusion (DSR) during LAD angioplasty (abstract). *JACC* 11: 132A, 1988.

Beyar, R. and Sideman, S. Time-dependent coronary blood flow distribution in left ventricular wall. *Am J Physiol.*; 252(2 Pt 2):H417-33, 1987.

Beyar, R., Guerci, A.D., Halperin, H.R., Tsitlik, J.E. and Weisfeldt, M.L. Intermittent coronary sinus occlusion after coronary arterial ligation results in venous retroperfusion. *Circ Res.*; 65(3):695-707, 1989.

Boekstegers, P., Giehrl, W. and von Degenfeld, G. Selective suction and pressure-regulated retroinfusion: an effective and safe approach to retrograde protection against myocardial ischemia in patients undergoing normal and high risk percutaneous transluminal coronary angioplasty. *J Am Coll Cardiol*; 31:1525-33, 1998.

Boekstegers, P. and Kupatt, C. Current concepts and applications of coronary venous retroinfusion. *Basic Res Cardiol*; 99:373-81, 2004.

Bruinsma, P., Arts, T., Dankelman, J. and Spaan, J.A. Model of the coronary circulation based on pressure dependence of coronary resistance and compliance. *Basic Res Cardiol.*; 83(5):510-24, 1988.

Burghart, C. *ECG Interpretation Made Incredibly Easy!*, 5th Ed. Wolters Kluwer, Lippincott Williams & Wilkins, Philadelphia, Baltimore, New York, London, Buenos Aires, Hong Kong, Sydney, Tokyo, 2011.

Chang, B.L., Drury, J.K., Meerbaum, S., Fishbein, M.C., Whiting, J.S. and Corday, E. Enhanced myocardial washout and retrograde blood delivery with synchronized retroperfusion during acute myocardial ischemia. *J Am Coll Cardiol.*; 9(5):1091-8, 1987.

Downey, J.M., Lee, J. and Chambers, D.E. Location and magnitude of the coronary artery capacitance. In: Mates, R.E., Nerem, R.M. and Stein, P.D., editors, *Mechanics of the Coronary Circulation.* The American Society of Mechanical Engineers, New York; 45-48, 1983.

Drury, J.K., Yamazaki, S., Fishbein, M.C., Meerbaum, S. and Corday, E. Synchronized diastolic coronary venous retroperfusion: results of a preclinical safety and efficacy study. *J Am Coll Cardiol*; 6:328-35, 1985.

Eckstein, R.W., Gregg, D.E. and Pritchard, W.H. The magnitude and time of development of the collateral circulation in occluded femoral, carotid and coronary arteries. *Amer. J. Physiol.* 132, 351, 1941.

Eckstein, R.W., Roberts, J.T., Gregg, D.E. and Wearn, J.T. Observation on the role of the Thebesian veins and luminal vessels in the right ventricle. *Amer. J. Physiol.* 132, 648, 1941.

Eckstein, R.W., Stroud, M., Dowling, C.V., Eckel, R. and Pritchard, W.H. Response of coronary blood flow following stimulation of cardiac accelerator nerves. *Fed. Proc.* 8, 38, 1949.

Eckstein, R.W., Stroud, M., Eckel, R., Dowling, C.V. and Pritchard, W.H. Effects of control of cardiac work upon coronary flow and O2-consumption after sympathetic nerve stimulation. *Amer. J. Physiol.* 163, 539, 1950.

Eckstein, R.W., Smith, G., Eleff, M. and Demming, J. Effect of arterialization of coronary sinus in dogs on mortality following acute coronary occlusion. *Circulation* 6, 16, 1952.

Eckstein, R.W., Hornberger, J.C. and Sano, T. Acute effects of elevation of coronary sinus pressure. *Circulation* 7, 422, 1953.

Egred, M., Bagnall, A., Spyridopoulos, I., Purcell, I., Das, R., Palmer, N., Grech, E., Jain, A., Stone, G., Nijveldt, R., Kessels, R. and Zaman, A. Pressure-controlled intermittent coronary sinus occlusion reduces infarct size and results in functional recovery after STEMI. *Journal Of The American College Of Cardiology*, Vol. 68, No. 18, Suppl B, 2016.

Egred, M., Kessels, R., Bagnall, A., Spyridopoulos, I., Palmer, N., Grech, E., Jain, A., Stone, G., Nijveldt, R and McAndrew, T. Pressure-controlled intermittent coronary sinus occlusion reduces infarct size after primary PCI: A propensity-controlled matched study. *Journal Of The American College Of Cardiology*, Vol. 70, No. 18, Suppl B, 2017.

Faber, J.E and Stouffer, G.A. Introduction to basic hemodynamic principles. In, Stouffer, G.A., Klein J.L. and McLaughlin, D.P., editors, *Cardiovascular Hemodynamics for the Clinician.* 2nd Ed. England, Wiley Blackwell, 2017.

Fanghäel, J., Pera, F., Anderhuber, F. and Nitsch, R. *Waldeyer - Anatomie des Menschen.* 17. Auflage, Walter de Gruyter, Berlin, New York, 2003.

Farcot, J.C., Meerbaum, S., Lang, T.W., Kaplan, L. and Corday, E. Synchronized retroperfusion of coronary veins for circulatory support of jeopardized ischemic myocardium. *Am J Cardiol.*; 41:1191-1201, 1978.

Faxon, D. Coronary venous interventions. *Circ Cardiovasc Interv.*; 8:e002743, 2015.

Faxon, D.P. Pros and cons - coronary sinus interventions vs. conventional therapy. In Mohl W., editor, *Coronary Sinus Library Volume 4, Coronary sinus interventions and interventional therapy*, pages 74-80. Clinics of CSI, 2003.

Fishbein, G.A, Fishbein, M.C. and Buja, L.M. Myocardial ischemia and its complications. In Butnay, J. and Buja, M. L., editors, *Cardiovascular Pathology*, 4th Ed., Academic Press, Amsterdam, Boston, Heidelberg, London, New York, Oxford, Paris, San Diego, San Francisco, Singapore, Sydney, Tokyo, 2016.

Ginat, D.T., Fong, M.W., Tuttle, D.J., Hobbs, S.K. and Vyas, R.C. Cardiac imaging part 1 MR pulse sequences, imaging planes, and basic anatomy. *AJR*; 197:808-815, 2011.

Gore, J.M., Weiner, B.H., Benotti, J.R., Sloan, K.M., Okike, O.N., Cuénoud, H.F., Gaca, J.M., Alpert, J.S. and Dalen, J.E. Preliminary experience with synchronized coronary sinus retroperfusion in humans. *Circulation*; 74(2):381-8, 1986.

Standring, S. *Gray's Anatomy - The Anatomical Basis of Clinical Practice.* 40th Ed. Elsevier Limited, Spain, 2008.

Gregg, D.E. and Dewald, D. The immediate effects of the occlusion of the coronary veins on collateral blood flow in the coronary arteries. *Am. J. Physiol.* 124: 435, 1938a.

Gregg, D.E. and Dewald, D. The immediate effects of the occlusion of the coronary veins on the dynamics of the coronary circulation. *Am. J. Physiol.* 124: 444, 1938b.

Gregg, D.E. and Green, H.D. Effects of viscosity, ischemia, cardiac output and aortic pressure on coronary blood flow measured under a constant perfusion pressure. *Amer. J. Physiol.* 130, 108, 1940.

Gregg, D.E. and Shipley, R.E. Studies of the venous drainage of the heart. *Amer. J. Physiol.* 151, 13, 1947.

Gregg, D.E. *Coronary circulation in health and disease.* Lea & Febiger, Philadelphia; pp 79-89, 1950.

Grover, V.P.P., Tognarelli, J.M., Crossey, M.M.E., Cox, I.J., Taylor-Robinson, S.D and McPhail, M.J.W. Magnetic resonance imaging: principles and techniques: lessons for clinicians. *Journal of Clinical and Experimental Hepatology*, Vol. 5, No. 3, 246-255, September 2015.

Gross, L., Blum, L. and Silverman, G. Experimental attempts to increase blood supply in the dogs heart by means of coronary sinus occlusion. *J Exp Med.*;65:91-108, 1937.

Guerci, A.D., Ciuffo, A.A., DiPaula, A.F. and Weisfeldt, M.L. Intermittent coronary sinus occlusion in dogs: reduction of infarct size 10 days after reperfusion. *J Am Coll Cardiol.*; 9(5):1075-81, 1987.

Gundry, S.R. and Kirsh, M.M. A comparison of retrograde cardioplegia vs antegrade cardioplegia in the presence of coronary artery obstruction. *Ann Thorac Surg* 38 (2): 124-127, 1984.

Hall, J.E., and Guyton, A.C. *Textbook of Medical Physiology.*, 12th Ed. Saunders Elsevier, United States of America, 2011.

Habib, A., Lachman, N., Christensen, K.N. and Asirvatham, S.J. The anatomy of the coronary sinus venous system for the cardiac electrophysiologist. *Europace* 11, v15-v21, 2009.

Heineman, F.W. and Grayson, J. Transmural distribution of intramyocardial pressure measured by micropipette technique. *Am. J. Physiol.*, 249:H1216-H1223, 1985.

Henriques, J.P., Zijlstra, F., van't Hof, A.W., de Boer, M.J., Dambrink, J.H., Gosselink, A.T., Hoorntje, J.C., Ottervanger, J.P. and Suryapranata, H. Primary percutaneous coronary intervention versus thrombolytic treatment: long term follow up according to infarct location. *Heart*; 92(1):75-9, 2006.

Ibanez, B., James, S., Agewall, S., Antunes, M.J., Bucciarelli-Ducci, C., Bueno, H., Caforio, A.L.P., Crea, F., Goudevenos, J.A., Halvorsen, S., Hindricks, G., Kastrati, A., Lenzen, M.J., Prescott, E., Roffi, M., Valgimigli, M., Varenhorst, C., Vranckx, P. and WidimskÃ$\frac{1}{2}$, P. 2017 ESC Guidelines for the management of acute myocardial infarction in patients presenting with ST-segment elevation. *European Heart Journal*, 00, 1-66, 2017.

Ikeoka, K., Nakagawa, Y., Kawashima, S., Fujitani, K. and Iwasaki, T. Effects of intermittent coronary sinus occlusion on experimental myocardial infarction and reperfusion hemorrhage. *Jpn Circ J*; 54:1258-73, 1990.

International working group on coronary sinus internventions, In Mohl, W., editor, *(Sec Gen) 2nd Surgical Clinic*, University of Vienna, Austria.

Jacobs A. K. Coronary sinus interventions: clinical application. In Mohl W., editor, *Coronary Sinus Library Volume 4, Coronary sinus interventions and interventional therapy*, pages 37-49. Clinics of CSI, 2003a.

Jacobs, A.K., Faxon, D.P., Coats, W.D., Vogel, W.M. and Ryan, T.J. Coronary sinus occlusion: effect on ischemic left ventricular dysfunction and reactive hyperemia. *Am Heart J.*; 121(2 pt 1):442-449, 1991.

Jacobs, A.K., Faxon, D.P., Coats, W.D., Mohl, W. and Ryan, T.J. The effect of pressure controlled intermittent coronary sinus occlusion during reperfusion. In Mohl W., editor, *Coronary Sinus Library Volume 6, ICSO and PICSO*, pages 13-18. Clinics of CSI, 2003b.

Jacobs, A.K., Faxon, D.P., Mohl, W., Coats, W.D., Gottsman, S.B. and Ryan T.J. Pressure controlled intermittent coronary sinus occlusion (PICSO) during reperfusion markedly reduces infarct size. *Clin Res* 33:197A, 1985.

Kajgana, I. Effects of coronary sinus pressure elevation on myocardial blood flow. *Technical University of Vienna*, Dissertation, 2004.

Kar, S., Drury, J.K., Eigler, N., Buchbinder, N., Litvack, F., Thessomboon, S., Hajduczki, I. and Corday, E. Amelioration of ischemia during PTCA with diastolic coronary venous retroperfusion (abstract). *JACC* 2: 64A, 1988.

Kenner, T., Moser, M. and Mohl, W. Arteriovenous difference of the blood density in the coronary circulation. *J Biomech Eng* ;107:34-40, 1985.

Kessels, R., Bouchard, A., Guy, L.G., LeClerc, G., Korkmaz, H. I., Niessen, H.W. and Stone, G.W. Early PICSO preserves LVEF in porcine acute myocardial infarction. *Journal Of The American College Of Cardiology.* Vol. 66. No. 15, Suppl B, 2015.

Komamura, K., Mishima, M. and Kodama, K. Preliminary clinical experience with intermittent coronary sinus occlusion in combination with thrombolytic therapy in acute myocardial infarction. *Jpn Circ J*; 53:1152-63, 1989.

Kumar, A. and Cannon, C.P. Acute coronary syndromes diagnosis and management, Part I. *Mayo Clin Proc.*; 84(10):917-938, 2009.

Kusmic, C., Barsanti, C., Matteucci, M., Vesentini, N., Pelosi, G., Abraham, N.G. and L'Abbate, A. Up-regulation of heme oxygenase-1 after infarct initiation reduces mortality, infarct size and left ventricular remodeling: experimental evidence and proof of concept. *J Transl Med*;12:89, 2014.

Lazar, H.L., Treanor, P., Rivers, S., Bernard, S. and Shemin, R.J. Combining percutaneous bypass with coronary retroperfusion limits myocardial necrosis. *Ann Thorac Surg.*; 59:373-378, 1995.

Mangano, D.T., Miao, Y., Tudor, I.C. and Dietzel, C. Post-reperfusion myocardial infarction: Long-term survival improvement using adenosine regulation with acadesine. *J Am Coll Cardiol*; 48: 206 -214, 2006.

Matsuhashi, H., Hasebe, N. and Kawamura, Y. The effect of intermittent coronary sinus occlusion on coronary sinus pressure dynamics and coronary arterial flow. *Jpn Circ J*; 56:272-85, 1992.

Mates, R.E., Burns, T., Canty, J.M., Greenberg, R. and Neeson, J. Modeling diastolic impedance to coronary blood flow. In Mates, R.E., Nerem, R.M. and Stein, P.D., editors, *Mechanics of the coronary circulation.* American Society of Mechanical Engineers, New York, pp 41-44, 1983.

McLaughlin, D.P., Wu, S.S. and Stouffer, G.A. Coronary hemodynamics. In, Stouffer, G.A., Klein J.L. and McLaughlin, D.P., editors, *Cardiovascular Hemodynamics for the Clinician*. 2nd Ed. England, Wiley Blackwell, 2017.

Meerbaum, S., Haendchen, R.V. and Corday, E. Hypothermic coronary venous phased retroperfusion: a closed-chest treatment of acute regional myocardial ischemia. *Circulation*; 65:1435-45, 1982.

Meerbaum, S., Lang, T.W. and Osher, J.V. Diastolic retroperfusion of acutely ischemic myocardium. *Am J Cardiol*; 37:588-98, 1976.

Meerbaum, S., Lang, T.W. and Povzhitkov, M. Retrograde lysis of coronary artery thrombus by coronary venous streptokinase administration. *J Am Coll Cardiol*; 1:1262-7, 1983.

Meerbaum, S. Clinically oriented phased retroperfusion systems. In Meerbaum, S., editor, *Myocardial Perfusion, Reperfusion, Coronary Venous Retroperfusion*, pages 221-242. Springer-Verlag Berlin Heidelberg, 1990.

Miracor Medical SA. PiCSO^{AMI} Impulse Console and PiCSO Impulse Catheter, accessed 2018-01-17, <http://www.miracormedical.com/pisco-therapy/pisco-in-ami/picso-impulse-system/>.

Mohl, W., Gangl, C., Jusic, A., Aschacher, T., De Jonge, M. and Rattay, F. PICSO: from myocardial salvage to tissue regeneration. *Cardiovascular Revascularization Medicine*, 16:36-46, 2015.

Mohl, W. The momentum of coronary sinus interventions clinically. *Circulation*; 77; 6-12, 1988a.

Mohl, W., Faxon, D., Glogar, D., Gore, J. M., Jacobs, A. Mai, D., Meerbaum, S., Moser, M., Juhasz-Nagy, A., Punzengruber, C., Raberger, G., Roberts, A., Tritthart, H., Winters, E., and Wolner, E. Report of the international working group on coronary sinus interventions. In Mohl W., editor, *Coronary Sinus Library Volume 4, Coronary sinus interventions and interventional therapy*, pages 28-36. Clinics of CSI, 2003b.

Mohl, W. The development and rationale of pressure-controlled intermittent coronary sinus occlusion - a new approach to protect ischemic myocardium. *Wien Klin Wochenschr.*; 96(1):20-5, 1984a.

Mohl, W. and Roberts, A.J. Coronary sinus retroperfusion and pressure-controlled intermittent coronary sinus occlusion (PICSO) for myocardial protection. *Surg Clin North Am.*;65:477-495, 1985a.

Mohl, W., Simon, P., Neumann, F., Schreiner, W., and Punzengruber, C. Clinical evaluation of pressure-controlled intermittent coronary sinus occlusion: a randomized trial during cardiac surgery. *Ann Thorac Surg.*; 46:192-201, 1988b.

Mohl, W., Komamura, K., Kasahara, H., Heinze, G., Glogar, D., Hirayama, A., and Kodama, K. Myocardial protection via the coronary sinus - long-term effects of intermittent coronary sinus occlusion as an adjunct to reperfusion in acute myocardial infarction. *Circ J*; 72: 526-533, 2008.

Mohl, W., Khazen, M., Milasinovic, D., Rama, Q., Aschacher, T., Macfelda, K. and Mader, R.M. PICSO during electrode implantation results in risk reduction in heart failure patients long term. *Eur J Heart Fail*; 16(Suppl. 2):46, 2014.

Mohl, W., Kajgana, I., Bergmeister, H. and Rattay, F. Intermittent pressure elevation of the coronary venous system as a method to protect ischemic myocardium. *Interact Cardiovasc Thorac Surg*; 4:66-9, 2005.

Mohl, W., Glogar, D.H., Mayr, H., Losert, U., Sochor, H., Pachinger, O., Kaindl, F. and Wolner, E. Reduction of infarct size induced by pressure-controlled intermittent coronary sinus occlusion. *Am J Cardiol.*; 53(7):923-8, 1984b.

Mohl, W., Punzengruber, C., Moser, M., Kenner, T., Heimisch, W., Haendchen, R., Meerbaum, S., Maurer, G. and Corday E. Effects of pressure-controlled intermittent coronary sinus occlusion on regional ischemic myocardial function. *J Am Coll Cardiol.*; 5(4):939-47, 1985b.

Mohl, W. PICSO (pressure controlled intermittent coronary sinus occlusion) - developments and current concepts. In Mohl W., editor, *Coronary Sinus Library Volume 6, ICSO and PICSO*, pages 13-18. Clinics of CSI, 2003a.

Mohl, W., Golgar, D., Mayr, H., et al. Effects of intermittent coronary sinus occlusion (ICSO) on infarct size and myocardial function (abstr). *Thorac Cardiovasc Surg*; 30(suppl 1):1-18, 1982.

Moll, J.W., Dzieatkoviak, A.J., Edelman, M., Iljin, W., Ratajczyk-Pakalska, E. and Stengert, K. Arterialization of the coronary veins in diffuse coronary arteriosclerosis. *J Cardiovasc Surg* 16: 520, 1975.

Moser, E., Stadlbauer, A., Windischberger, C., Quick, H.H. and Ladd, M.E. Magnetic resonance imaging methodology. *Eur J Nucl Med Mol Imaging*, 36 (Suppl 1):S30-S41, 2009.

Muers, M.F. and Sleight, P. The reflex cardiovascular depression caused by occlusion of the coronary sinus in the dog. *J Physiol* ;221:259-82, 1972a.

Muers, M.F. and Sleight, P. Action potentials from ventricular mechanoreceptors stimulated by occlusion of the coronary sinus in the dog. *J Physiol* ;221:283-309, 1972b.

Nakazawa, H.K., Roberts, D.L. and Klocke, F.J. Quantitation of anterior descending vs. circumflex venous drainage in the canine great cardiac vein and coronary sinus. *Am J Physiol.*;234(2):H163-6, 1978.

Netter, F.H. Heart: *The Ciba Collection of Medical Illustrations*. Thieme-Verlag, Stuttgart, New York, 1983.

Neumann, F., Mohl, W. and Schreiner, W. Coronary sinus pressure and arterial flow during intermittent coronary sinus occlusion. *Am J Physiol.*; 256(3 Pt 2):H906-15, 1989.

Oswald, E. Modell zur Bestimmung von Druck, Volumen und Fluss in den Herzkranzgefäßen. *Technical University of Vienna*, Diploma Thesis, 2004.

Ota, S., Nishikawa, H., Takeuchi, M., Nakajima, K., Nakamura, T., Okamoto, S., Setsuda, M., Makino, K., Yamakado, T. and Nakano, T. Impact of nicorandil to prevent reperfusion injury in patients with acute myocardial infarction: Sigmart Multicenter Angioplasty Revascularization Trial (SMART). *Circ J*; 70:1099- 1104, 2006.

Patel, A.N., Geffner, L., Vina, R.F., Saslavsky, J., Urschel, H.C. Jr., Kormos, R. and Benetti, F. Surgical treatment for congestive heart failure with autologous adult stem cell transplantation: A prospective randomized study. *J Thorac Cardiovasc Surg*; 130: 1631- 1638, 2005.

Pedersen, F., Butrymovich, V., Kelbaek, H., Wachtell, K., Helqvist, S., Kastrup, J., Holmvang, L., Clemmensen, P., Engstrom, T., Grande, P., Saunamäki, K. and Jorgensen, E. Short- and long-term cause of death in patients treated with primary PCI for STEMI. *JACC*, VOL. 64, NO. 20:2101-2108, 2014.

Porth, C.M. and Matfin, G. *Pathophysiology: Concepts of Altered Health States.* 8th Ed. Wolters Kluwer Health/Lippincott Williams & Wilkins, Philadelphia, PA, 2009.

Pratt, F.H. The nutrition of the heart through the vessels of Thebesius and the coronary veins. *Am. J Physiol*; 1:86-103, 1898.

Pries, A.R. and Secomb, T.W. Blood Flow in Microvascular Networks. In Tuma, R.F., Durán, W.N. and Ley, K. editors, *Microcirculation.* 2nd Ed. Amsterdam, Boston, Elsevier/Academic Press, 2008.

Raake, P., von Degenfeld, G., Hinkel, R., Vachenauer, R., Sandner, T., Beller, S., Andrees, M., Kupatt, C., Schuler, G. and Boekstegers, P. Myocardial gene transfer by selective pressure-regulated retroinfusion of coronary veins: comparison with surgical and percutaneous intramyocardial gene delivery. *J Am Coll Cardiol*; 44:1124-9, 2004.

Roberts, A.J. An overview on myocardial protection in open-heart surgery. In Mohl W., editor, *Coronary Sinus Library Volume 5, Myocardial Protection Via The Coronary Sinus During Surgery*, pages 1-12. Clinics of CSI, 2003.

Sabbah, H.N. and Stein, P.D. Effect of acute regional ischemia on pressure in the subepicardium and subendocardium. *Am J Physiol.*; 242(2):H240-4, 1982.

Schreiner, W. and Neumann, F. Mathematical modeling of coronary sinus interventions. In Meerbaum, S., editor, *Myocardial Perfusion, Reperfusion, Coronary Venous Retroperfusion*, pages 221-242. Springer-Verlag Berlin Heidelberg, 1990b.

Schreiner, W., Neumann, F., Schuster, J., Froehlich, K.C. and Mohl, W. Computation of derived diagnostic quantities during intermittent coronary sinus occlusion in dogs. *Cardiovasc. Res.*, 22:265-276, 1988a.

Schreiner, W., Neumann, F., Schuster, J., Simon, P., Froehlich, K.C. and Mohl, W. Intermittent coronary sinus occlusion in humans: pressure dynamics and calculation of diagnostic quantities. *Cardiovasc Res.*; 22(4):277-86, 1988b.

Schreiner, W., Mohl, W., Neumann, F. and Schuster, J. Model of the haemodynamic reactions to intermittent coronary sinus occlusion. *J Biomed Eng*; 9:141-147, 1987.

Schreiner W., Neumann, F. and Mohl, W. Coronary perfusion pressure and inflow resistance have different influence on intramyocardial flows during coronary sinus interventions. *Am. Assoc. Phys. Med.* 17 (6), 1990a.

Schreiner, W., Neumann, F., Mohl, W. The role of intramyocardial pressure during coronary sinus interventions: a computer model study. *IEEE Transaction On Biomedical Engineering*, Vol. 37, NO. 10, 1990d.

Schreiner, W., Neumann, F. and Mohl, W. Simulation of coronary circulation with special regard to the venous bed and coronary sinus occlusion. *J. Biomed. Eng.*, 12:429-443, 1990c.

Schreiner, W., Neumann, F., Schuster, J., Froehlich, K.C., Sun, Y. And Mohl, W. Computation of diagnostic data from coronary sinus pressure: a comparison between two possible models. *J. Biomed. Eng.*, Vol. 11, 1989.

Seko, Y., Takahashi, N., Shibuya, M. and Yazaki, Y. Pulsatile stretch stimulates vascular endothelial growth factor (VEGF) secretion by cultured rat cardiac myocytes. *Biochem Biophys Res Commun*; 254: 462-465, 1999.

Stein, P.D., Sabbah, H.N., Marzilli, M. and Blick, E.F. Comparison of the distribution of intramyocardial pressure across the canine left ventricular wall in the beating heart during diastole and in the arrested heart. Evidence of epicardial muscle tone during diastole. *Circ Res.*; 47(2):258-67, 1980.

Stoller, M., Traupe, T., Khattab, A.A., de Marchi, S.F., Steck, H. And Seiler, C. Effects of coronary sinus occlusion on myocardial ischaemia in humans: role of coronary collateral function. *Heart*; 99:548-55, 2013.

Sun, Y. and Mohl, W. Characterization of the reactive hyperemic response time during intermittent coronary sinus occlusion. In Mohl W., editor, *Coronary Sinus Library Volume 6, ICSO and PICSO*, pages 45-52. Clinics of CSI, 2003.

Sun, Y. and Gewirtz, H. Estimation of intramyocardial pressure and coronary blood flow distribution. *Am J Physiol.*; 255(3 Pt 2):H664-72, 1988.

Syeda, B., Schukro, C., Heinze, G., Modaressi, K., Glogar, D., Maurer, G. and Mohl, W. The salvage potential of coronary sinus interventions: Metaanalysis and pathophysiologic consequences. *J Thorac Cardiovasc Surg*; 127: 1703- 1712, 2004.

Thygesen, K., Alpert, J.S., Jaffe, A.S., Simoons, M.L., Chaitman, B.R. and White, H.D. Third universal definition of myocardial infarction. *Circulation*, 126:2020-2035, 2012.

Toggart, E.J., Nellis, S.H. and Liedtke, A.J. The efficacy of intermittent coronary sinus occlusion in the absence of coronary artery collaterals. *Circulation*; 76:667-77, 1987.

Trägårdh, E., Claesson, M., Wagner, G.S., Zhou, S. and Pahlm O. Detection of acute myocardial infarction using the 12-lead ECG plus inverted leads versus the 16-lead ECG (with additional posterior and right-sided chest electrodes). *Clinical physiology and functional imaging*, Vol: 27, Issue: 6, pp. 368-74, 2007.

Tuma, J., Fernandez-Vina, R., Carrasco, A., Castillo, J., Cruz, C., Carrillo, A., Ercilla, J., Yarleque, C., Cunza, J., Henry, T.D. and Patel, A.M. Safety and feasibility of percutaneous retrograde coronary sinus delivery of autologous bone marrow mononuclear cell transplantation in patients with chronic refractory angina. *J Transl Med*; 9:183, 2011.

Tziroglou, A.G., Raphael, S.S., Troulinos, A.E. and Arealis, E.G. Attempts to increase the blood supply to an acutely ischemic area of the myocardium by intermittent occlusion of the coronary sinus. *Proc Eur Soc Artif Organs*, 6, pp. 45-49, 1979.

van de Hoef, T., Nijveldt, R., van der Ent, M., Neunteufl, T., Meuwissen, M., Khattab, A., Berger, R., Kuijt, W., Wykrzykowska, J., Tijssen, J., van Rossum, A., Stone, G., and Piek, J. Pressure-controlled intermittent coronary sinus occlusion (PICSO) in acute ST-segment elevation myocardial infarction: results of the Prepare RAMSES safety and feasibility study. *EuroIntervention*; 11:37-44, 2015.

van de Hoef, T.P, Nolte, F., Delewi, R., Henriques, J.P.S., Spaan, J.A.E., Tijssen, J.G.P., Siebes, M., Wykrzykowska, J.J., Stone, G.W. and Piek, J.J. Intracoronary hemodynamic effects of pressure-controlled intermittent coronary sinus occlusion (PICSO): Results from the first-in-man Prepare PICSO study. *J Interven Cardiol*; 25:549-556, 2012.

Vatner, S.F. Correlation between acute reductions in myocardial blood flow and function in conscious dogs. *Circ Res.*; 47(2):201-7, 1980.

Vergroesen, I., Noble, M.I. and Spaan, J.A. Intramyocardial blood volume change in first moments of cardiac arrest in anesthetized goats. *Am J Physiol.*; 253(2 Pt 2):H307-16, 1987.

Weigel, G., Kajgana, I., Bergmeister, H., Riedl, G., Glogar, H.D., Gyöngyösi, M., Blasnig, S., Heinze, G. and Mohl, W. Beck and back: A paradigm change in coronary sinus interventions-pulsatile stretch on intact coronary venous endothelium. *J Thorac Cardiovasc Surg* ;133:1581-7 ,2007.

World Health Organization. Cardiovascular diseases. WHO fact sheet May 2017, accessed 2018-01-30, <http://www.who.int/mediacentre/factsheets/fs317/en/>.

Wong, A.Y., Armour, J.A., Klassen, G.A. and Lee, B. The dynamics of the coronary venous system in the dog. *J Biomech.*; 17(3):173-83, 1984.

Xu, S., Bendeck, M. and Gotlieb, A.I. Atherosclerosis and Large Vessel Disease. In Butnay, J. and Buja, M. L., editors, *Cardiovascular Pathology*, 4th Ed., Academic Press, Amsterdam, Boston, Heidelberg, London, New York, Oxford, Paris, San Diego, San Francisco, Singapore, Sydney, Tokyo, 2016.

Yamamoto, K., Takahashi, T., Asahara, T., Ohura, N., Sokabe, T., Kamiya, A. and Ando, J. Proliferation, differentiation, and tube formation by endothelial progenitor cells in response to shear stress. *J Appl Physiol.*;95(5):2081-8, 2003.

Zalewski, A., Goldberg, S., Slysh, S. and Maroko, P.R. Myocardial protection via coronary sinus interventions: superior effects of arterialization compared with intermittent occlusion. *Circulation*; 71(6):1215-23, 1985.